The Hydraulic WILMER Tweezer

Design and Development of a Hydraulic Voluntary Closing Mechanism within a Body Powered Split-Hook Prosthesis

MSc Thesis

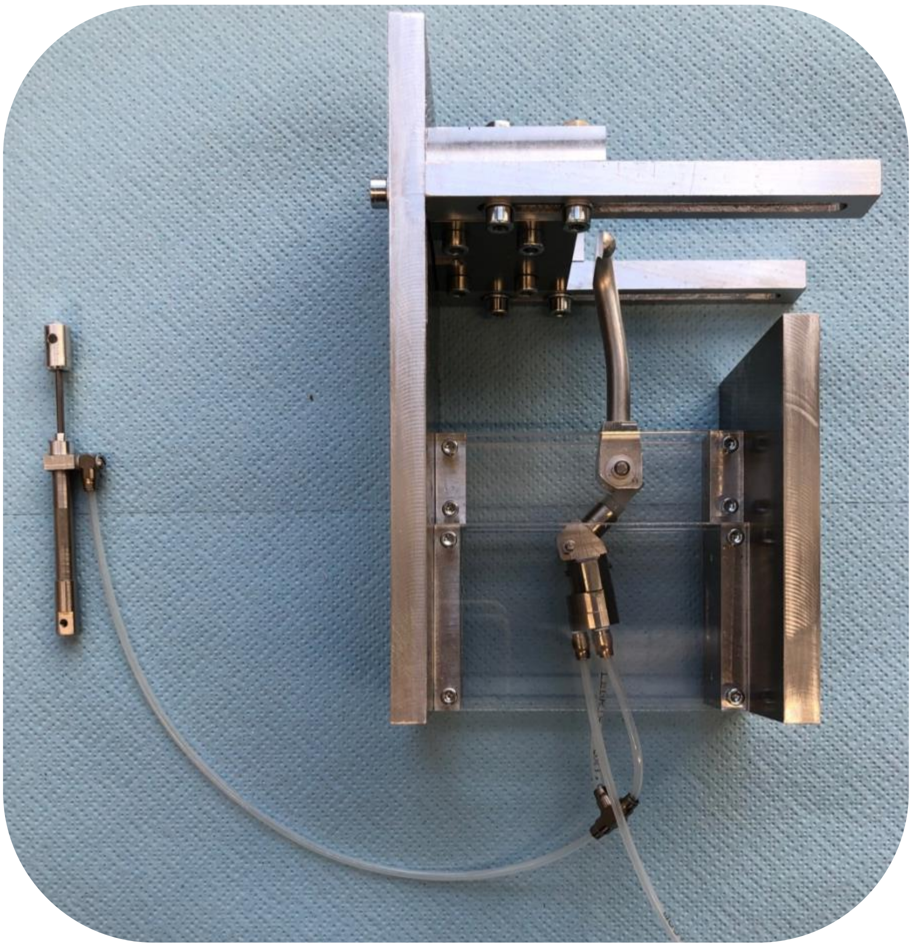

Rogier J. Panhuyzen
4272730

July 9, 2020
15:00 – 17:30h

Dr. Ir. Dick H. Plettenburg (Supervisor)
Dr. Ir. Gerwin Smit (Graduation Committee)
Dr. Ir. Tim Horeman (Graduation Committee)

Delft University of Technology
Faculty of Mechanical, Maritime and Materials (3mE)

TUDelft

Table of Contents

Scientific Paper

Abstract

Background
Despite its high demand, prostheses are too often abandoned because they fail to meet the main requirements control, comfort and cosmesis. Body-powered hook prostheses provide good control due to their proprioceptive feedback but are in general not efficient nor appealing. The WILMER group has developed an appealing voluntary-opening prehensor by building all mechanical parts inside the prosthetic cover. The voluntary closing (VC) version, the Tweezer, has slight advantages over the voluntary opening but failed to provide sufficient energy transmission within the available space to which hydraulics offer the solution. The objective is to develop and evaluate a hydraulic VC mechanism within a body powered hook prosthesis that meets the main requirements.

Methods
A hydraulic system was designed. The system shall transmit a 32 N and a 6.4 N actuation force, when holding objects for a prolonged time, to a 7 N pinch force. A maximum 40 mm actuation displacement shall close the hook from a 50° open to a 0° closed position. The system shall fit inside the prosthetic cover and have a maximum mass of 43 g. A prototype was built and tested to measure its performance.

Results
The design consists of three hydraulic actuators: a master cylinder, a slave cylinder and a pressure intensifier. The user actuates the master cylinder, which is incorporated in the harness, causing fluid to be transferred to a slave cylinder in the prosthesis that closes the hook to grasp objects. When an object is met the pressure intensifier amplifies the pressure of the slave to increase the pinch force to 45 – 53 N and 9 – 11 N for actuation forces 32 and 6.4 N respectively. The actuation displacement equals 26 mm.
The prototype failed to be manufactured properly within the given time and a simplified version, equal to the inactive pressure intensifier, has been made to prove part of the concept. Theoretically, the simplified version closes the hook with an actuation displacement of 11 mm and reaches pinch forces of 5 – 6 N over the hook range. The prototype closes the hook with 12 mm and reaches pinch forces 3 – 5 N. It takes 4 N to reopen the hook. The simplified version weighs only 15 g and fits easily inside the prosthetic cover. The mechanism provides proprioceptive feedback at the master cylinder.

Conclusion
Part of the concept has been proven. Theoretically, by adjusting the simplified versions parameters the 32 N actuation force could generate pinch forces 16 – 19 N with a 34 mm actuation displacement. It would outperform other body powered prostheses in terms of force transmission. The hydraulic VC mechanism has the potential to transfer a comfortable actuation force and displacement into the required pinch force within the available space of the Tweezer. Thus, a voluntary closing hook prosthesis is designed that can satisfy all user requirements control, comfort and cosmesis.

1. Background

In the United States of America nearly 541,000 individuals in 2005 have an upper limb amputation, and that number is predicted to double by 2050 [1]. There is no question for the demand for prostheses, yet they are far from perfect. Approximately 27% of the amputees do not actively use their device and an additional 20% stop wearing it. Many studies have been conducted and report rejection rates from 35% for body powered prostheses and 25% up to above 50% for electric powered prostheses [2] [3] [4] [5]. What is the problem? Many prostheses are not being used due to the discrepancy between the expectations of the amputees and reality [6]. Research on children's acceptance of prostheses highlighted the main problems of the device being unreliable, uncomfortable, unaesthetic or too heavy [7] [8] [9] [10]. According to Dr. Plettenburg, the three basic requirements to solve these problems are cosmetic appearance, easy and reliable control and comfort in wearing and using [6]. Dr. Biddiss recommends increased comfort and decreased mass [7] and Dr. Schulz aim for more functionality and a better cosmetic appearance [11] [12]. Research is needed to lend people a helping hand in providing what they truly need.

Two types of active upper-arm prostheses exist: electric powered prostheses (EPP) and body-powered prostheses (BPP) [13]. There is no consensus which is better. EPP are cosmetically more appealing and less rejected but are more expensive, noisy, vulnerable and heavy to wear due to the electric components inside the arm [7] [14] [15] [16] [17]. BPP provide direct proprioceptive feedback at the body part that provides input which makes the user feel the prosthesis is an extension of its own body thus improving its control (Figure 1) [18] [19]. Yet, BPP are inefficient, as they need high actuation forces (61–131 N) but generate low pinch forces (~15 N) [20]. Making BPP more appealing and efficient could decrease the rejection rates for BPP.

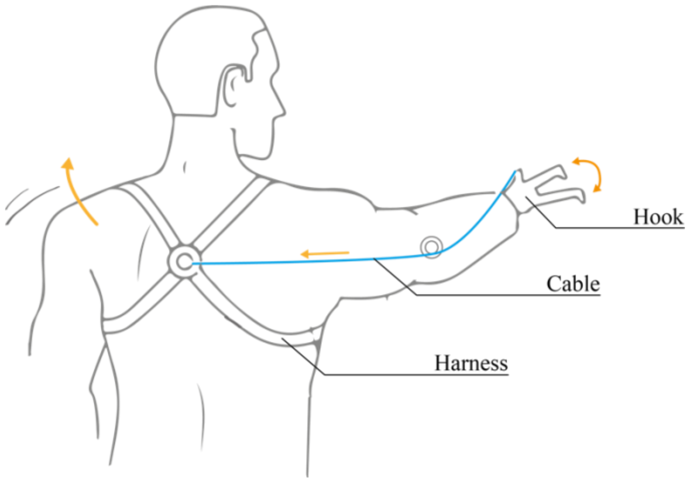

Figure 1. Body powered hook prostheses can provide proprioceptive feedback. The user puts tension on the cable with its shoulder that is strapped in a harness and thus opens or closes the hook. The tension is directly felt in the shoulder.

The WILMER group, a research group on prosthesis and orthosis in Delft, has developed a BP hook prosthesis, the Appealing Prehensor, that solves the cosmetic requirement by building all mechanical parts inside the cosmetic cover (base) (Figure 2) [21].

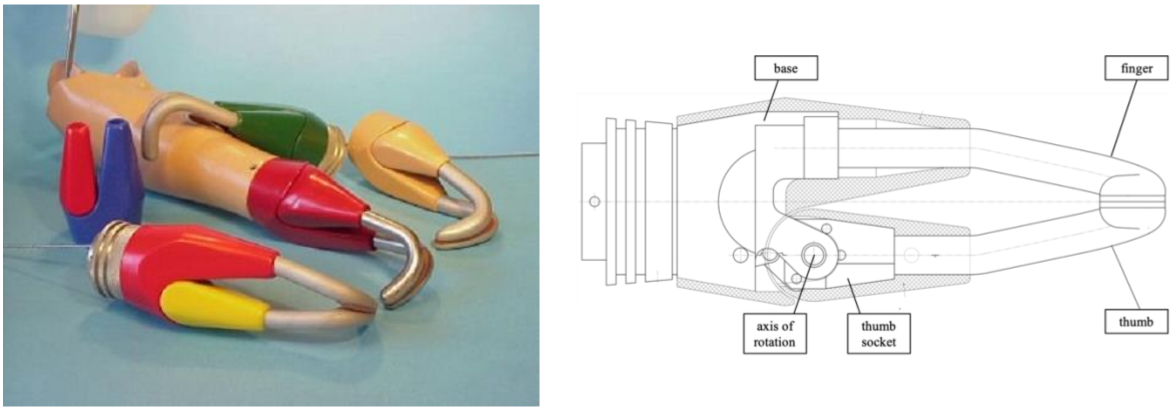

Figure 2. The WILMER Appealing Prehensor – a cosmetically accepted body powered split-hook prosthesis (left). highlighted parts of the WILMER Prehensor (right).

The WILMER Prehensor is a voluntary opening (VO) prosthesis. The moveable hook, the thumb, is opened by the user and closed by a spring to grasp objects (Figure 3a). The antagonist of VO is voluntary closing (VC). The hook is opened by a spring and closed by the user (Figure 3b). The main advantages of VC are the extended proprioceptive feedback: the direct relationship between pinch and actuation force [22]. Closing the terminal device at will makes it, unlike VO, physiological intuitive to operate [23]. VC has a faster response time than VO in the Southampton Hand Assessment Procedure Test (SHAP) [24] by 1.3s [25]. Research on 37 limb-deficient children 3-5 years old using BPP showed VC is more energy-efficient than VO [26]. The authors also concluded VO is not feasible for children. A more recent study proved that VC is more accurate, shows less variability in low grip forces (0.49 – 4 N) and mostly resembles the anatomical hand [27]. However, for higher pinch forces the required actuation force for VC is higher than VO, because it uses body power to grasp objects where VO uses spring force [28]. This induces user strain during or after usage [7]. In particular when developing the VC version of the Prehensor, the WILMER Tweezer, creating sufficient mechanical advantage within the available space was the biggest obstacle [29].

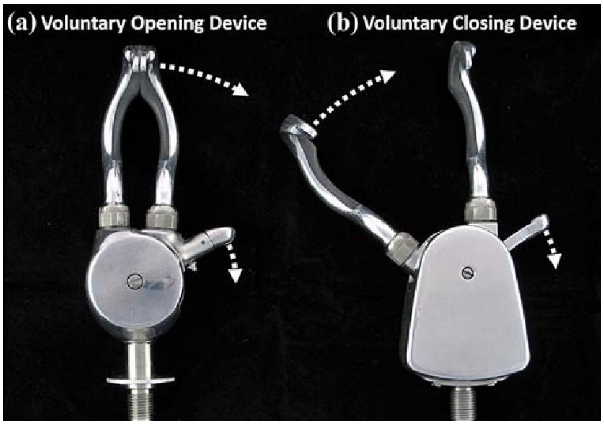

Figure 3. Two operating principles of a BP hook prosthesis: a) voluntary opening, the hook opens upon user input b) voluntary closing, the hook closes upon user input.

Hydraulics prove to be a promising principle to acquire the desired actuation to pinch force ratio [30]. Hydraulic transmissions can provide a more efficient alternative compared to a similar cable mechanism [31] as the friction losses are typically low [17]. Next, they have small response time, are quiet, have good control of prehension force and closing speed [32]. Hydraulic systems are excellent for power transmission and can be shaped into forms that fit in a tiny space.

2. Problem Definition

Body-powered prostheses have high rejection rates due to poor cosmetic appearance and energy inefficiency. The WILMER Prehensor solves the cosmetic problem by building all parts inside the prosthetic cover, but the voluntary opening principle is counter-intuitive. A previous attempt to design a voluntary closing version, the WILMER Tweezer, got stuck on generating sufficient mechanical advantage within the available space to translate a comfortable actuation force and displacement into the required pinch force.

3. Objective

The objective is to develop and evaluate a hydraulic VC mechanism within a body powered hook prosthesis that meets the user requirements control, comfort and cosmesis. The mechanism needs to be actuated by body powered from the harness. This actuation force shall be transferred to the prosthetic base where the mechanism rotates the thumb to provide pinch force for everyday objects. The user group comprises of children from 4 to 9 years old which uses the smallest size of the WILMER Tweezer. The mechanism shall transfer a comfortable actuation force and displacement, within the available space of the Tweezer, into the required pinch force and full closure of the split-hook. The mechanism shall allow full opening of the split-hook to reposition the thumb to grasp everyday objects. The mechanism will be verified to evaluate if the requirements are met.

4. Methodology

I. System Requirements

A hydraulic VC mechanism for the Tweezer was designed. Requirements were set up to describe what the mechanism needs to perform and what corresponding values to satisfy.

1. **Force transmission:** The mechanism shall transmit a comfortable actuation force less than 32 N that produces a pinch force of 7 N at the grip surface of the hook (70 mm) to grasp everyday objects. 32 N is the 200 N adult force scaled down anatomically for 4-year old's [33] [34] and 7 N pinch force is equal to the WILMER Prehensor. When holding an object for a prolonged time the mechanism shall transmit the accepted upper limit of 20% of the actuation force (6.4 N) to the same pinch force [33].
2. **Actuation & hook displacement**: The mechanism shall allow a maximum actuation displacement of 40 mm to move the thumb from 50 to 0 degrees for full closure. The thumb angle range (50 degrees) is equal to the Prehensor and allows grasping of everyday objects. 80 mm is the maximum actuation displacement of adults and for children it is anatomically scaled to half this length [34] [35].
3. **Return to open position:** The mechanism shall return the thumb to an open thumb position of 50 degrees from any position to reposition the thumb to grasp everyday objects.
4. **Cosmetic Conservation:** In order to conserve the cosmetic appealing appearance, the mechanism shall be built inside the cosmetic cover (base) of the Tweezer version for children 4 – 9 years old (Figure 4).
5. **Mass**: The mechanism's mass shall be minimized to prevent fatigue in the upper arm. The mechanism shall weigh less than the hand of a 4-year old which is 120 g [34]. Since the Prehensor's cover and hook weigh 77 g the designed system shall weigh maximally 43 g.
6. **BP control:** The mechanism shall be actuated by movement of a body part in the harness. The actuation force shall be transferred to the mechanism in the base and provide proprioceptive feedback.

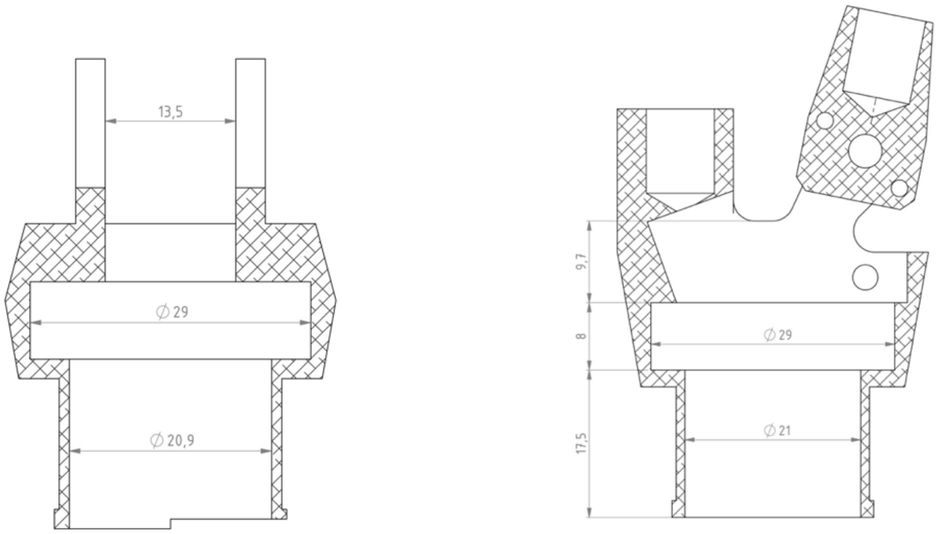

Figure 4. Dimensions of the WILMER Tweezer in mm: right section view of the base (left), front section view of the base and the thumb socket (right).

II. Verification Plan

Verification has been performed to measure to what degree the requirements were accomplished. The system was put in a test rack with similar dimensions to the base. The test rack has a mechanical stop on both sides to verify the thumb opening from 50 to 0 degrees. The masses of the filled subsystems, as they would be put into the prosthesis, were measured by a scale (Mettler PJ360 DeltaRange).

Five experiments have been performed (Figure 5)

1. **Pressure test**: five different actuation forces were applied (12, 22, 32, 42 and 52 N), and the pressure put into the system was measured to estimate mechanical losses. The test has been repeated 3 times.
2. **Pressure test by pinch force**: similar to the pressure test but the pinch force was measured at the closed hook of 0 degrees to estimate mechanical losses. The pressure has been calculated from the measured pinch forces.
3. **Close test**: The hook was fully closed from 50 to 0 degrees, without pinching for 4 sessions. The hook was opened manually. The actuation displacement was measured. The test has been repeated 3 times.
4. **Re-open test**: Stepwise increasing actuation force was applied until the hook fully opened from 0 to 50 degrees. The minimum actuation force has been measured.
5. **Pinch test**: The pinch force was measured at 6 different thumb angles set by a goniometer: 0, 10, 20, 30, 40 and 50 degrees. A 32 N and 6.4 N force was applied for 4 sessions of 5 s each and which are separated by 10 s of rest.

The input pressure in the hydraulic system has been measured by a pressure sensor (SICK PBT 6038640 [36]) to determine the true output pressure that generates the pinch force. The pinch force has been measured by a load cell (Futek FLLSB200 S-Beam Jr. [37]). Test weights were used to apply the actuation forces. A calliper measures the displacement. The load cell and pressure sensor are connected to an Analog Signal Conditioner (Scaime CPJ Rail [38]). A DAQ device (NI USB-6008 [39]) loads the data via Labview into MATLAB.

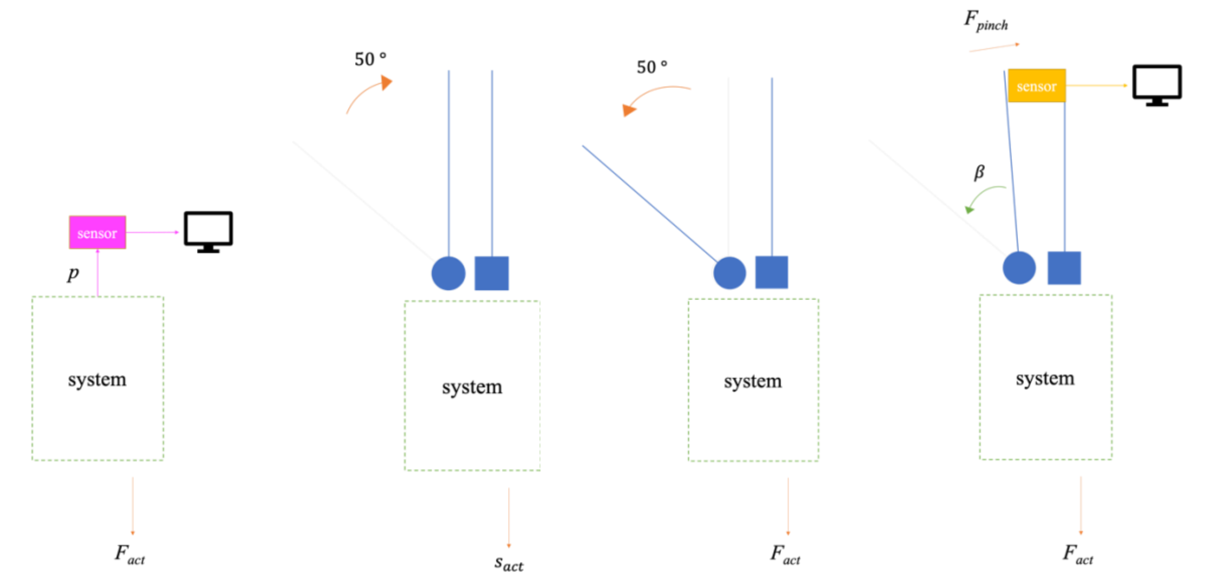

a) **b)** **c)** **d)**

Figure 5. The five test that were performed. a) The pressure test, where an actuation force is put into the system and the output pressure is measured. b) The close test, where an actuation displacement is put into the system to close the thumb. c) The re-open test, where an incremental actuation force is put into the system and re-opens the thumb. d) The pinch test, where an actuation force is put into the system and the pinch force is measured at specific thumb angles (β). The pressure test by pinch force follows same procedure as the pinch test but calculated the pressure from the pinch force.

5. Results

I. Prototype

The system starts at the Master Cylinder located at the harness transmitting user force and displacement to fluid pressure and movement (Figure 6). The fluid is guided by a hydraulic hose to the Pressure Intensifier (PI) inside the Tweezer's base which amplifies pressure when activated. The pressure is transferred to the Slave Cylinder which transmits it to a force to the thumb socket via the piston. The force on the thumb socket is transferred into rotation of the thumb socket closing the thumb and generating a pinch force. The slave cylinder pivots on an axle connected to the base that also provides the reaction force of the pinch force. A to be defined return system exerts a force on the thumb socket to preserve an open position.

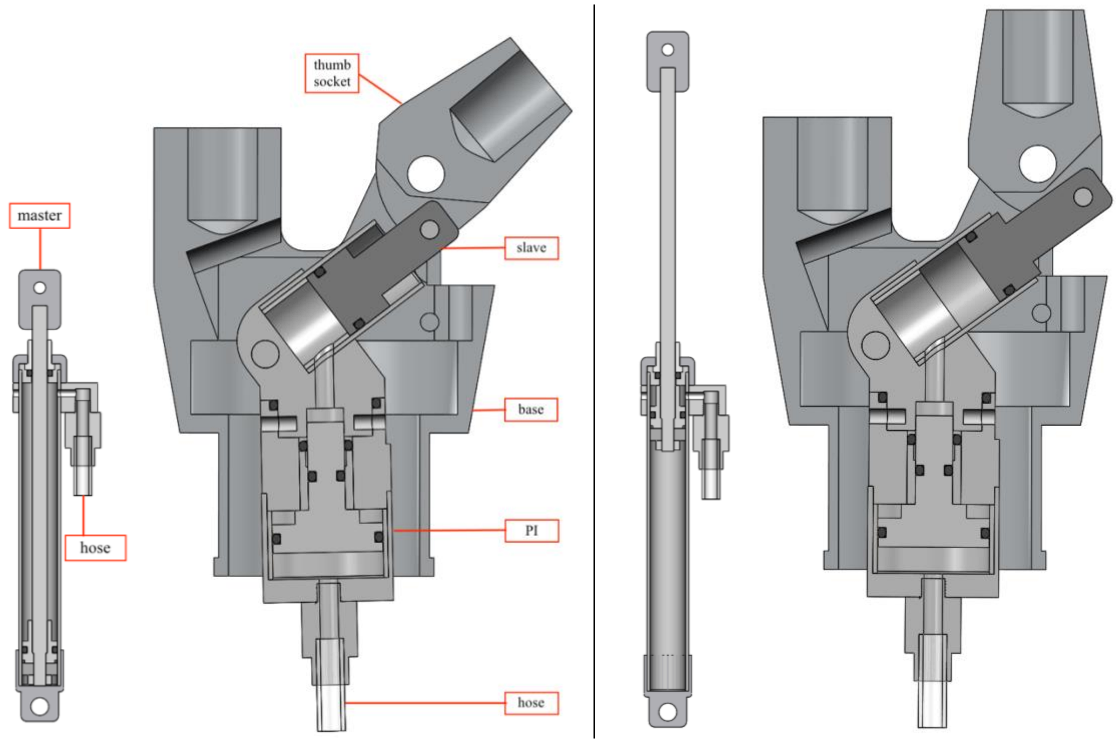

Figure 6. A section view of the final design of the Tweezer excluding the return system. The thumb is at an open position of 50 degrees, the master cylinder is in the neutral position (left). The thumb is in closed position at 0 degrees, the master cylinder is in the maximum position (right).

Fluid System

1. **Medium:** Water has been chosen as the medium to minimize leaking damage to the user's skin or fabric. It is also used in other miniature hydraulics [17] [40] [41].
2. **Sealing:** Leakage in the hydraulic systems decreases the pressure and fluid volume and consequently the performance and efficiency. Contact seals are elastic rings interfacing piston and cylinder stopping leakage between mating components and are the most useful for moving components [41]. O-rings were used for their very small size availability and robustness [42]. The O-rings have a cross-section width of 1 mm and inner diameters 2.5, 4, 6 and 10 mm which withstand pressures up to 13 MPa [43]. Loctite 648 is used to seal the assembled parts and provide a strong connection [44].
3. **Hydraulic Hose & Fittings:** A hydraulic hose transfers fluid from the master cylinder at the harness to the pressure intensifier inside the base. The hose needs to be compliant to allow effortless arm movements by the user. Festo's PUN-H-3x0.5 was chosen because it handles high pressures (over 10 bar), is compliant and small to allow more design space [45]. A Legris fitting connects the hose to the actuators [46]. Festo's QSMY-3 Y-junction was used to split the hose for the two fluid entries of the pressure intensifier [47].

Hydraulic Actuators

Master Cylinder

The master cylinder is a hydraulic pull actuator. The cylinder is fixed to the harness and by moving the shoulder the piston is pulled causing fluid pressure and movement. The piston consists of a rod and a head and its effective surface ($A_{m,eff}$) determine the pressure in the system. Designing as small as possible allows more design space and increases efficiency in the cylinder (Fig. C.10, [41]), yet small diameters result in high pressures that can damage the system. The diameters of the rod ($d_{m,rod}$) and head ($d_{m,head}$) are 6 and 2.5 mm respectively and generate at the maximum actuation force ($F_{act} =$ 32 N) a pressure (p_m) of 1.37 MPa without losses.

$$p_m = \frac{F_{act}}{A_{m,eff}} \tag{1}$$

$$A_{m,eff} = \frac{\pi}{4}\left(d_{m,head}^2 - d_{m,rod}^2\right) \tag{2}$$

The master cylinder's length enables 40 mm piston displacement equal to the maximum required actuation displacement. The master piston needs to displace a volume to displace the slave cylinder for full hook closure, to activate the pressure intensifier and to account for springback within the system. Elastic deformation will take place because the system and the object cannot have infinite stiffnesses. The springback of the hook was taken as 5 mm at a distance of 70 mm. This translated to an extra slave displacement of 0.43 mm. In total the master piston was predicted to move 25.7 mm for full system operation.

Slave Cylinder

The slave cylinder is a hydraulic push actuator that generates a force in the direction of the expanding fluid. The cylinder pivots on an axle connected to the base (maximum 2.7°) and is connected to the thumb by the piston (Figure 7). The angle (ϕ) between slave piston and the thumb arm (r_T) changes over the thumb angle (β). It defines with the pinching moment (M_{pinch}) the needed force by the slave piston (F_s)

$$F_s = \frac{M_{pinch}}{r_T \cos(\phi - 90°)} \tag{3}$$

The pinching moment is the product of the pinch force (F_{pinch}) and the length of the thumb hook (r_{hook}) which is 70 mm. The cylinder is placed perpendicular r_T at $\beta = 19°$ such that it fits the boundaries of the base and has the best force distribution over all angles. The maximum needed F_s is 97 N at $\beta = 50°$ and $\phi = 123°$. The inner diameter of the slave cylinder (d_s) is 8 mm. The maximum pressure needed by the slave cylinder (p_s) was predicted to be 1.94 MPa.

$$p_s = \frac{4F_s}{\pi d_s^2} \tag{4}$$

The displacement of the slave piston to fully close the hook equals 5.1 mm. The piston was made from polychlorotrifluoroethylene (PCTFE) to function as a bearing in the cylinder. PCTFE does not absorb water and has high strengths [48].

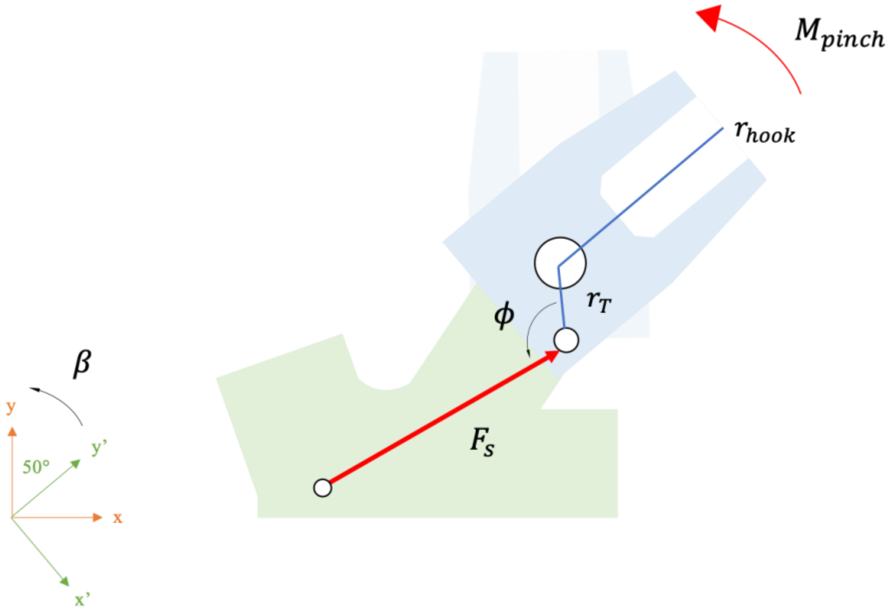

Figure 7. Kinematics of the slave (red) and the thumb socket (blue) in the base (green). The slave piston exerts a force at the thumb arm which pivots around its axis of rotation and closes the thumb providing a pinch moment.

Pressure Intensifier

The PI is a hydraulic actuator invented by J. van Frankenhuyzen [49]. The PI consists of two chambers with each a fluid entrance. A piston between the chambers is held in place by a spring in the large chamber. When no pinch force is present the PI is inactive because the spring holds the piston in place and the fluid passes through the small chamber directly to the slave cylinder. From master to slave the system is closed and liquids are non-compressible meaning the pressures are equal ($p_m = p_s$). Combined with the Conservation of Energy, a relation between the diameters ($d_{m,head}$, $d_{m,rod}$ & d_s) and displacements (s_m & s_s) of the master and slave can be found.

$$\frac{d_s^2}{d_{m,head}^2 - d_{m,rod}^2} = \frac{s_m}{s_s} \tag{5}$$

Inserting the diameters and slave displacement the actuation displacement is computed and the hook can fully close with an accepted 10.8 mm when the PI is inactive.

The PI activated when an object is encountered. The pressure generated by the pinch force exceeds the spring force in the large chamber and the piston moves until the small chamber is closed off (Figure 8). The output pressure onto the slave (p_s) is then intensified by the piston force and its surface ratio. The pistons large diameter ($d_{PI,l}$) is 12 mm and small ($d_{PI,s}$) 4 mm which can intensify the pressure by a factor (I) 9.

$$p_s = \frac{A_l}{A_s} p_m \tag{6}$$

$$I = \frac{p_{in}}{p_{out}} = \frac{A_l}{A_s} = \left(\frac{d_{PI,l}}{d_{PI,s}}\right)^2 = 9 \tag{7}$$

With an actuation input of 32 N a pressure of 12.3 MPa is generated. This enables pinch forces from 44.55 N to 53.15 N over the thumb opening angle (Figure 9). When holding an object for a prolonged time with 6.4 N of actuation force the intensified force is 8.92 N to 10.63 N which satisfies the required 7 N pinch force.

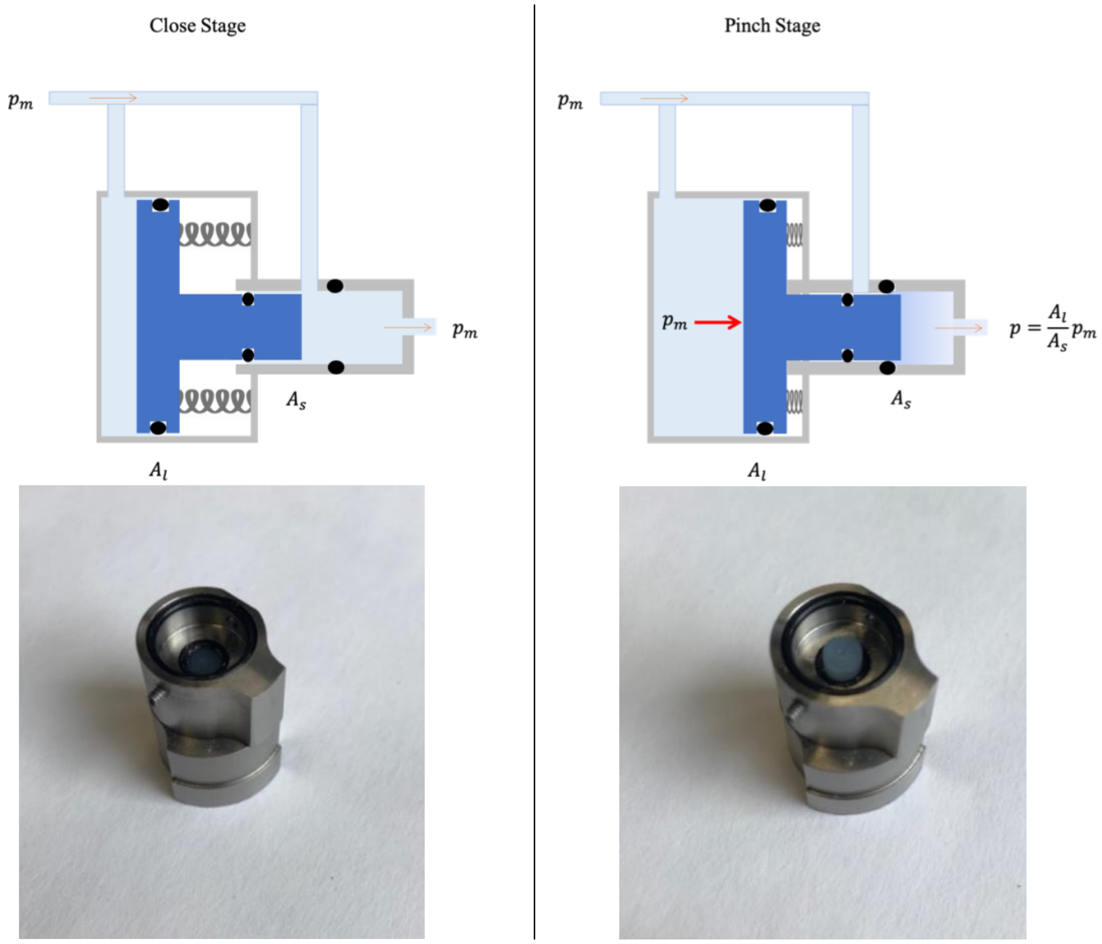

Figure 8. working principle of the pressure intensifier. PI is inactive when closing the hook (left), PI is activated when pinching an object thus intensifying the pressure (right).

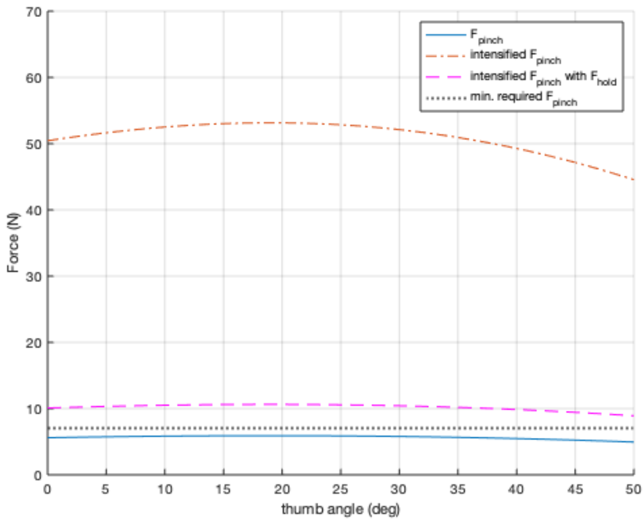

Figure 9: theoretical pinch force w.r.t. thumb angle with an actuation force of 32 N.

II. Test setup

The prototype was assembled in a test rack of similar dimensions of the Tweezer's base (Figure 10). Test weights were applied at the master cylinder which is connected by the hose to the hydraulic mechanism in the test rack (Figure 11). The load cell was placed in a 2 DOF case that allows correct positioning for measuring the force at different angles (Figure 12). The cell was clamped to ensure a pure compressive force indifferent of the angle of the hook.

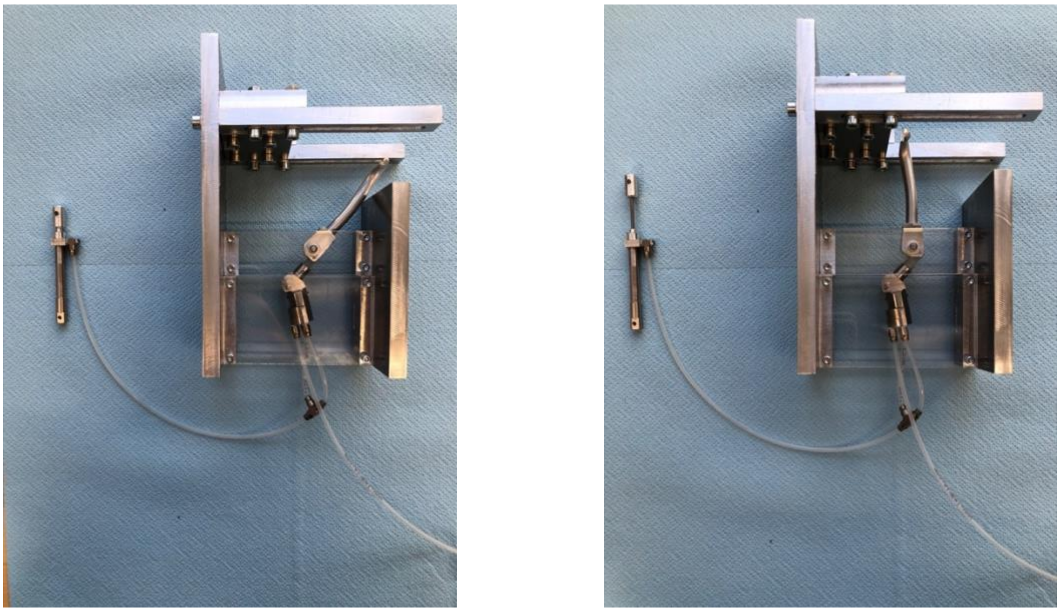

Figure 10. The prototype inside the test rack. The thumb is at an open position of 50 degrees, the master cylinder is in the neutral position (left). The master piston is pulled and closes the hook (right).

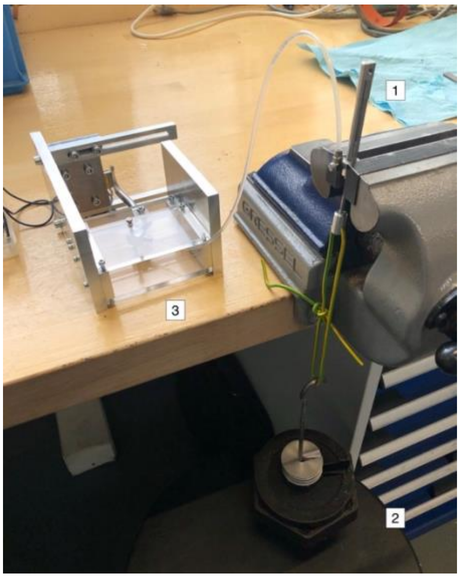

Figure 11. The master cylinder (1) is subjected to an actuation force by the test weights (2) to measure the pinch force in the test rack (3).

Figure 12. The placement of the load cell clamped in the case placed in the test rack: the thumb is at 0 degrees (left) and 50 degrees (right)

III. The Simplified Version

Unfortunately, the PI system failed to work for proper test results due to leakage. The Corona Crises gave me an unexpected opportunity to manufacture my design, yet it failed to meet the high precision that professionals can deliver. Re-manufacturing cost too much time and did not guarantee success for its high precision requirements.

A simplified version (SV) has been manufactured that fulfils the same function as the PI in its inactive state. The SV is a connecting element with the base and slave cylinder without the PI element. The master cylinder is directly connected to the slave cylinder (Figure 13). The tests were performed with the SV. The 6.4 N actuation force is not tested since it can only be satisfied using the PI.

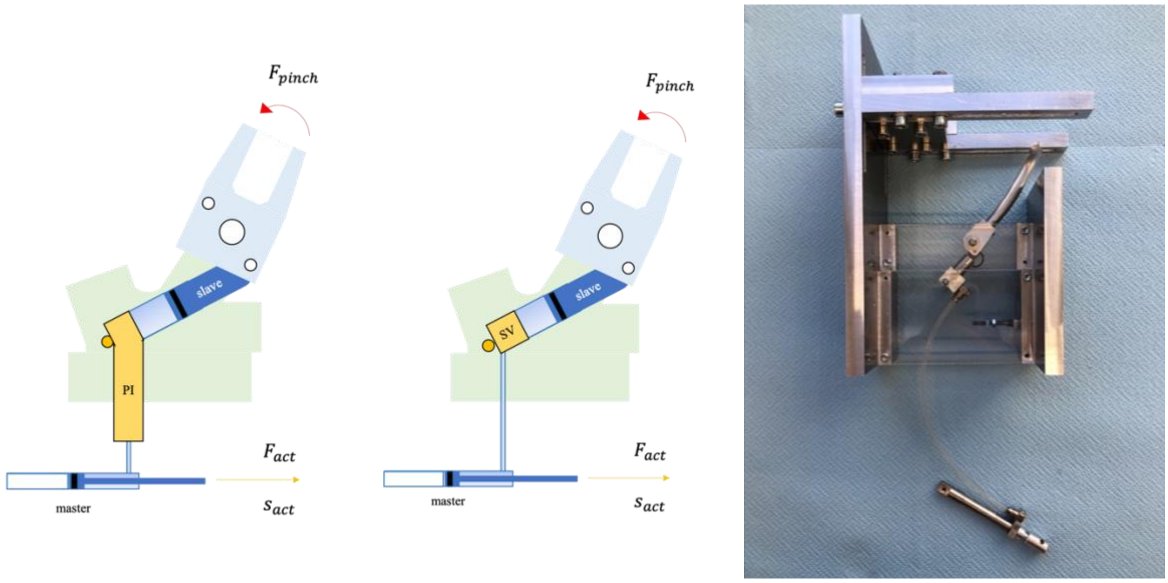

Figure 13. The design of the simplified version. The complete system with PI (left). The simplified version where the master cylinder is directly connected to the angled slave cylinder (middle). The prototype of the simplified version inside the test rack (right).

IV. Verification Results

1. **Pressure Test of the Master Cylinder**: The input pressure is the pressure from the master cylinder. The measured pressure was compared to the theoretical pressure (Figure 14). The mean pressure is lower than the theoretical pressure. At 32 N the mean measured pressure equals 11.5 ± 0.1 bar

which is 1.6 bar lower than the theoretical pressure 13.1 bar. The mean calculated pressure is 10.4 bar.

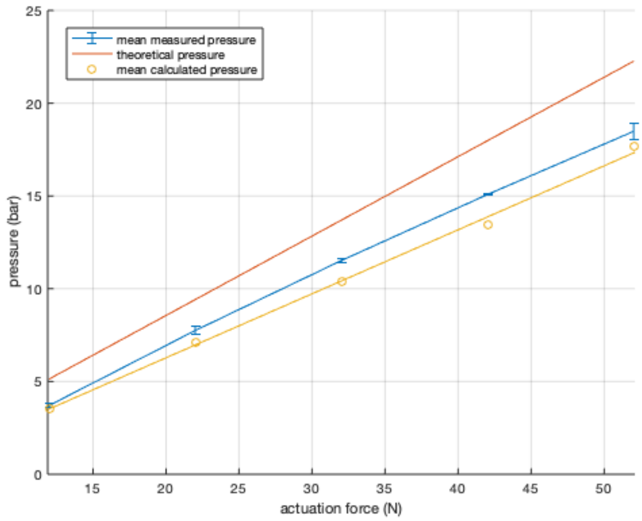

Figure 14. The theoretical pressure, the mean of the measured pressure and the mean of the calculated pressure with respect to the actuation force.

2. **Closing and re-opening the hook:** The 3 test results were similar (Figure 15). On average there is a loss in displacement of 0.21 mm (1.8%) after 4 sessions. The average displacement difference between the theory and practice is 0.83 ± 0.04 mm (7.7%). Because the hydraulic system is a closed system pushing back the master cylinder causes the hook to re-open. Adding a weight 382.8 ± 5 g (3.76 ± 0.05 N) will return the master cylinder.

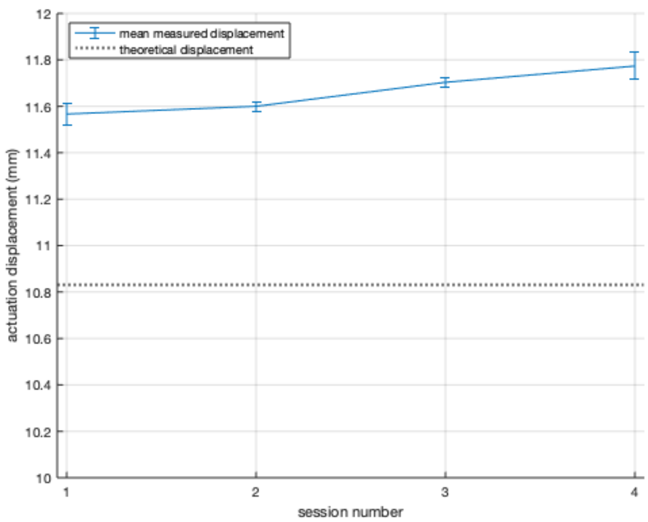

Figure 15. The actuation displacement to completely close the hook per session.

3. **Pinch force:** At every angle the system showed no sign of force loss with the sessions. The measured force was compared to the theoretical pinch force (Figure 16) and the theoretical pinch force corrected with the measured pressure by the master cylinder. The mean of the pinch force is taken to mitigate any forces by impact from the data. The measured pinch force ranges from 2.87 ± 0.04 to 4.96 ± 0.09 N at $\beta = 50°$ and $\beta = 20°$ respectively, as expected. The measurements follow the curve of the theory with a loss corrected with the measured master pressure between 0.01 N (0.1% difference) and 1.3 N (32% difference).

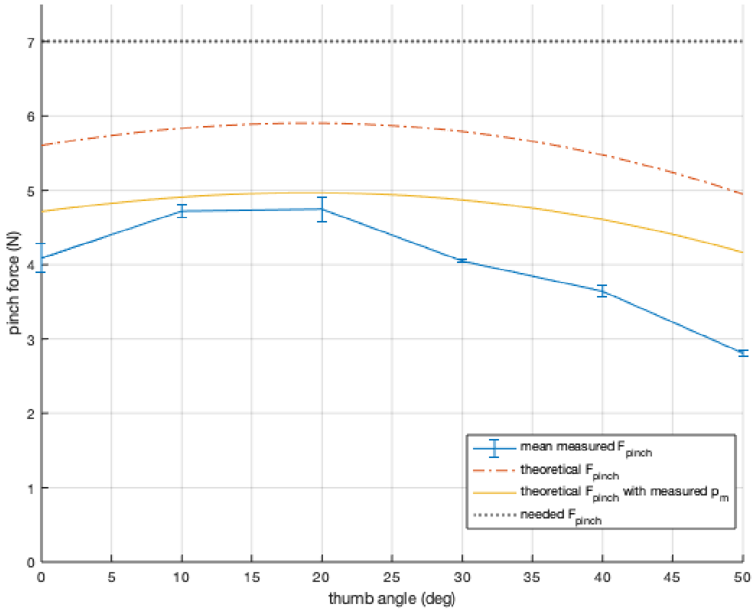

Figure 16. Comparing the measured pinch force with the theoretical pinch force over the thumb angle range.

4. **Mass**: The systems were weighted. The PI with slave weighs 41.68 g but for testing it uses a stainless-steel piston instead of PCTFE. The 3 fittings weigh together 3.0 g [46] and the Y-junction 3.7 g [50]. Together the system in the prosthetic cover weighs 48.38 g. The simplified version weighs 5 g but needs to be made of stainless steel instead of aluminium. Using the density of SS316 (7,780 kg/m^3) [51] and Al7075 (2,810 kg/m^3) [52] the stainless steel simplified version weighs 14 g. The master cylinder is located outside the prosthesis but adds weight to the harness. It weighs, including fitting, 14 g and filled 18 g. The hose weight is distributed over the arm and weights 4.2 g/m [53]. With an average length users arm length of 580-793 mm [54] and filled with fluid it adds a total of 4.25 – 5.81 g distributed over the arm.

6. Discussion

I. Evaluation of the Requirements

Table 1 shows an overview of the evaluation of the requirements. Below, detailed explanation is given per requirement.

1. **Force transmission:** The required pinch force of 7 N is not met with the tested simplified prototype. The pressure tests show pressure and mechanical losses. The pressure loss of 1.6 bar (12%) is probably caused by static friction of the O-rings on the piston head and piston rod, static friction between the bearing element on the piston and the cylinder wall, leakage of the master cylinder and viscous friction of the fluid. When the master cylinder is leaking the piston moves static friction becomes kinetic friction. It is hard to estimate or mitigate these causes.

   The difference between the theoretical pressure and the measured pressures increases with the applied force as is true for the friction force. The difference between the mean pressure and the calculated pressure of 1.1 bar is a consequence of mechanical losses in the test rack due to imprecision. This causes friction in the connection axes between the test rack and the system that suspend the system.

   There exists variation in the difference between the measured and the theoretical pinch force at the angles. The difference at 20 degrees is the smallest for which the system is designed to have the maximum pinch force. The pinch force losses range from 1.1 N (19%) to 2.1 N (43%).

The pinch force from a 32 N actuation force of the Hydraulic Tweezer (HT) variants is compared with other BPP (Figure 17). The BPP pinch forces were converted from their measured actuation forces [20] [55], assuming this relationship is linear. The BPP pinch forces were measured using a 10 mm thick force sensor which is equivalent to a 10 degrees thumb angle. The SV is a measured value and the PI active and optimized versions are predicted. The HT with activated PI would score highest. The SV prototype scores average but is expected to outperform the other prostheses when optimized. Note that the Lightweight Hand, being a hydraulic prosthesis, can also be customized to for the most optimal force transmission.

2. **Actuation & hook displacement:** The simplified prototype closes the hook completely with an average displacement of 11.57 mm at the first session which is close to the predicted displacement of 10.8 mm and far below the maximum actuation displacement of 40 mm. The difference between the measured and theoretical displacement can be caused by air in the system when filling it with fluid. Inevitably, when pulling the piston, the two O-rings at the master and one at the slave will be compressed inside the groove by the pressure (Figure 18). A new volume has arisen where water flows to and more water needs to be displaced to move the slave piston.

   The loss after the sessions indicates minor leakage at the master, fluid system or slave. To check for leakage the master cylinder was subjected to 32 N for 60 min. Each 15 min the displacement is measured. The system is placed on kitchen paper to see any fluid leakage. The difference between the displacement measured at the start and the end was 1.02 mm. The leakage was present at the piston head. To compensate for the loss in displacement the prototype needs to be manufactured with higher precision.
3. **Return to open position**: Three possible solutions exist to return the hook to open position: implementing a spring inside the Tweezer, implementing a spring at the master or designing the master to enable push input by shoulder relaxation at the harness. The third solution is preferred because implementing a spring adds force to the needed actuation force. The second solution requires a spring with a stiffness that generates a spring force of 3.76 N. The spring in the master needs to be longer than in the slave to displace the master piston (≤ 40 mm). As the spring force increases with deformation this might be a problem. The increased spring force by deformation is less a problem in the first solution because the elongation is independent of the undeformed spring length and equals 2.45 mm. Yet, the spring force needs to be higher due to the high transmission ratio between the thumb arm and hook.
4. **Mass**: With a mass of 48.67 g the prototype does not yet satisfy the 43 g requirement. Replacing the stainless-steel PI piston by a PCTFE one and reducing the weight of the connector would satisfy the requirement. The added mass outside the prosthetic cover, hose and master cylinder, is estimated to be comfortable by the user. The stainless-steel simplified version weighs 15 g (65% less than required).
5. **Cosmetic conservation**: The system fits inside the Tweezer's base and its outside remains unchanged. The appealing appearance is conserved.
6. **BP control:** The hydraulic mechanism provides extended proprioceptive feedback. When pulling the master cylinder by hand an increasing pinch force was felt as it required more muscle force. The mechanical losses decrease the degree of proprioceptive feedback. This degree and the severity of the losses need to be evaluated by the user.

Table 1. Evaluation of the requirements

requirement	**target**	**result**	**verified**
Pinch force	7 N	2.87 to 4.96 N (SV)	no
Actuation & hook displacement	50 – 0 degrees < 40 mm	11.58 mm (SV)	yes
Return to open position	0 – 50 degrees	3.76 N at the master cylinder	yes
Mass	< 43 g	48.38 g (with PI) 15 g (SV)	no yes
Cosmetic conservation	Fit inside the base	Fits inside the base	yes
BP control	Actuate by body part Proprioceptive feedback	Accomplished User evaluation needed	yes no

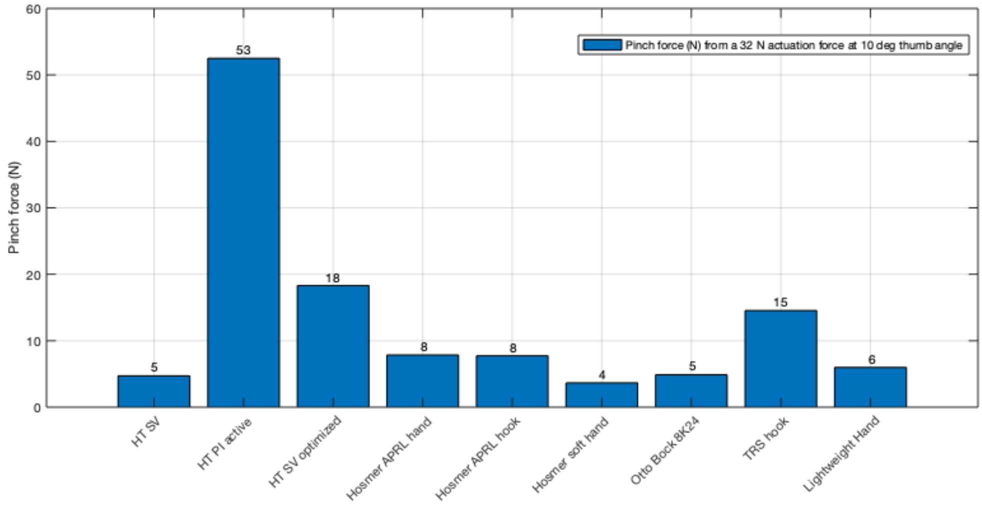

Figure 17. Comparing the force transmission of the Hydraulic Tweezer (HT) with other BPP. Plotted is the pinch force from a 32 N actuation force at a thumb angle of 10 degrees. The pinch forces of HT PI active and HT SV optimized are predictions.

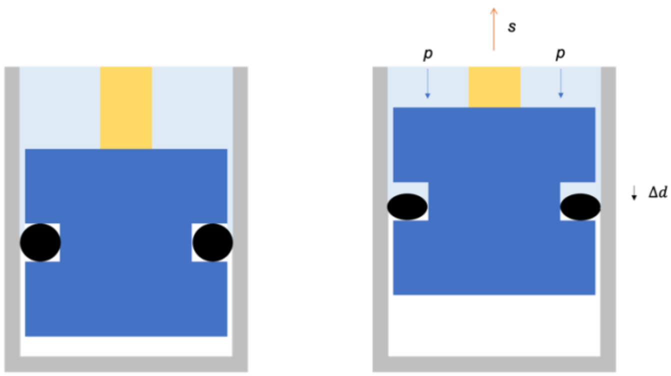

Figure 18. Compression of the O-ring in the groove. The piston is in rest position (left). The piston moves, pressure is exerted on piston, the O-ring diameter changes and fluid flows in the emerged volume (right).

II. Limitations & Recommendations

The study is limited by the prototype verification of the PI. The PI needs improvements in design for assembly. Detachable parts are wanted but for the smallest Tweezer this was too large, and consequently its design needs to take into account the flow of glue during assembly. The prototype failed during assembly when the glue flowed to the wrong places causing either leakage or blocked movement of fluid or parts.

Since force transmission was the key requirement of this research implementing a PI was a priority. It was unknown what force losses would occur and it was interesting to see how much force the PI could generate. Given the PI would have worked, manufacturability had been more important than choosing the actuation displacement to be close to 40 mm. Also, leaving space for a return system the slave cylinder's outer diameter should not exceed 9 mm.

The experiments showed that the simplified prototype works, and a spring is not needed when the user re-opens the thumb by a 3.76 N actuation force. Although limited by design space and manufacturability, different master and slave piston diameters can be chosen to adjust to the desired pinch force and actuation displacement. This gives much freedom for experimentation and customization for the user. The system can easily be upscaled for older users. For example, choosing the diameters of master rod, head and slave as 2, 4 and 9 mm the pinch forces would be 15.53-18.53 N and the actuation displacement 34.0 mm where the losses need to be determined. An adjusted simplified version could theoretically fulfil the requirements but given the time this could not be proven in practice.

Whether the PI is truly needed remains a question. Holding an object for a prolonged time with 20% of the actuation force is not possible without a PI but so far, no other prosthesis takes this requirement into account except by using a locking mechanism. The maximum pinch force for an everyday task is inserting a plug into an outlet under the most slippery condition with 31.4 N [56] requires a PI when the maximum actuation force is 32 N. On the other hand, the user could put in more force for these tasks and given the 7 N pinch force requirement it disputable how often these extremes are encountered by a 4 to 9-year-old. User evaluation in pinch force, actuation forces and displacement are strongly recommended to answer the necessity of the PI and the right master and slave ratio.

To compare the efficiency of the HT with other BPP's the hysteresis needs to be measured. Smit and Plettenburg defined hysteresis as the difference between the amount of work required to close a prosthesis and the work returned by the prosthesis [20]. The HT was not tested for hysteresis because the return system was undefined and consequently the work returned.

Further research could be on the implementation of the master cylinder to the harness and a locking mechanism to hold objects for a prolonged time. Next, the shape of the Tweezer's base should be adjusted to place the slave cylinder under a 25-degree angle to increase the lowest pinch force at 50 degrees. When the prototype is optimized, and correct requirements have been identified it needs to be tested for reliability.

7. Conclusion

This study presents the Hydraulic WILMER Tweezer, a hydraulic voluntary closing (VC) mechanism within a body-powered prosthesis for children between 4 and 9 years old. The main goal to transfer a 32 N and 6.4 N input to a 7 N pinch force with a maximum actuation displacement of 40 mm to pinch and hold objects has not been accomplished due to manufacturing failures of the prototype. Manufacturing the pressure intensifier needs very high precision.

A simplified version (SV) has been manufactured to prove part of the concept. The simplified version closes the thumb with 11.6 ± 0.04 mm displacement and reaches pinch forces between 2.87 ± 0.04 to 4.96 ± 0.09 N over the complete thumb range with an actuation force of 32 N. It takes 3.76 N to re-open the hook. The simplified version weighs just 15 g, fits inside the prosthesis to conserve its appealing appearance and its body-powered actuation provides the user with proprioceptive feedback. With design optimization the simplified version could theoretically reach pinch forces of 15.53-18.53 N, exceeding the 7 N requirement, and an actuation displacement of 34.0 mm below the maximum of 40 mm. This optimized version would outperform other body powered prostheses in terms of force transmission.

The hydraulic VC mechanism has the potential to transfer a comfortable actuation force and displacement into the required pinch force within the available space of the Tweezer. Thus, a voluntary closing hook prosthesis is designed that can satisfy all user requirements control, comfort and cosmesis.

Acknowledgements

I would like to thank TU Delft for the education that has led me to become an engineer. Dr. Dick Plettenburg for his enthusiasm and allowing me to be independent. Jan van Frankenhuyzen, Nisse Linskens and Reinier van Antwerpen for their collaboration in design and manufacturing – I deeply enjoyed manufacturing my own design and gained incredible practical knowledge in Design for Manufacturability and Assembly. I am very motivated to continue and use technology as a tool to improve the world.

Appendices

A. Thesis Outline

This chapter is the reader's guide to the methodology of the design and development of the Hydraulic Tweezer (Figure 19). The design and development processes are inspired on the books Product Design and Development [57] and Engineering Design [58].

First the problem is described, and requirements are specified. The use sequence which describes how the product is being used helps setting up the requirements. Solutions to the requirements are found internally and externally and displayed in a morphological table. The solutions are screened, and infeasible solutions are eliminated.

The remaining solutions are combined into concepts that solve the problem. Assumptions and simplifications are made to estimate the life-cycle performance, manufacturability, performance and simplicity of the concepts. The concepts are scored on these evaluation criteria using a Pugh Chart. The highest scoring concept is the most suitable and will be designed in detail.

In the embodiment design the system architecture is laid down. This defines the physical elements that perform the required functions and its relations such as kinematics and energy flow. The geometric model of each subsystem is to be derived. First the subsystem's architecture is laid down. Next, the significant parameters are determined and optimized leading to the subsystem's dimensions. Design for Manufacturing and Assembly plays a significant role and the design continuously iterated with manufacturer. Critical parts of the model are verified using simulations and requirement fulfilment is estimated.

The design has been completed and is manufactured and assembled. The prototype will be verified to measure to what degree the requirements are accomplished. The results are documented and discussed thus concluding the thesis.

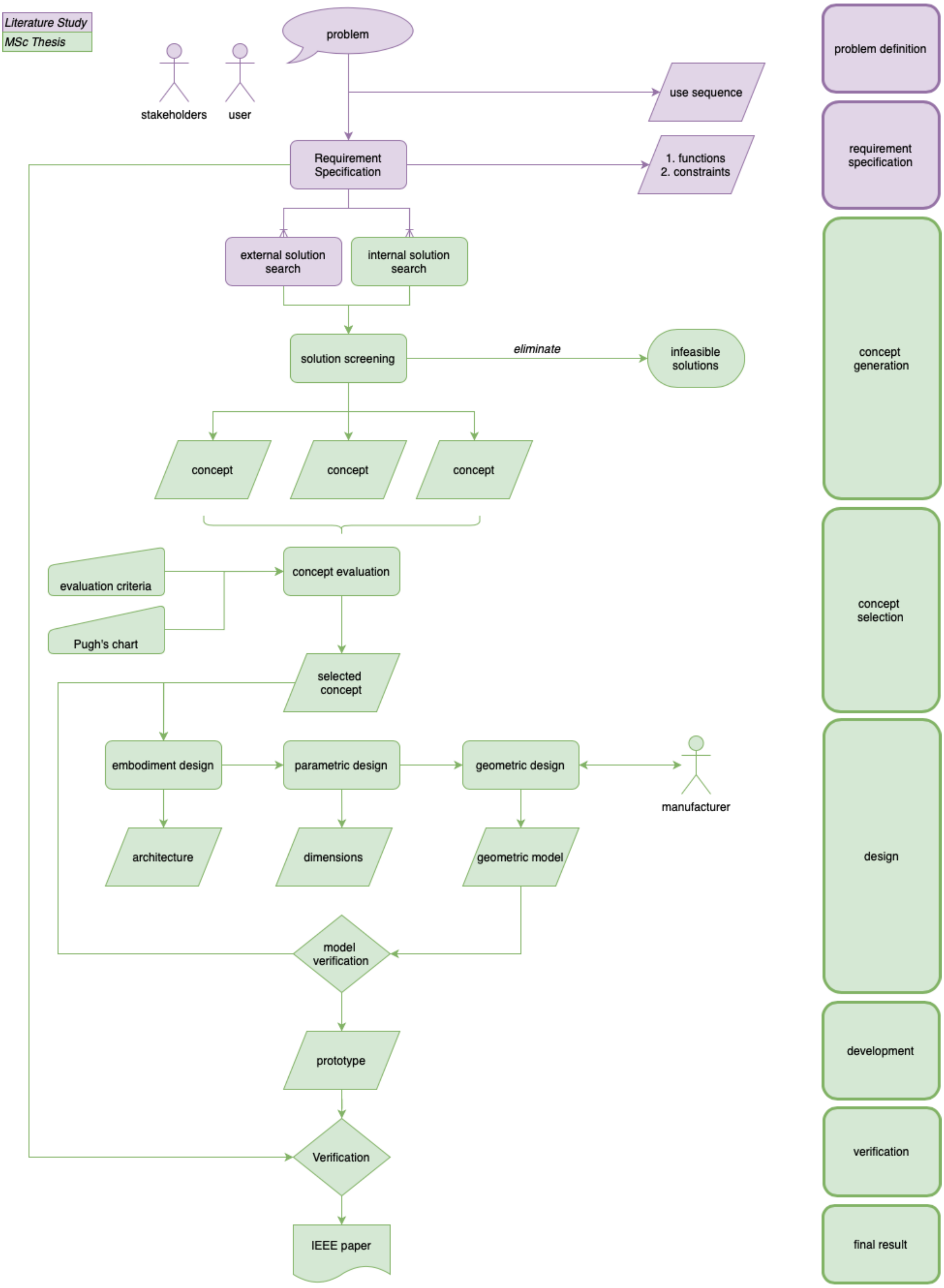

Figure 19: The roadmap of the thesis.

B. Solution Search

Solutions to the requirements are determined. The solutions are found externally, by means of literature, and internally. All solutions are displayed in a morphological table related to their functions.

The four main functions are derived from the requirements:
1. **Force transmission:** The mechanism needs to transmit a comfortable actuation force into the required pinch force.
2. **Transferring translation into rotation**: The mechanism needs to transfer a translational input into rotation of the thumb.
3. **Transfer force:** The system needs to transfer force from the harness to the prosthesis.
4. **Return to open position:** The mechanism shall return the thumb to the open position.

I. Force Transmission

The following solutions accomplish the function Force Transmission.

Mechanical Principles

N. Sclater categorized in his book "Mechanisms and Mechanical Devices Sourcebook" [60] all mechanical mechanisms. Useful mechanisms for our application are described (Table 2). The mechanisms work on the Conservation of Energy. Assuming the friction losses are negligible the conservation of energy is equal to the conservation of moments. The forces can be described as a ratio of their moment arms.

$$F_2 = \frac{r_2}{r_1} F_1 \qquad \text{(B. 1)}$$

When $r_2 > r_1$ positive mechanical advantage has been created and $F_2 > F_1$.

Table 2. classification of mechanical mechanisms transmitting mechanical advantage

Class	Description	Figure
Gears	A gear is toothed wheel that can be connected to other gears and can generate mechanical advantage by radially different sized wheel	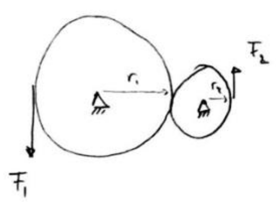
Lever (class I)	Rigid bar resting on a pivot. Physical effort at one side of the bar will move a load on the other end. The pivot is located between the ends of the bar.	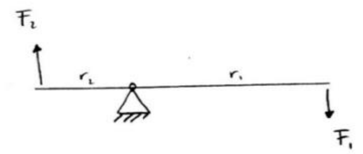
Lever (class II)	A lever where the pivot is located at the end of the bar.	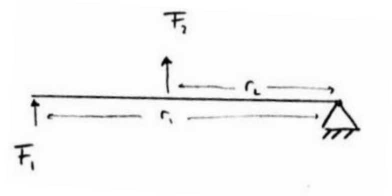

Winch	Winches can convert linear motion to rotary motion. By difference in bar length and wheel radius mechanical advantage can be created.	
Pulley & Belts	Transfer rotating motion from one shaft to another by a belt that moves a wheel by friction. By radius difference in the wheels mechanical advantage can be transmitted	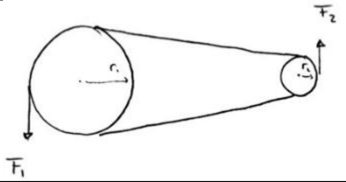
Sprockets & Chains	Sprockets have a similar working principle to the pulley but use a chain to rotate the sprockets	*Similar schematic as Pulley & Belts*

The BP Prehensor of D. Frey and L. Carlson [61] uses a mechanical VMA. At the close stage, the lever rotates over the pivot of the hook allowing high hook displacement with low actuation displacement. At the start of the pinch stage, when the object is met, the input lever comes in contact with the quadrant and the mechanism switches into high MA mode (Figure 20). In 2009 the research has been revised because of its poor performance gripping very compliant objects [61]. They solved the problem incorporating a switch to allow it to be used in free-wheel mode i.e. switching of VMA.

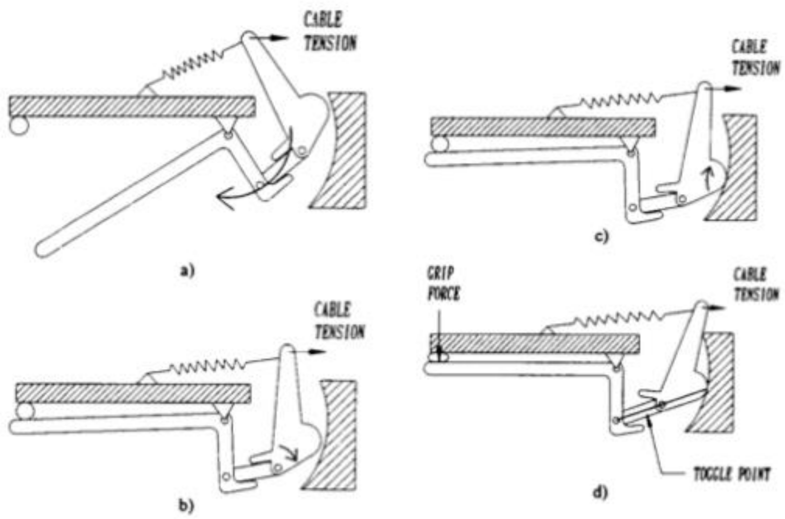

Figure 20. The working principle of VMA (Fig. 2, [61]). Operation of the VMA prehensor. a) The prehensor closes to grasp an object. b) The mechanism changes to high mechanical advantage operation when the object is met and the input lever touches with a quadrant. c) The lever rolls over the quadrant. d) The mechanism comes into the toggle point to hold objects.

Hydraulic Mechanical Advantage

Hydraulic systems are excellent for power transmission and can be shaped into forms that fit in a tiny space. Because liquids are non-compressible the pressure everywhere in the liquid is constant.

$$P = P_1 = P_2 \tag{B.2}$$

Figure 21 displays a hydraulic press that transmits the input force F_1 into a greater force F_2 due to the difference in piston surface area.

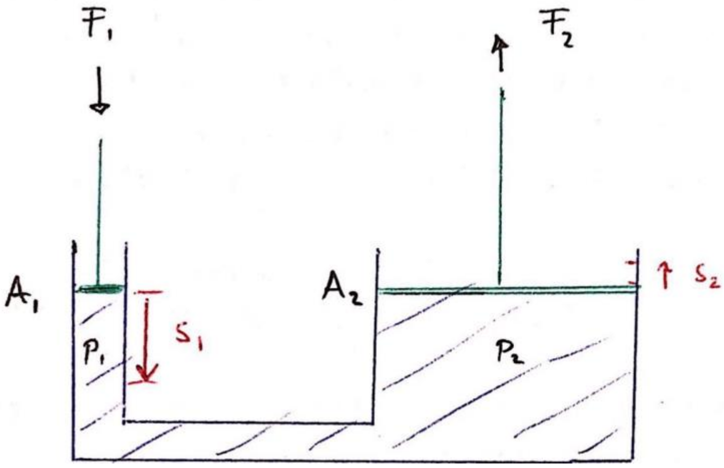

Figure 21. Schematic working principle of a hydraulic press. The output force and displacement are different from the input when the surfaces are not equal. The output force and displacement are inversely proportional.

Pressure is equal to the force times the area and since pressure is constant everywhere in the liquid the following force ratio can be derived.

$$P = F_1 A_1 = F_2 A_2 \tag{B.3}$$

$$F_2 = \frac{A_2}{A_1} F_1 \tag{B.4}$$

With $A_2 > A_1$ the $F_2 > F_1$.

The beauty of the hydraulic force intensifier is that it can be separated over a long distance by dividing the system into two cylinders connected with a hose.

The thesis of E.Versluis designs an active thumb to the Lightweight Hand. The mechanism uses an interesting element: the Two-Phase Cylinder designed by J. van Frankenhuyzen and Dr. D. Plettenburg (Figure 22). The two-phase cylinder is inspired by a braking system in vehicles by J. van Frankenhuyzen [62]. The driver can brake slowly by exerting low actuation input but also brake hard when exerting high actuation force. When a pressure threshold is passed the system generates a much larger force. Similar happens when grasping. In the close stage, there is a low actuation force without pinch force. High force transmission is not needed as that would result in high unfavorable actuation displacement. The next stage, pinch stage, the hook hits and pinches an object thus needing a large pinch force. Higher force transmission is generated when going in the cylinders the second phase thus limiting the actuation force. This could potentially solve the major problem of the trade-off sketched before

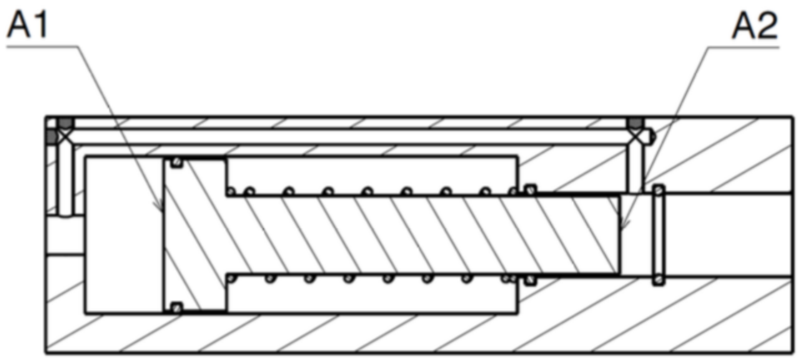

Figure 22. The cross-section of the two-phase cylinder (Fig 14) [63].

With a two-phase cylinder it is possible to have large thumb movements for the free movement of the thumb. When a large thumb force is needed, the pressure in the master cylinder will increase above the threshold

In the pinch stage, a large force is needed at the hook and thus the pressure in the master cylinder will exceed the threshold. This will close off the channel that connects the input and output chambers. The pressure in the slave cylinder will be a factor A1/A2 times the master cylinders pressure which allows for higher pinch forces with a low actuation force.

Challenge of Mechanical Advantage

Force transmission comes with a trade-off. Applying the Principle of Conservation of Energy, a high input displacement results in a low output displacement $s_2 < s_1$.

$$\begin{aligned} W_1 &= W_2 \\ W &= F \cdot s \\ s_2 &= \frac{F_2}{F_1} s_1 \end{aligned} \tag{B.5}$$

As for all MA systems this is a challenge for the Tweezer as high force transmission is wanted, while high actuation displacement for a low hook displacement is not.

II. Transferring Translation to Rotation

In order to close the split-hook by one-directional force input the mechanism needs to transfer translation into rotation. The classes of mechanical mechanisms, from N. Sclater's "Mechanisms and Mechanical Devices Sourcebook" [60], that perform this are displayed (Table 3).

Table 3. Classification of mechanical mechanisms transferring translation to rotation.

Class	Description	Figure
Cam	Cams can transmit motion to a follower by direct contact	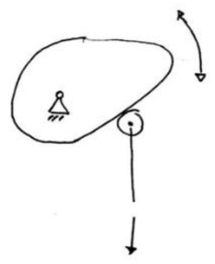
Linkages	Linkages can be designed to change the direction of motion	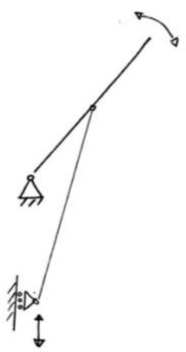

Winch	Winches can convert linear motion to rotary motion	
Ternary link	A rigid angled link rotating around an axis [64]. Either a rocker link (a) or bell crank link (b)	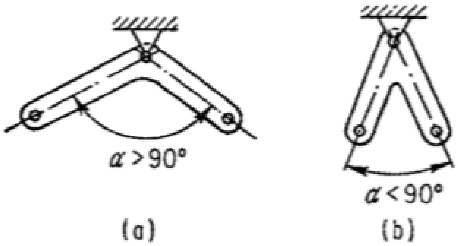

The VC Elbow [23] is an elbow-controlled prosthesis (Figure 23). Upon elbow flexion a cable is pulled. The cable is connected in the hand to a whippletree which provides tension input in the thumb and finger mechanism. The thumb and finger rotate towards each other using rolling link mechanisms. Rolling link mechanism is a system of links that roll directly on each other [65]. Rolling link mechanisms minimize friction [23].

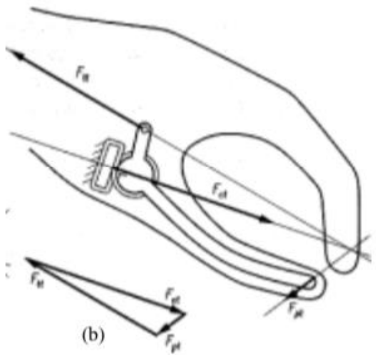

Figure 23: The thumb mechanism in the hand prosthesis uses a rolling mechanism to transfer translation of the cable into rotation of the thumb and thereby closing the hand (Fig. 5, [23])

The Fluidhand uses flexible fluidic actuator (FFA) to bend the fingers (Figure 24) [66]. The invention is inspired by the knee joint of a spider. The actuator consists of bellows that once filled with liquid or air increase in volume and apply torque to the joint such that the finger bends [67]. Its advantages are high power with low weight in combination with the inherent compliance of the actuators and the possibility of complex movements [68] [69].

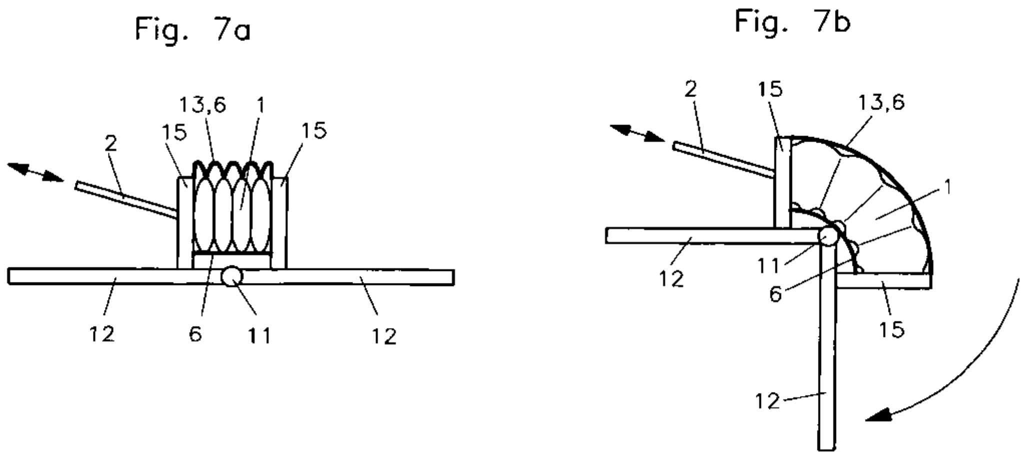

Figure 24. Working principle of Flexible Fluidic Actuator (Fig 7, [75]). Fig. 7a: deflated position actuator and hinge in the extended position. Fig 7b: the actuator gets inflated and hinge flexes.

D. Ray designed a haptic glove with an artificial muscle. A hydraulic master cylinder is actuated by a motor. The fluid system is connected to an artificial muscle consisting of a braided veil around an elastic tube. When pressure is generated in the master cylinder the tube fills with fluid. Because of the construction of the muscle thickens and shortens thus providing a compression force. Mounted on a hinge, the muscle can allow the hinge to flex or extend. The artificial muscle is implemented alongside the finger. This could be done for the Tweezer.

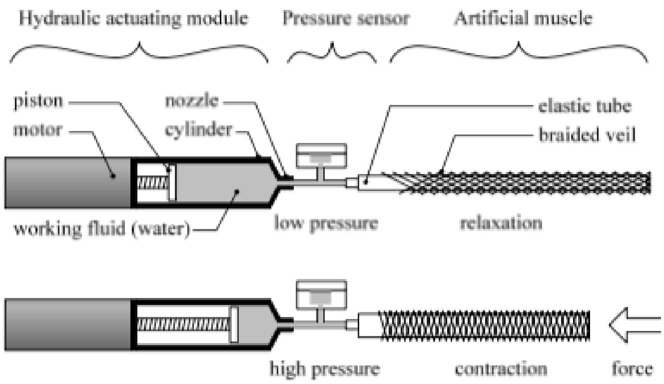

Figure 25. The working principle of the artificial muscle: under pressure the muscle fills with fluid and shrinks. Mounted on alongside a finger on a hinge it can bend the finger (Fig.2, [70]).

The wrist prosthesis of Dr. D. Plettenburg and Dr. G. Smit [71] developed a curved hydraulic cylinder to close the hook of the prosthesis. The curved cylinder eliminates an extra link, joint or mechanism that closes the hook from a linear actuation of straight cylinders (Figure 26). Part elimination means extra space, less friction and no unwanted forces on the actuator. Curved cylinders are not that easy to manufacture as machining a curved hole is not possible. Plettenburg and his team solved this using a carbon fiber formed around a male mold.

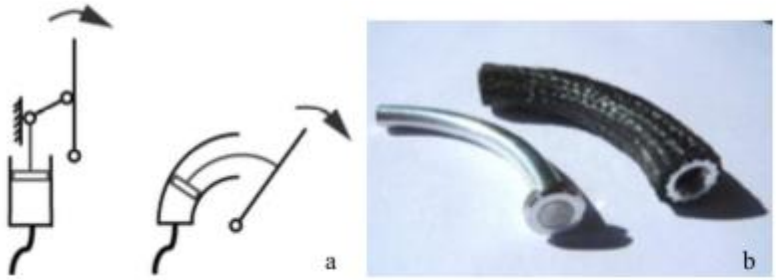

Figure 26. The curved cylinder compared to a straight cylinder. a) eliminating extra link b) curved cylinder prototype (Fig. 3, [71]).

III. Transfer Force

The most used form of transferring force from the harness to the prosthesis is the Bowden cable. Most hydraulic prostheses replace the Bowden cable by a hydraulic hose. The Bowden cable has high and variable static friction mainly due to cable curves [72] [73]. Hydraulic hoses do not reduce the system's efficiency [74]. The Lightweight Hand has the master cylinder connected to the upper body of the user and the slave cylinders in the fingers [17]. A hydraulic hose connects the master cylinder with the slave cylinders.

IV. Returning to open position

The thumb needs to return to a neutral position. Without external energy it can only be moved when stored potential energy is released. Electrical, chemical and nuclear energy are opted out and gravitational potential energy is unpractical when manipulating the Tweezer in certain configurations. The remaining potential energy is elastic energy and is stored by passive components.

Spring

A spring stores elastic energy when brought out its equilibrium state and returns to equilibrium when external forces resign.

Interesting springs for the Tweezers application are compression springs, extension springs and torsion springs (Figure 27). Other springs are not analysed, e.g. leaf springs are subjected to bending and gas springs are too complicated relative to the mechanical springs.

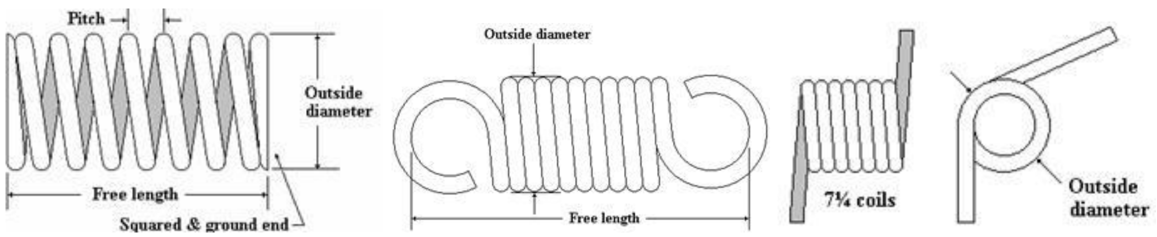

Figure 27. Spring types for the Tweezer: (left) compression spring, (middle) extension spring, (right) torsion spring [75]

Passive elements inside hydraulic systems

Hydraulic cylinder returns to its neutral state when a passive element is introduced in the cylinder (Figure 28). Because of the properties of the hydraulic fluid, it is assumed that a damper inside a hydraulic cylinder is not needed. The figures below display possible configurations of the passive element for a push-push cylinder and pull-push cylinder (Figure 29).

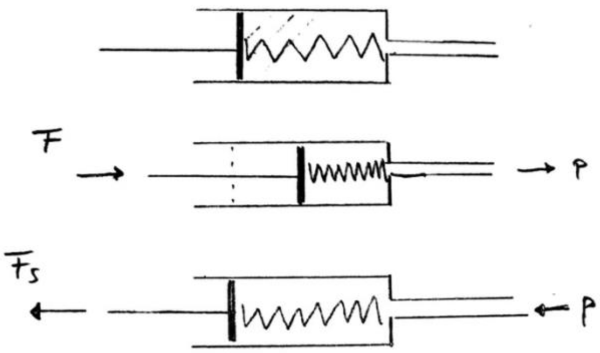

Figure 28. Working principle of equilibrium recovery of a hydraulic cylinder. (top) neutral position, (middle) force applies and spring stores energy, (bottom) force resigns and spring releases energy

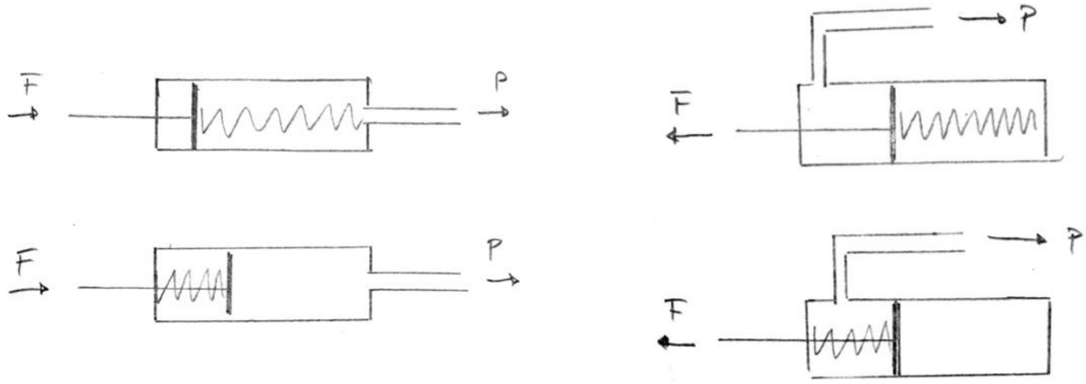

Figure 29. Configurations of a passive element for a push-push cylinder (a) and pull-push cylinder (b)

Return by force

Although not preferred a closed hydraulic system could return the hook when providing actuation force in the opposite direction. It needs to be researched what this force would be.

V. Morphological Table

The table below displays per function the solutions found [76].

Table 4.Solutions per function

Closing Tweezer	Force Transmission	Return to open position	Transfer Force
FFA	VMA mechanical	Torsion	Hydraulic pull-push
Artificial Muscle	2-phase cylinder	Extension	Hydraulic pull-pull
Ternary Link	Gears	Compression	Bowden Cable
Winch	Pulley & Belt	Hydraulic spring	
Pulley & Belt	Sprocket & Chains	Return by force	
Sprocket & Chains	Lever (class I)		
Curved Cylinder	Lever (class II)		
Cam	Hydraulic transmission		
Gears			
Rolling-Link Mechanism			
Linkages			

C. Conceptual Design

This section describes the conceptual design phase. First, all solutions are screened to eliminate infeasible solutions. From the residual solutions, concepts are generated and analysed. The most suitable concept is selected based on selection criteria and is to be designed. The sub-system's architecture is defined.

I. Solution Screening

In order to generate concepts that have the potential for product success, all solutions are screened to eliminate unfeasible solutions [58]. When screening the solutions, it is important to ask two questions: is the solution feasible and will the solution meet the requirements? The following solutions have been eliminated.

The hydraulic VMA [77] is eliminated because it is a prototype and rather large for our application. Both FFA and artificial muscles do not fit because of their implementation alongside the thumb. The curved cylinder is a concept that has not yet been proven. It is difficult to manufacture without leakage. It would be a risk to take it into the design. The design of a cam to rotate the Thumb would not fit inside the Tweezer. Moreover, cams are prone to friction, fatigue, and wear and are expensive and difficult to manufacture [78]. Sprocket and chains are nearly equivalent to pulley and belt but more complex. The pulley and belt will be investigated, and this solution is eliminated.

Since a hydraulic component is to be implemented it does not make sense to use a Bowden cable between the hydraulic cylinders. In all concepts, it is desired to use micro hydraulic cylinders as well as a hydraulic VMA since this provides only advantages. The choice of the 2-phase cylinder is independent of the concepts and is decided in the detailed design phase.

Compared to tension springs which can be hooked easily within a tiny space, compression springs are difficult to mount in the tiny space. Moreover, compression springs can loosen from its mounting position. Torsion springs have the lowest energy to volume ratio [79]. Even though the predicted energy is low it requires more volume than other spring types but could still provide an opportunity.

J. Kuntz modeled its Rolling-Link Mechanism, using a direct rolling contact between two linear tracks, inside the Prehensor (Figure 30) [80]. Even though this concept predicted an increased efficiency from 56% to 92% compared to the Prehensor design of 1995, the concept was never put into proof. The clamping of the rolling cylinders remained an unsolved challenge. Therefore, it is decided not to investigate further.

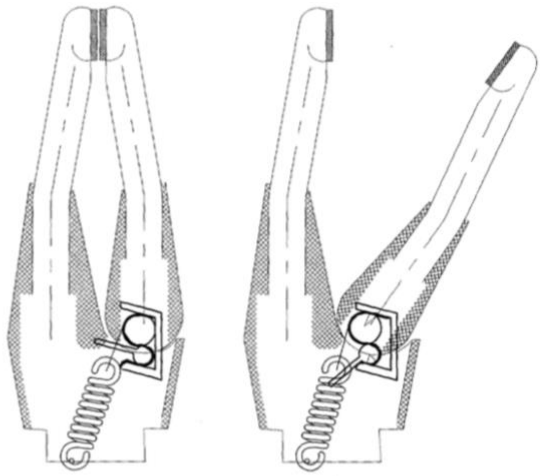

Figure 30. A VO operation mechanism within the Prehensor (Fig 7.26, [80]).

The VMA (Figure 31) is eliminated due to its complexity. It requires a wall that needs to be manufactured precisely and is subjected to wear. Moreover, it cannot grasp compliant objects which would limit the functionality of the Tweezer [81].

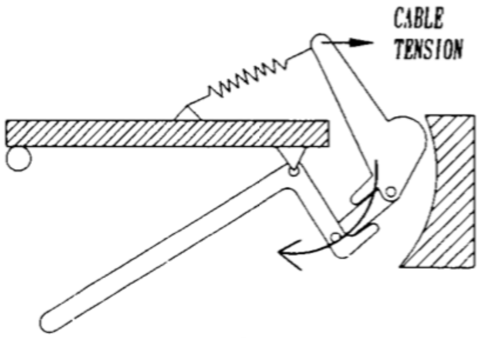

Figure 31. Operation of the VMA prehensor (Fig 2a, [81])

The spring inside the hydraulic system is to be tested in the detailed design. A hydraulic VMA is always implemented since it minimizes actuation displacement while providing the required pinch force. Without the VMA mechanism, the actuation displacement is at its maximum.
The residual solutions are mapped in the morphological table.

Table 5. Morphological Table after solution screening.

Closing Tweezer	Energy Transmission	Passive Element	Transfer Force
Gears	Gears	Torsion	Hydraulic pull-push
Pulley & Belt	Pulley & Belt	Extension	Hydraulic pull-pull
Ternary Link	2-phase cylinder	Hydraulic spring	
Winch	Hydraulic transmission		
Linkages	Lever (class II)		

II. Estimated Performance Test

To generate and compare concepts a test is derived that mostly resembles the final verification.

For full closure the mechanism needs to move the thumb from 50 to 0 degrees. At all angles the maximum pinch force of 7 N is required. The concepts are analysed at providing the pinch force at the mean angle of 25 degrees. This all is illustrated in the figure below (Figure 32).

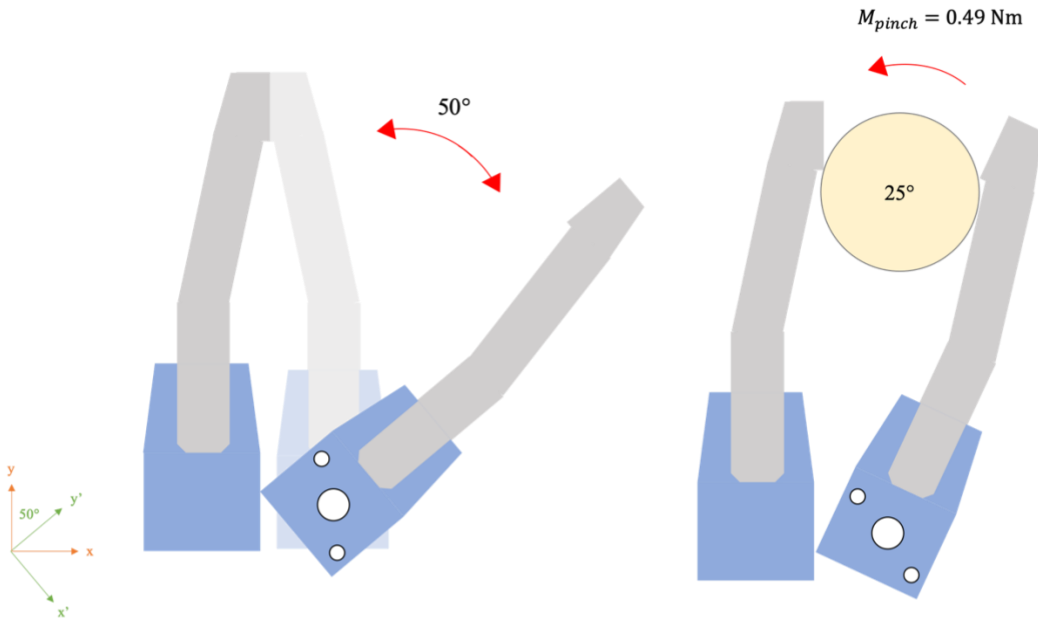

Figure 32. The estimated performance test; (left) open position movement 0 to 50 degrees and back, (right) 25 degrees providing the required pinch force.

All this needs to fit in the dimensions of the Tweezer's base. A 2D representation is sufficient. It is assumed the spring force to be small relative to the input forces of the mechanism and the joint forces to be negligible. Furthermore, static equilibrium is used to get an easy calculation of energy transmission. The force on the slave cylinder is compared per concept.

The piston needs to remain concentrically aligned to prevent leakage or jamming of the piston in the cylinder (Figure 33). Radial loads on the piston are to be nullified. Radial load estimates are compared per concept.

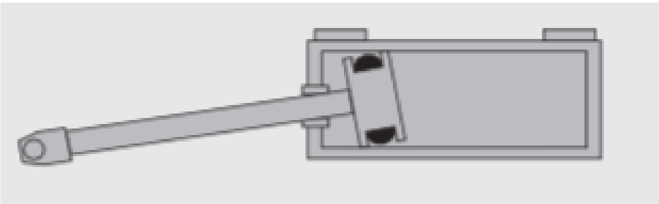

Figure 33. A rod bearing failure of a hydraulic cylinder [82].

For clarification the kinematics of the thumb socket is displayed (Figure 34). The thumb arms are vectors relative to the pivot point $O_T = (0,0)$.

$$r_{T,left}(0°) = \begin{bmatrix} -5.41 \\ 2.6 \end{bmatrix} \quad \& \quad r_{T,right}(0°) = \begin{bmatrix} 4.85 \\ -3.54 \end{bmatrix}$$

The clockwise rotation matrix rotates the thumb arms around a pivot point to acquire all configurations closed to open $\beta = 0 - 50°$.

$$R = \begin{bmatrix} \cos\beta & \sin\beta \\ -\sin\beta & \cos\beta \end{bmatrix} \tag{C.2}$$

$$r_T = R \cdot r_i(0°) \;\; i = left, right$$

All concepts consist of a hydraulic system with annotated variables (Figure 35). Kinematically the cylinders can be modelled as two rods with a prismatic joint (Figure 36). When performing a force analysis on the cylinders the pull cylinders' piston consists of a rod and a head and the push cylinders' piston consists of one part (Figure 37).

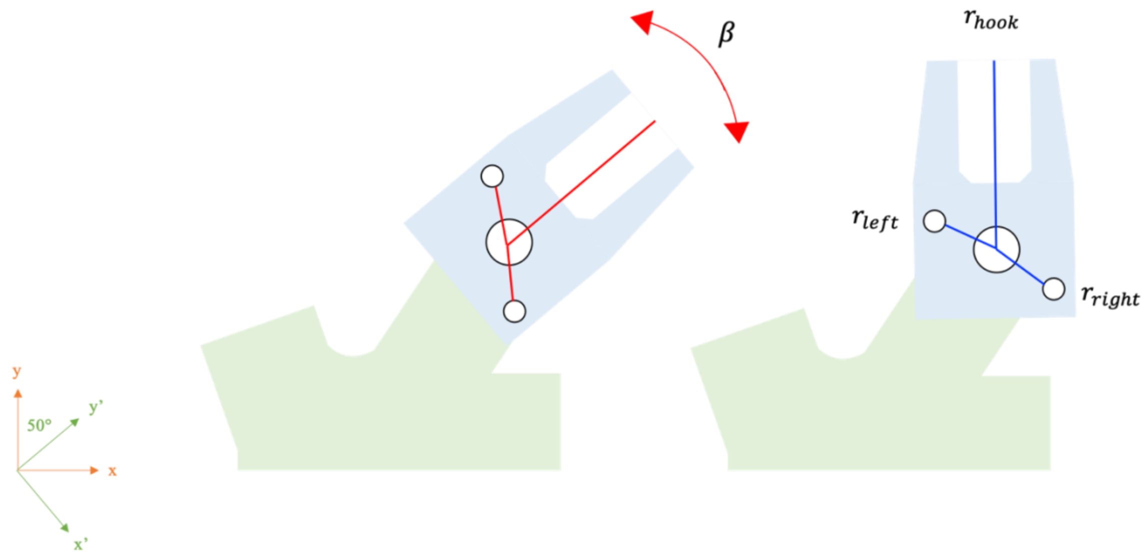

Figure 34. Kinematics of the thumb socket.

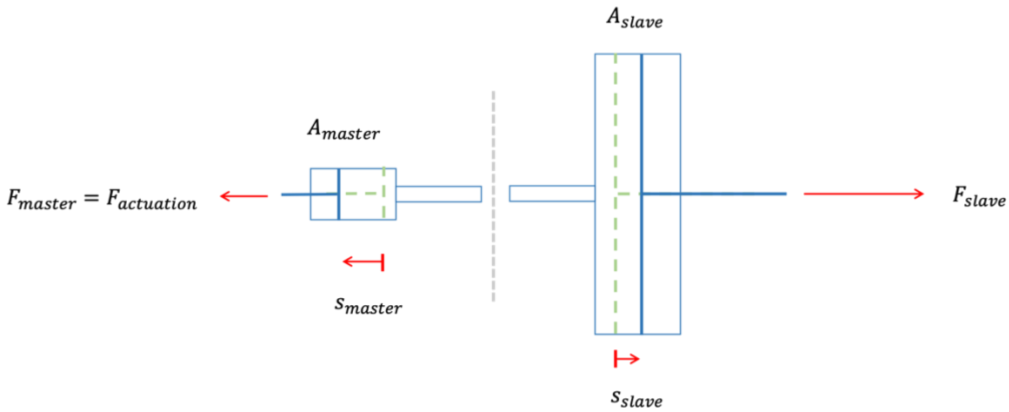

Figure 35. Hydraulic system variables. This example is a pull-push principle.

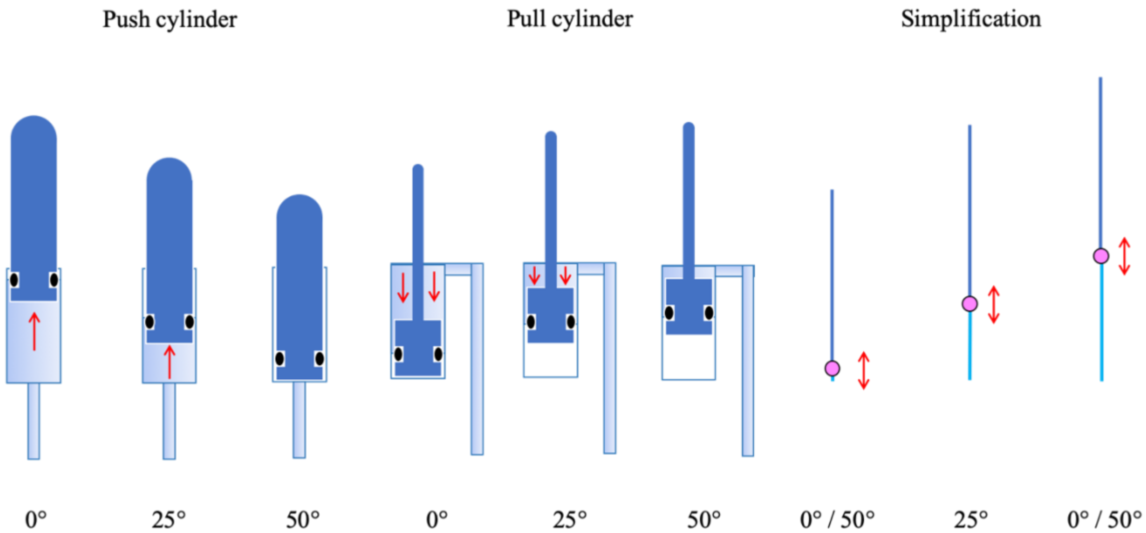

Figure 36. Different configurations of (left) push cylinder, (middle) pull cylinder, (right) cylinder modelled as two rods with prismatic joint

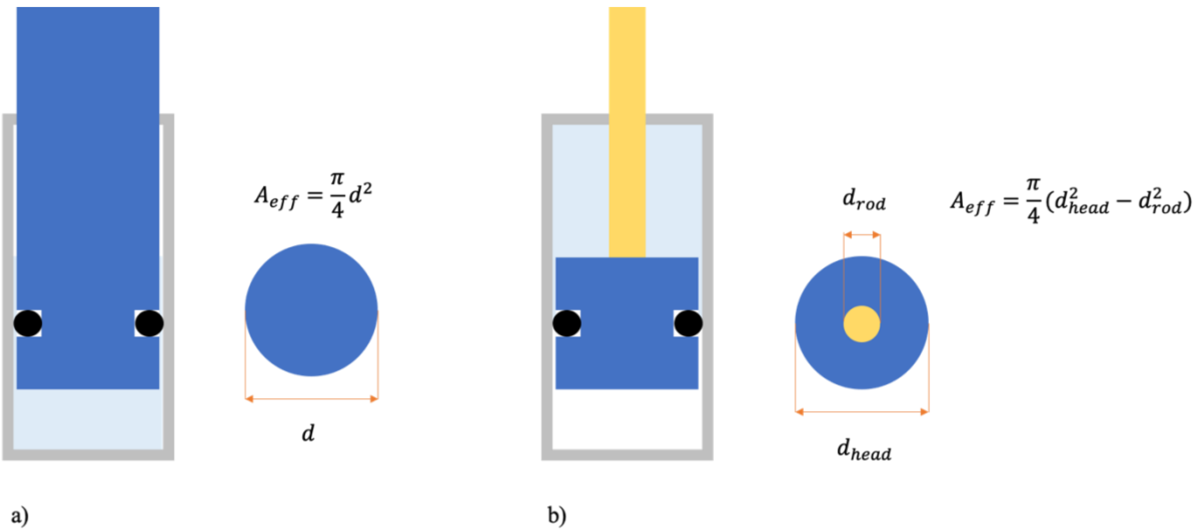

Figure 37. Effective surface of a hydraulic cylinder. a) push cylinder b) pull cylinder.

The effective surface of the push cylinder

$$A_{eff} = \frac{\pi}{4} d^2 \tag{C.3}$$

The effective surface of the pull cylinder

$$A_{eff} = \frac{\pi}{4}\left(d_{head}^2 - d_{rod}^2\right) \tag{C.4}$$

III. Concept Generation

Four concepts have been generated from a combination of the function solutions.

Concept A: Inverse Prehensor

This concept is inspired by the Prehensor [83]. Instead of having a pull input of the cable, it uses a pivoting hydraulic cylinder to push the ternary link upward which, via a connecting rod, closes the Tweezer. The ternary link is a class II lever and provides a mechanical advantage to obtain the required pinch force. At the pinch stage at 25 degrees both forces on the ternary link and thumb socket act perpendicular providing the optimum force. A hydraulic spring is used to preserve an open position.

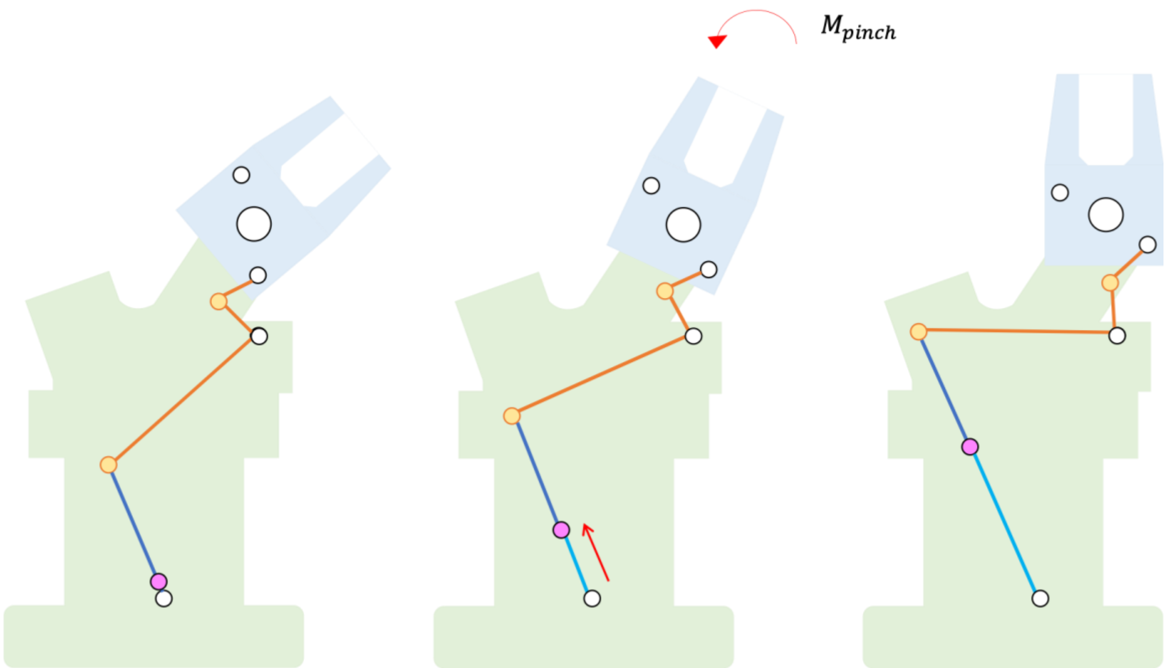

Figure 38. Working principle of Concept A: (left) neutral position, (middle) pinching at 25 degrees, (right) closed position.

A force analysis is done (Figure 39). The relation between the force of the slave cylinder and the pinch force, neglecting the joint force and small spring force, is

$$F_{b2} = \frac{M_{pinch}}{r_T} \tag{C.5}$$

$$F_s = F_{b,2} \cdot \frac{r_{b,2}}{r_{b,1}} \tag{C.6}$$

For performance estimation, the ternary link is scaled from the original technical drawings and thus the arm ratio equals

$$\frac{r_{b,2}}{r_{b,1}} \approx 0.21$$

Solving for the force the slave cylinder needs to exert at 25 degrees.

$$F_s = \frac{r_{b1}}{r_{b2}} \cdot \frac{M_{pinch}}{r_T} = 0.21 \cdot \frac{0.49}{0.006} = 17.5 \text{ N}$$

The needed force will increase due to the angle between the arm r_{b1} and the piston. From the kinematic diagram (Figure 38) the angle is approximated to be 25 degrees on both sides. This means a maximum force change of

$$F_{s,max} = \frac{17.5}{\cos\left(\frac{25\pi}{180}\right)} \approx 19 \text{ N}$$

The radial forces are estimated

$$F_{rad} = \sin\left(\frac{25\pi}{180}\right) \cdot F_{slave,max} \approx 8 \text{ N}$$

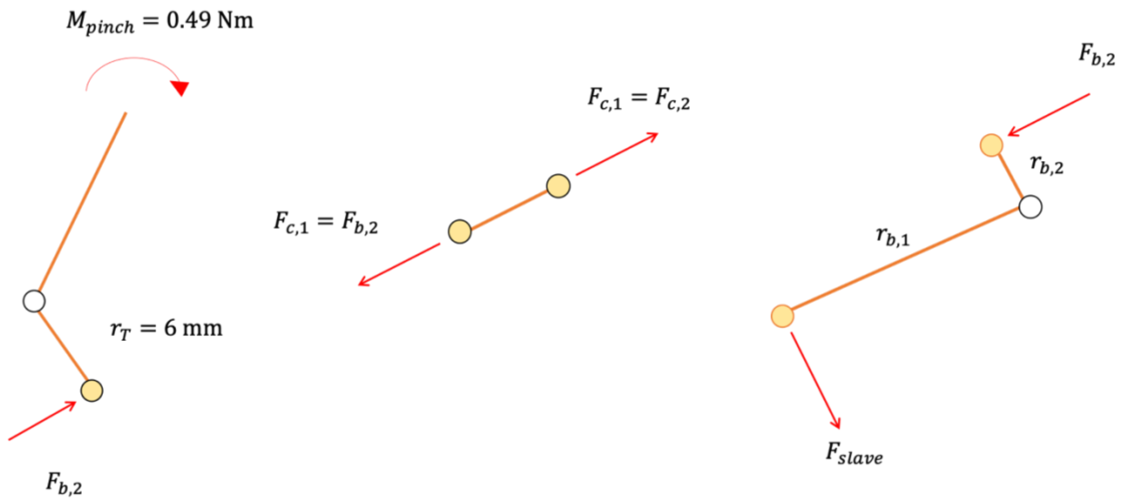

Figure 39: FBD at 25 degrees: (left) thumb socket modeled as ternary link, (middle) connecting rod, (right) ternary link.

A rough approximation of the sketches defines the arm $r_{b1} = 3 \cdot r_T$ and an angular displacement of 50°. The displacement equals the arc length.

$$s_s = \frac{50\pi}{180} \cdot 18 \approx 16 \text{ mm}$$

Concept B: Pulley Cable

This concept uses a cable sliding over a pulley connected to a pulling hydraulic cylinder to close the thumb and guide the force of the slave cylinder to the thumb. This configuration allows perfect alignment of the slave cylinder without radial forces and the highest diameter placing it in the centre. The concept needs a spring returning the thumb to the original position as the cable cannot transfer compressive forces.

All concepts aim to position a perpendicular force on the thumb arm at 25 degrees. Choosing perpendicularity at 25 degrees places the pulley outside the base. The pulley is thus perpendicular at $\beta = 0°$. The concept is illustrated in Figure 41.

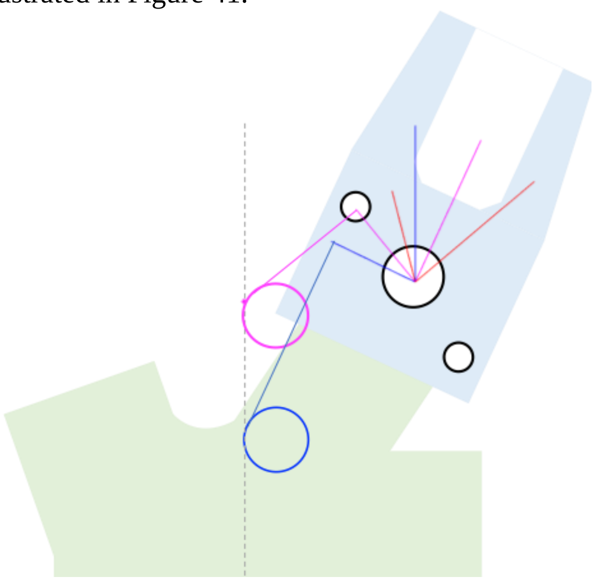
Figure 40. Perpendicularity of the cable: (magenta) pulley at 25 degrees is outside base, (blue) pulley at 0 degrees is inside the base.

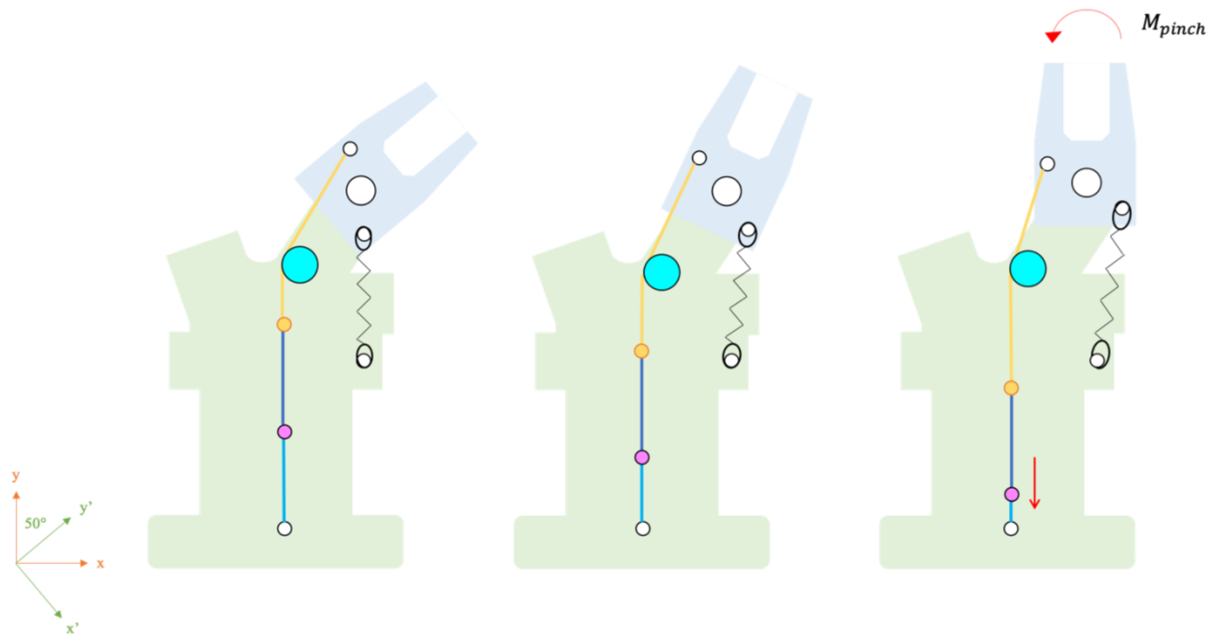

Figure 41. Working principle of Concept B: (left) neutral position, (middle) pinching at 25 degrees, (right) closed position.

The kinematic diagram is given from open to closed (Figure 42). The slave force is derived from the force analysis (Figure 42)

$$F_s = \frac{M_{pinch}}{r_T \cos(\theta)} \tag{C.7}$$

Since at 0 degrees the thumb arm and the cable are perpendicular the maximum angle is found at an open position of the thumb socket and equals 43°. The maximum slave force is 111.5 N (Figure 43).

The displacement of the cable and consequently of the piston is then computed as follows

$$s_s = |u_{50}| - \cos\alpha\, |u_0| = 4.6 \text{ mm} \tag{C.8}$$

Where the angular displacement between the vectors is given as

$$\cos\alpha = \left(\frac{u_0 \cdot u_{50}}{|u_0| \cdot |u_{50}|}\right) \tag{C.9}$$

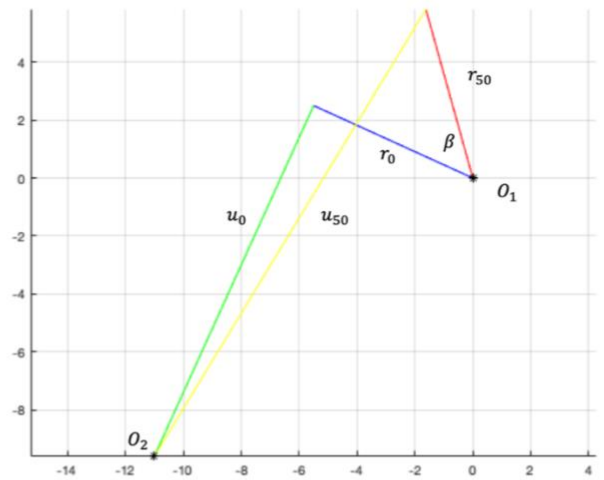

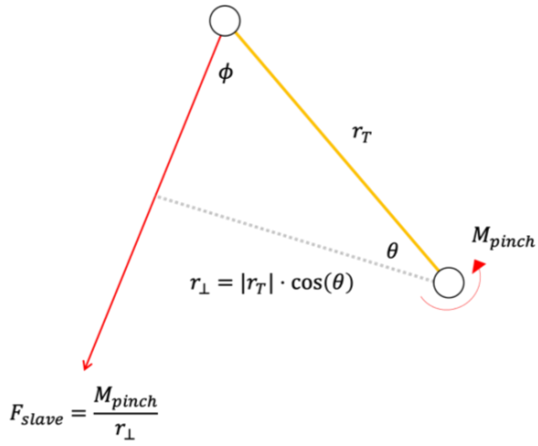

Figure 42. Kinematics of the pulley cable at 0 and 50 degrees (left). Force analysis on thumb socket from pulley cable (right).

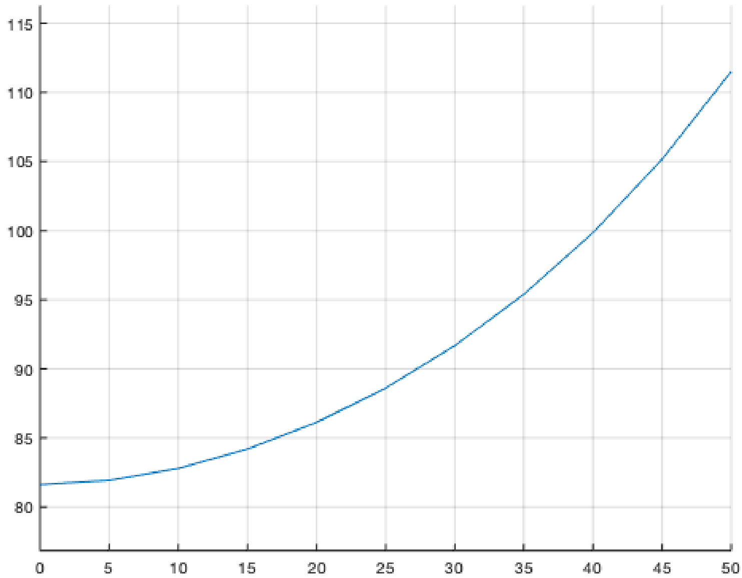

Figure 43. The needed slave force over the thumb angle.

Concept C: Gears

This concept uses gears to move the thumb and exert mechanical advantage. The slave cylinder exerts a pulling force on the lever connected to gear 1. Gear 2 transfers the force to gear 3 which is connected to the thumb socket. As the slave cylinder pulls the gears rotate and consequently the thumb closes. A hydraulic spring is used to preserve an open position.

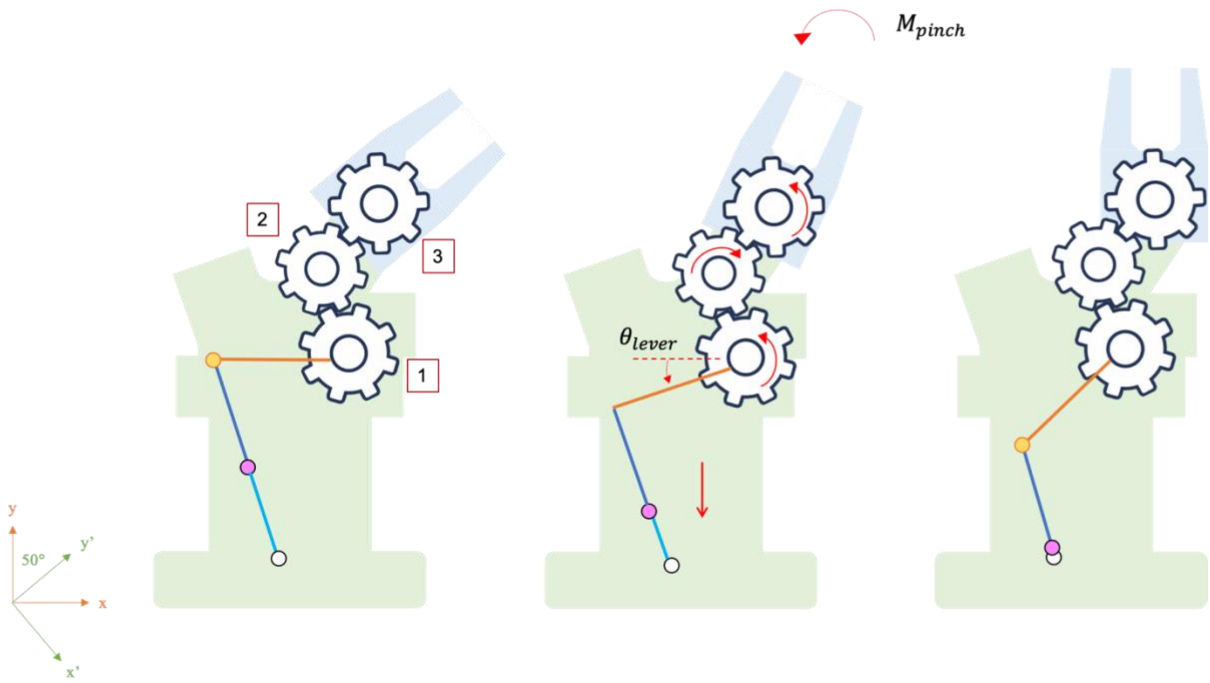

Figure 44. Working principle of Concept C: (left) neutral position, (middle) pinching at 25 degrees, (right) closed position.

The force analysis is analogous to the Pulley & Belt concept. Gear 2 is a guiding gear that merely transfers the force from gear 1 to gear 3.

$$F_{slave} = \frac{r_{gear1}}{r_{lever}} \cdot F_{gear} \tag{C.10}$$

$$F_{gear} = \frac{M_{pinch}}{r_{gear3}} \tag{C.11}$$

$$F_{slave} = \frac{r_{gear1}}{r_{gear3}} \cdot \frac{F_{pinch} \cdot r_{thumb}}{r_{lever}} \tag{C.12}$$

The gear radii and lever length are the parameters but are limited by the base's dimension. The length of the lever is chosen to be 15 mm and the lever movement angle (θ_{lever}) as 25 degrees. Because the tangential velocities on the gear are equal, the gear ratio can be calculated.

$$\frac{r_{gear1}}{r_{gear3}} = \frac{25°}{25°} = 1$$

A lower gear ratio is wanted to generate mechanical advantage. Yet, there exists a trade-off between lever movement angle and gear force amplification. To continue, the moment arm of the thumb is 70 mm. The force in the slave cylinder, with a pinch force of 7 N, can be calculated.

$$F_s = 1 \cdot \frac{7 \cdot 70}{15} = 33 \text{ N}$$

The same rough approximation is done as Concept A.

$$F_{s,max} = \frac{33}{\cos\left(\frac{25\pi}{180}\right)} \approx 36 \text{ N}$$

The radial forces are estimated

$$F_{rad} = \sin\left(\frac{25\pi}{180}\right) \cdot F_{slave,max} \approx 15 \text{ N}$$

And the piston displacement

$$s_s = \frac{50\pi}{180} \cdot 15 \approx 13 \text{ mm}$$

Concept D: Pivoting Push Cylinder

This concept uses a pivoting push cylinder. It uses the piston to directly rotate the thumb socket. The thumb socket is modelled as a ternary link rotating around its pivot thus closing the Tweezer. A hydraulic spring is used to preserve an open position. The needed force by the slave cylinder is calculated using (Figure 46)

$$F_s = \frac{M_{pinch}}{r\cos(\theta)} \tag{C.13}$$

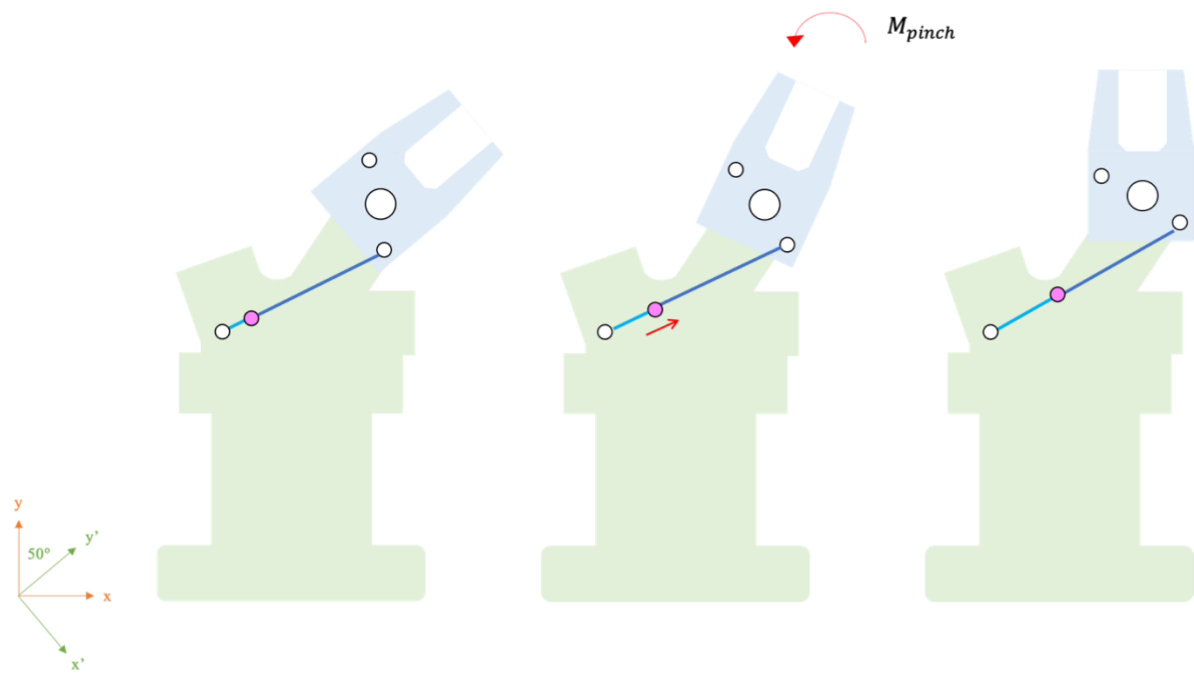

Figure 45. Working principle of Concept D: (left) neutral position, (middle) pinching at 25 degrees, (right) closed position.

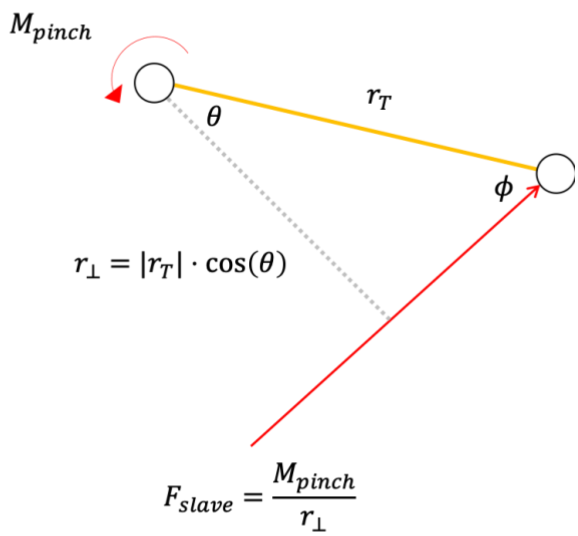

Figure 46. force analysis on thumb socket from the piston

From the kinematic diagram (Figure 47) can be seen that the cylinder barely rotates around its pivot point. Also, the angle between the piston and the thumb arm remains close to 90 degrees. This can be seen in the force plot of the needed slave force (Figure 48). The maximum required slave force $F_{slave,max} = 93$ N. The radial forces on the piston are computed $F_{rad} = \sin\theta \cdot F_{slave}$ with a maximum of $F_{rad,max} = 40.6$ N. The displacement is computed $s_{slave} = 5.1$ mm.

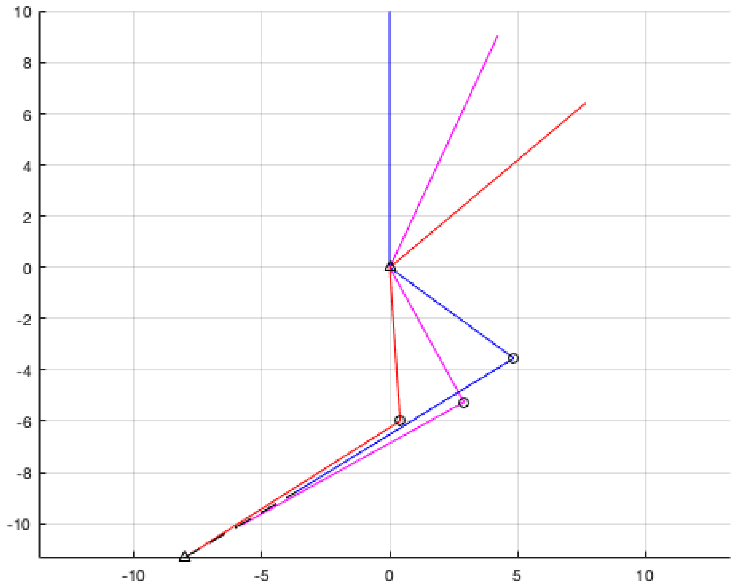

Figure 47. Kinematics of the pivoting push cylinder.

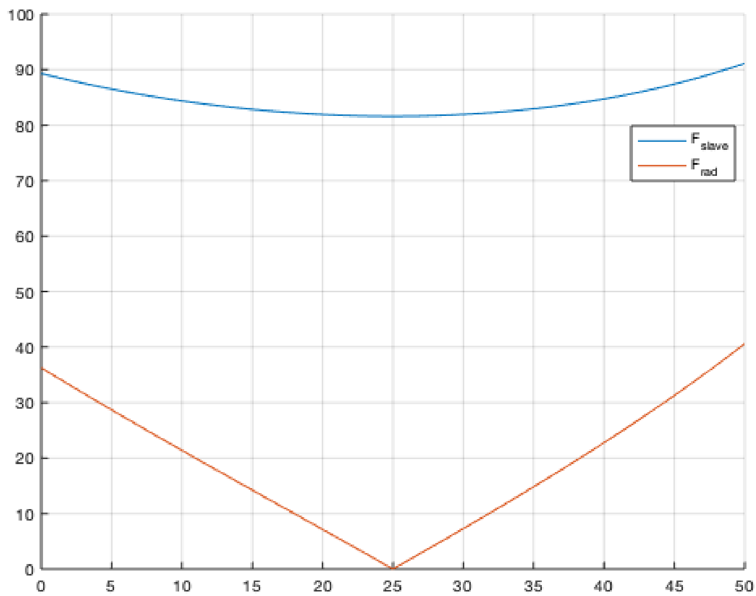

Figure 48. Force analysis of pivoting push cylinder.

D. Concept Selection

This section aims to find the most suitable concept by evaluating over selection criteria in a decision matrix. The most suitable concept(s) are selected for development.

Concept Selection Methodology

To select the most suitable concept the relative comparing method of S. Pugh is used (Table 6) [84]. First, selection criteria are established by which the concepts are evaluated. The concepts are put against the selection criteria in a matrix form. A datum concept is chosen by which the concept as a reference to grade the other concepts relative to the datum. The highest scoring concept is chosen as the new datum and the matrix is rerun until the datum is the most superior concept.

Table 6. Definition of the scoring of the concepts.

Score	Definition
2	Much better than the datum
1	Better than the datum
0	Similar to the datum
-1	Worse than the datum
-2	Much worse than the datum

Selection Criteria

Since concepts are not fully defined designs they cannot be verified against their concepts. independent selection criteria are created, originating from the requirements, to provide an estimation

1. **Life-Cycle Performance:** Reliability is the quality of consistent adequate performance. Robustness and durability are incorporated in this criterion. Durability is the ability to withstand external. Robustness is the quality to perform under non-ideal conditions. Both are measured as life-cycle performance.
2. **Manufacturability**: Manufacturability is designing in such a way that parts are easy to manufacture guaranteeing success in the development stage [85] and profound reduction of product costs [86]. Geometry, material, tolerances and production techniques influence manufacturability.
3. **Performance**: A rough force analysis is carried out to estimate the mechanism's performance. Influencing this criterion are mechanical efficiency and the potential for design optimization. Low piston radial forces, slave cylinder force and slave piston displacement score well. When the slave displacement relative to the master displacement is low higher transmission ratios can be utilized. The low slave force does not need high transmission ratios.
4. **Simplicity**: Simple design encompasses ease in the systems architecture and the interaction of the parts. A simple system is easy to assembly [87] and maintain. The degree of redesigning of neighbouring parts also plays a role.

Concept Evaluation

Each concept is evaluated with respect to the selection criteria.

1. **Life-cycle Performance:** The Pivoting Cylinder scores highest because it uses no additional parts to the hydraulic system. The Gears score low in reliability due to the gears. They are prone to failure when particles come into the system [88]. R. Bos tested several cables in terms of bending endurance for a similar setup and concluded that Dyneema SK99 has the longest fatigue life (Appendix B.4.2, [41]). There exists a trade-off between durability and mechanical efficiency. Dyneema performed far better than steel in durability but has a far lower E-modulus which results

in much elastic energy storage in the cable and consequently energy losses [55]. Moreover, cables have a risk of runoff. The Pulley & Cable scores average. The Inverse Prehensor is based on the Prehensor which is a verified product. Therefore, this concept is estimated to be reliable. Both Pulley & Cable and Gears have a pulling cylinder that needs extra lid closing off the cylinder comparing to the push cylinder. This can cause leakage.

2. **Manufacturability:** The Pivoting Cylinder has no additional parts but requires small cylinders that are challenging to manufacture. The inverse Prehensor requires customized but not complex parts. Gears are bought as standard products but connecting the lever to the gear and integrating a gear to the thumb socket will be a challenge. Pulley & cable and fittings can be standardized parts. J. Cool [89] researched the implementation of a cable pulley system in a hand orthosis which has the same challenge of limited working space. In his example, he concluded the pulley diameter needed to be much larger than the cable diameter to compensate for the bending stiffness relation. Large pulley diameters or curvatures are not possible inside the Tweezer.
3. **Performance:** The performance values per concept are stated in the table below (Table 7). External factors are taken into account. Cable elasticity depends on the thickness of the pulley and designing on a small-scale result in a high elasticity and energy losses. Gears have many parts which decrease efficiency. Radial forces on a push cylinder are less likely to cause jamming or leakage than for pull cylinders and are ranked better. A pull cylinder has a piston with a head and a rod. The rod diameter is small compared to the head to generate a large effective surface. A small rod diameter means a higher chance of bearing failure. The piston of the push cylinder is one part and thus can be modeled as fixed to the cylinder. A relative scoring chart is used to rank the concepts in terms of performance (Table 8).

Table 7. performance values

	Inverse Prehensor	Pulley-Cable	Gears	Pivoting Cylinder
Maximum required slave force (N)	19	111.5	36	93
Radial force (N)	8 (42%)	0	15 (42%)	40.6 (45%)
Piston displacement (mm)	16	4.6	13	5.1

Table 8. relative performance scoring of the concepts

	Inverse Prehensor	Pulley-Cable	Gears	Pivoting Cylinder
Maximum required slave force (N)	4	1	3	2
Radial force (N)	2	4	1	3
Piston displacement (mm)	1	4	2	3
External factors	3	2	1	4
TOTAL	10	11	7	12

4. **Simplicity:** The Pivoting Cylinder is the simplest concept with the least parts. The cable of Concept Pulley & Cable needs to be put on tension. This can be challenging during assembly in a small space. The Concept Gears is complex. It needs 3 gears and a lever that somehow is connected to the gear. Implementing gears requires the redesign of the thumb socket.

The evaluation is put as scores in the Pugh chart. The first iteration held Concept Inverse Prehensor as the datum and resulted in the Pivot Cylinder being the best (Table 9). To ensure a sound decision Concept Inverse Prehensor is held as a datum in the second iteration (Table 10). No concept scored higher this time. The concept the Pivoting Push Cylinder is selected for further development.

Table 9. Pugh chart first iteration with Concept A as datum

	inverse	pulley	gear	pivot

reliability	0	0	-1	+1
manufacturability	0	+1	+1	0
performance	0	+1	-1	+1
simplicity	0	-1	0	+2
TOTAL	0	1	-1	4

Table 10. Pugh chart second iteration with Concept Pivot Cylinder as datum

	inverse	pulley	gear	pivot
reliability	-1	-1	-1	0
manufacturability	0	0	-1	0
performance	-1	-1	-2	0
simplicity	-2	-1	-1	0
TOTAL	-4	-3	-5	0

E. Design Phase

This section describes the evolution from the chosen concept to a physical model i.e. “where meat is put on the bones” [58]. The architecture of the system describes the arrangement of the physical elements to perform the required functions. The derivation of each subsystem is described, and critical elements are verified. The system is implemented in the Tweezer and the final design is presented. During the design phase the mechanical losses are not incorporated. These are derived from the verification.

I. System Architecture

The system starts at the Master Cylinder. The Master Cylinder is located at the harness and transmits the user force to pressure of the fluid. The fluid is guided from the harness to the Tweezer’s base by the Fluid Transfer System to the Pressure Intensifier (PI) living in the Tweezer’s base. The PI is placed inside the base such that high pressure does not need to travel a long distance. The PI intensifies the pressure when active. The pressure is transferred to the Slave Cylinder which transmits it to a force at the piston’s end. The Slave cylinder is connected to the thumb socket and the base by revolute joints. The linear force on the thumb socket is transferred into rotation of the thumb socket closing the thumb and generating a pinch force. The Spring or return system exerts a force on the thumb socket to preserve an open position.

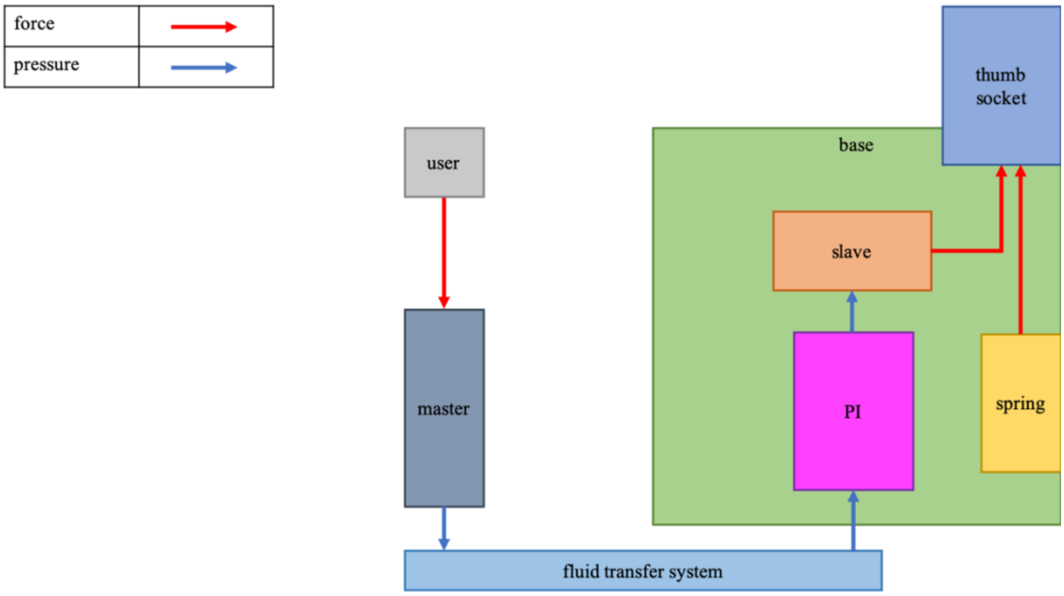

Figure 49. The system architecture of the hydraulic mechanism within the Tweezer.

II. Slave Cylinder

Architecture

The slave assembly consists of a cylinder containing fluid that provides support and smooth sliding for the piston. The piston moves with expanding fluid and transfers pressure into force at the thumb arm axle. The fluid is sealed off by the piston by a stretched O-ring 6x1 and by a cap on the other side. The cap has a fluid entry and is connected to the base acting as a pivot point of the slave assembly. A mechanical stop restricts the piston to surpass the fluid entry and ensures a maximum 50 degrees opening angle of the thumb.

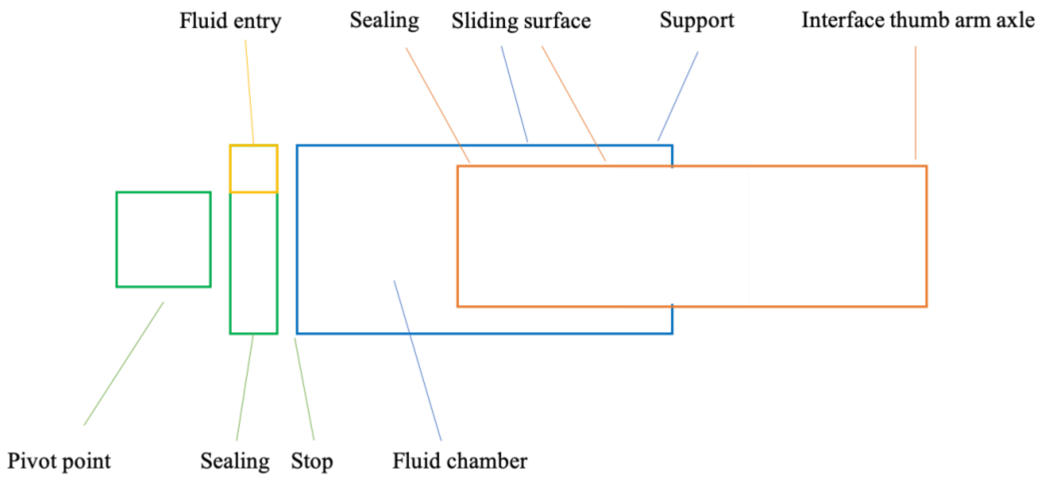

Figure 50. slave assembly architecture

Dimensioning

The dimensions of the slave cylinder are driven by the cylinder's inner diameter. The master and slave diameter are related to each other and to its displacement ratio. The conservation of pressure in a closed hydraulic system relates the diameter ratio of master and slave to the force ratio as

$$p_m = p_s \tag{E.1}$$

$$\frac{d_s^2}{d_{m,head}^2 - d_{m,rod}^2} = \frac{A_s}{A_{m,eff}} = \frac{F_s}{F_m}$$

Since the master cylinder is a pull cylinder the effective diameter needs to be taken to compute the effective surface $A_{m,eff}$ (Figure 37). The inner cylinder diameter equals the head diameter $d_m = d_{m,head}$.

Using Conservation of Energy, the displacement ratio relates to the same force ratio

$$W_m = W_s \tag{E.2}$$

$$\frac{s_m}{s_s} = \frac{F_s}{F_m}$$

The diameters between master and slave relate to the displacements as

$$\frac{d_s^2}{d_{m,head}^2 - d_{m,rod}^2} = \frac{s_m}{s_s} = N \tag{E.3}$$

It is wise to generate a mechanical advantage from master to slave such that the intensification factor of the pressure intensifier remains low. A high factor means a high diameter ratio in the PI which is limited by the same design space and manufacturing possibilities (explained later). Thus $d_s > d_m$ and $s_m > s_s$. From the concept the needed displacement of the slave piston to close the Tweezer is roughly 5 mm. By requirement maximum master displacement is 15 mm. A too small master displacement makes the system too sensitive. 10 mm displacement suits well and has a margin for possible losses. With these displacements the diameter ratio equals $N = 2$.

The diameter of the slave cylinder is constrained in maximum by the design and assembly space inside the base. Tiny slave or master diameters result in manufacturing limitations and inaccuracies. The generated pressure in the master cylinder is related to the slave diameter

$$p_m = \frac{F_m}{A_{m,eff}} = \frac{4NF_m}{\pi d_s^2} \tag{E.4}$$

A small slave cylinder diameter results in higher pressures. Stated before, high pressure requires thicker walls or stronger materials.

It is important the all inner cylinder diameters be a round number. This allows using standard cylinders with known quality and the possibility to ream the hole according to engineering fits [90]. Moreover, a rounded cylinder diameter means a rounded piston diameter to which standard O-rings will fit. It is decided the slave cylinder to have an inner diameter of 8 mm. The master cylinder inner diameter is set to 6 mm. The diameter of the master rod is set small to 2.5 mm. The master piston displacement then equals 11 mm.

The piston's length is a free variable and can be adjusted when the slave cylinder is implemented.

Geometric Model

The dimensions and architecture result in the design (Figure 51).

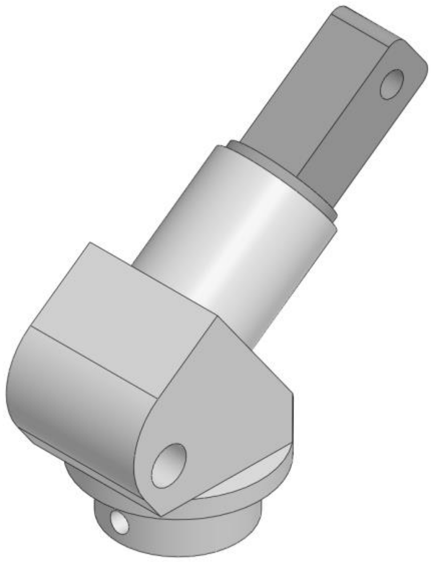

Figure 51. isometric view of the slave cylinder

When the hook closes the fluid in the cylinder expands and moves the piston upwards (Figure 52).

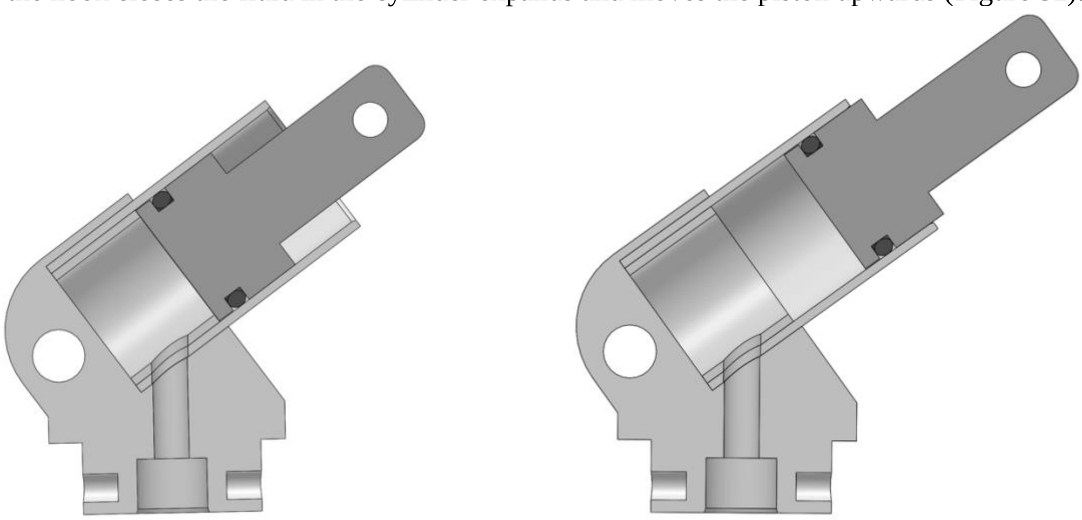

Figure 52. slave cylinder section view: inactive (left), active (right)

Model verification

An empty slave cylinder including the connector to the PI weighs 12 grams. The maximum weight contribution of the fluid is 0.25 gram at a volume with height 5.1 mm and 8 mm in diameter.

Loads are exerted on the piston and the slave cap by the thumb socket and the base respectively. The maximum force equals 97 N which is with $d = 8$ mm rounded off to 2 MPa pressure on the piston and the slave cap. The connector has been simulated being fixated at the hole and subjected to 2 MPa pressure. It is seen that all stresses are far below the yield stress of Stainless Steel (Figure 53).

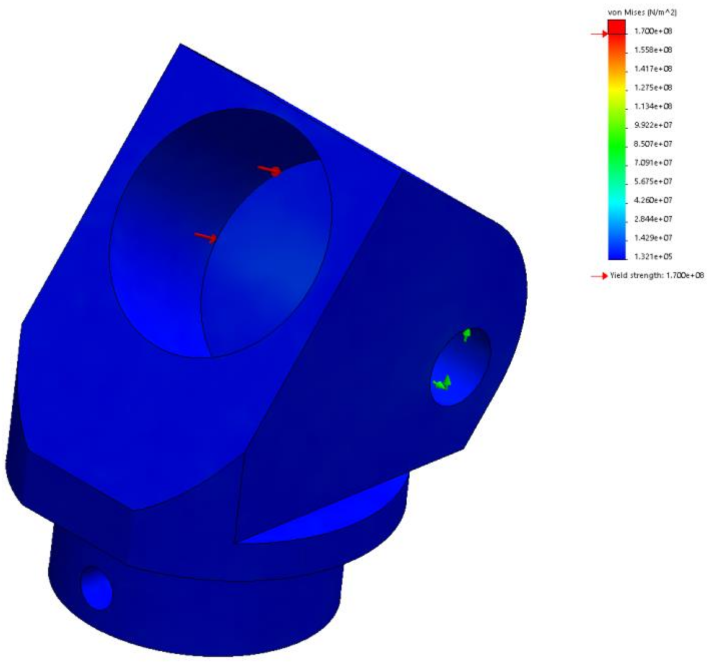

Figure 53. stress test of the connector subjected to a pressure of 2 MPa

The piston act as a revolute joint to the thumb axle. By making the piston completely of PCTFE no bearing is needed. Compared to other plastics PCTFE has high tensile strength and elastic modulus [91]. Simulating the piston, with a pressure of 2 MPa and fixated at the hole, it remains far below the yield stress of 38 MPa (Figure 54).

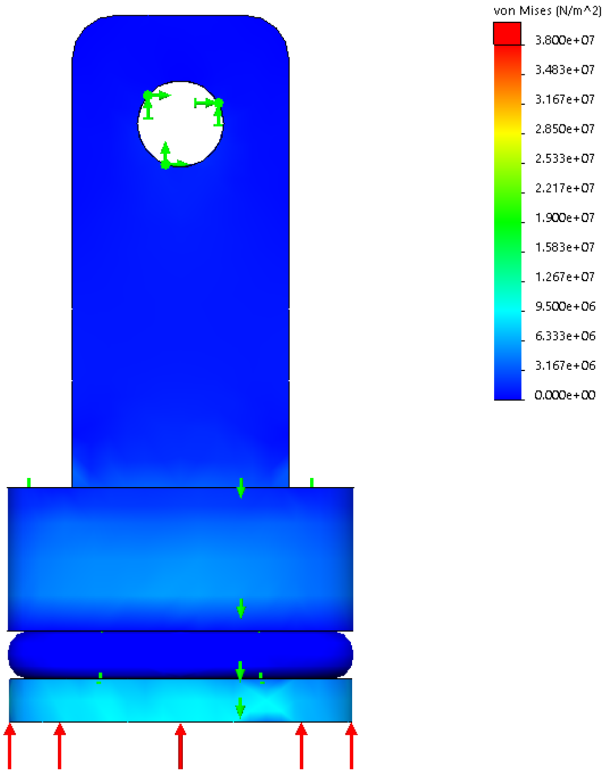

Figure 54. Stress test on the piston subjected to a pressure of 2 MPa with the piston hole fixated.

The cylindrical stresses are calculated. With a wall thickness of 0.5 mm, a pressure of 2 MPa and an inner diameter of 8 mm the hoop stress equals

$$\sigma_\theta = \frac{pd_m}{2t} = \frac{2 \cdot 10^6 \cdot (0.009 - 0.0005)}{2 \cdot 0.0005} = 17 \text{ MPa} \ll \sigma_{y,SS316} \qquad (E.5)$$

Longitudinal stress equals

$$\sigma_l = \frac{pd_m}{4t} = \frac{1}{2}\sigma_\theta = 8.5 \text{ MPa} \ll \sigma_{y,SS316} \qquad (E.6)$$

Both stresses are lower than the yield strength of Stainless Steel which is 290 MPa.

III. Master Cylinder

Architecture

The master assembly is a pulling cylinder. It consists of a cylinder and piston serving the same functions as the slave assembly, but where sealing is performed in the piston head by a stretched O-ring 4x1. A mechanical stop is introduced at piston to restrict the piston surpassing the fluid exit. The cap seals the cylinder by a compressed O-ring 2.5x1 and houses a bush bearing for the piston rod. Force and displacement are transmitted to pressure and movement of the fluid by the interface of the user input at the piston. On the other side a cap closes the cylinder and is connected to the harness.

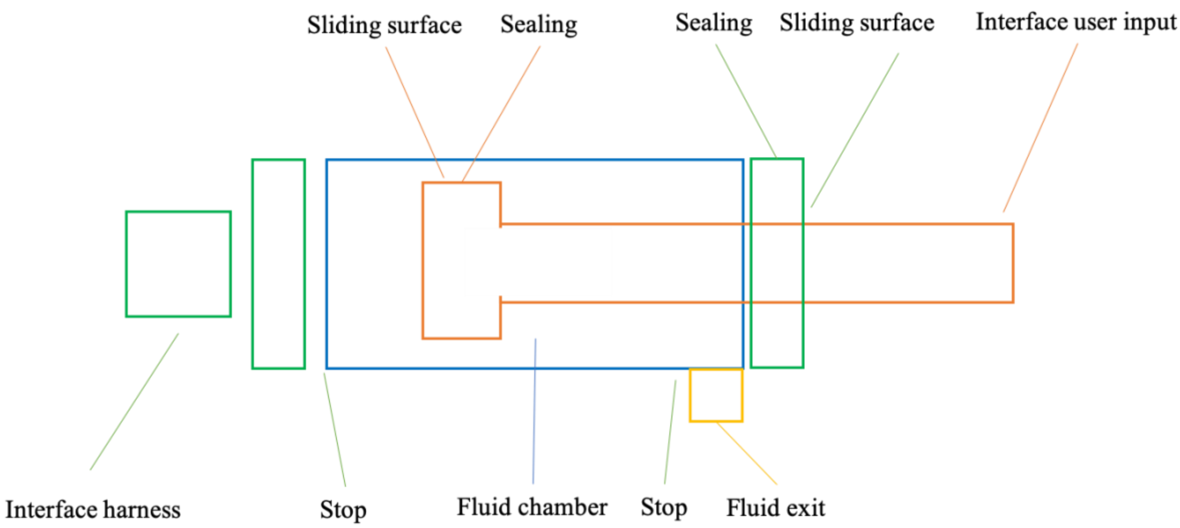

Figure 55. Master assembly architecture.

Dimensioning

The master cylinder is not restricted in space. The inner cylinder has a diameter of 6 mm and length 15 mm equal to the maximum displacement. The diameter of the piston head equals the inner cylinder and the piston rod is 2.5mm to allow tapering for an M2 hex nut.

The cap at the harness needs to have sufficient surface for the glue to remain connected to the cylinder when a force of 32 N applies.

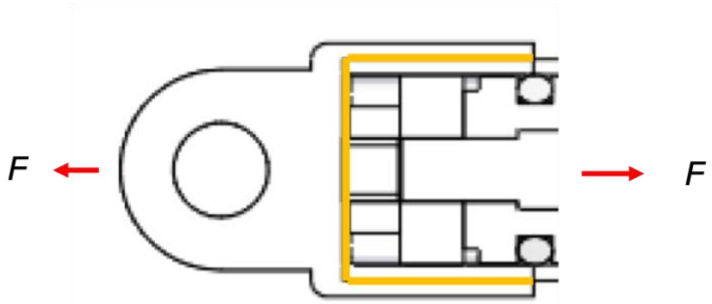

Figure 56. Section view of master cylinder gluing the cap over the cylinder (yellow).

Geometric Model

The figure below displays the master cylinder (Figure 57). By pulling the rod the master cylinder activates and transfers force into pressure.

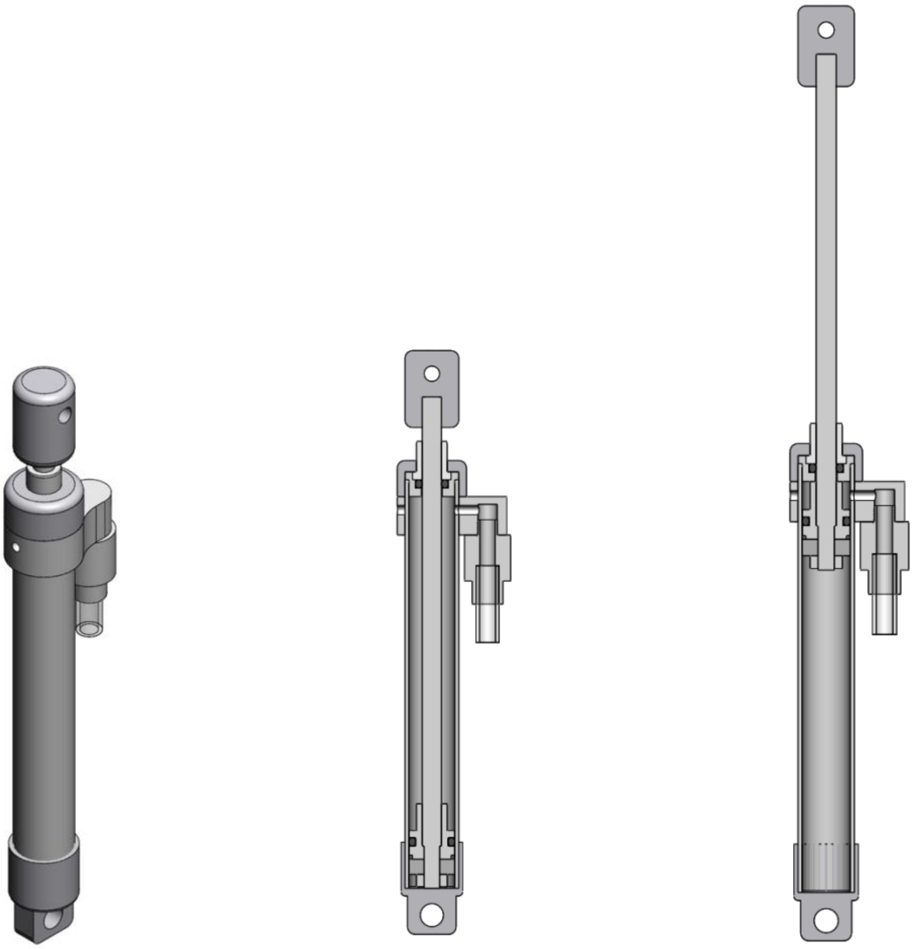

Figure 57. Master cylinder: isometric view (left), section view inactive (middle), section view active (right).

Model verification

An empty cylinder weighs 9 grams. The weight contribution of the fluid is 0.35 gram at a maximum volume with height 15 mm and the effective surface of $\frac{\pi}{4}(0.006^2 - 0.0025^2)$. It has no mass requirement, but a minimized mass is desired.

The cylindrical stresses are calculated. The wall thickness is 0.5 mm, the outer diameter is 7 mm and the maximum pressure is 1.1 MPa. Again, the stresses remain below the yield stress

$$\begin{bmatrix} \sigma_\theta \\ \sigma_l \end{bmatrix} = \begin{bmatrix} 7.2 \\ 3.6 \end{bmatrix} \text{ MPa} \ll \sigma_{y,SSS316} \tag{E.7}$$

IV. Pressure Intensifier

Working Principle

The pressure intensifier is a hydraulic component that intensifies the pressure when a threshold is passed (Figure 58). The system is invented by J. van Frankenhuyzen [49]. At the close stage there is no pinch force and the pressure generated by the master cylinder is sufficient to close the thumb. When an object is encountered and pinched the object exerts a pinch force around the thumb that needs to be satisfied by the slave cylinder. The pressure exceeds the spring force in the large chamber and the piston moves. The system is active. The piston closes the small chamber and due to area difference between the piston head in the large and small chamber the pressure gets intensified.

$$p = \frac{A_l}{A_s} p_m \tag{E.8}$$

The intensification factor is given by

$$I = \frac{A_l}{A_s} = \left(\frac{d_l}{d_s}\right)^2 \tag{E.9}$$

The spring force needs to be verified experimentally. Pressurized air is used to easily adjust the pressure in the air chamber and thus determine the required spring force (Figure 59).

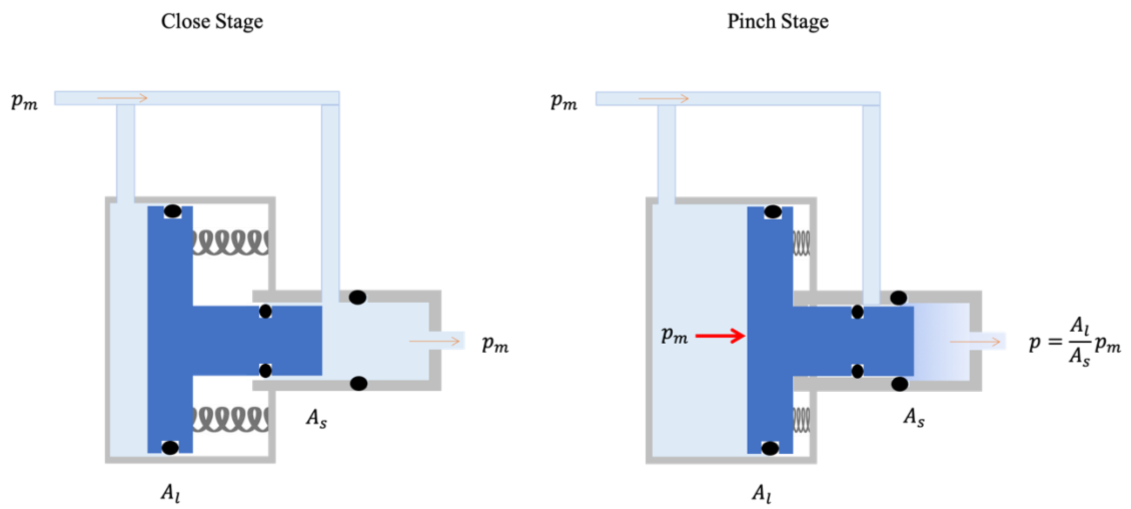

Figure 58. Working principle of the pressure intensifier.

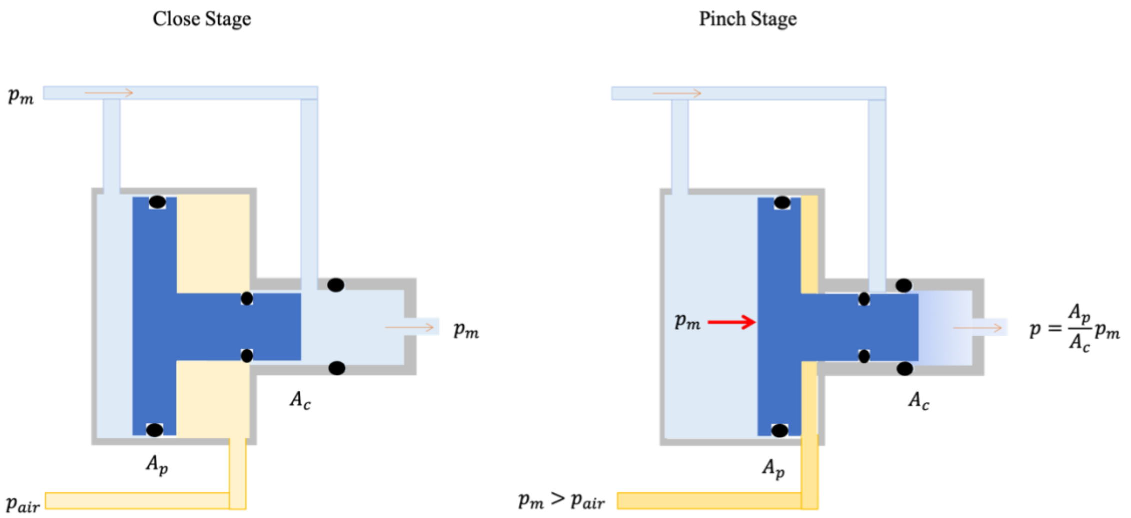

Figure 59. Inserting a channel for pressurized air.

Architecture

The PI consists of two smooth cylinders functioning as a large and small chamber. The large chamber encompasses the fluid and pressurized air. A cap seals the large chamber and provides a fluid entry. There exists a separate entry for the air. The piston is made from PCTFE for smooth sliding in the cylinder. The piston seals the large with a compressed O-ring 10x1 and closes of the small chamber with a stretched O-ring 4x1 when active. Fluid can enter the small chamber. A cap seals the small chamber by a compressed O-ring 6x1 and provides an exit for the fluid. The fluid exit is directly connected with the slave cylinder via a connector.

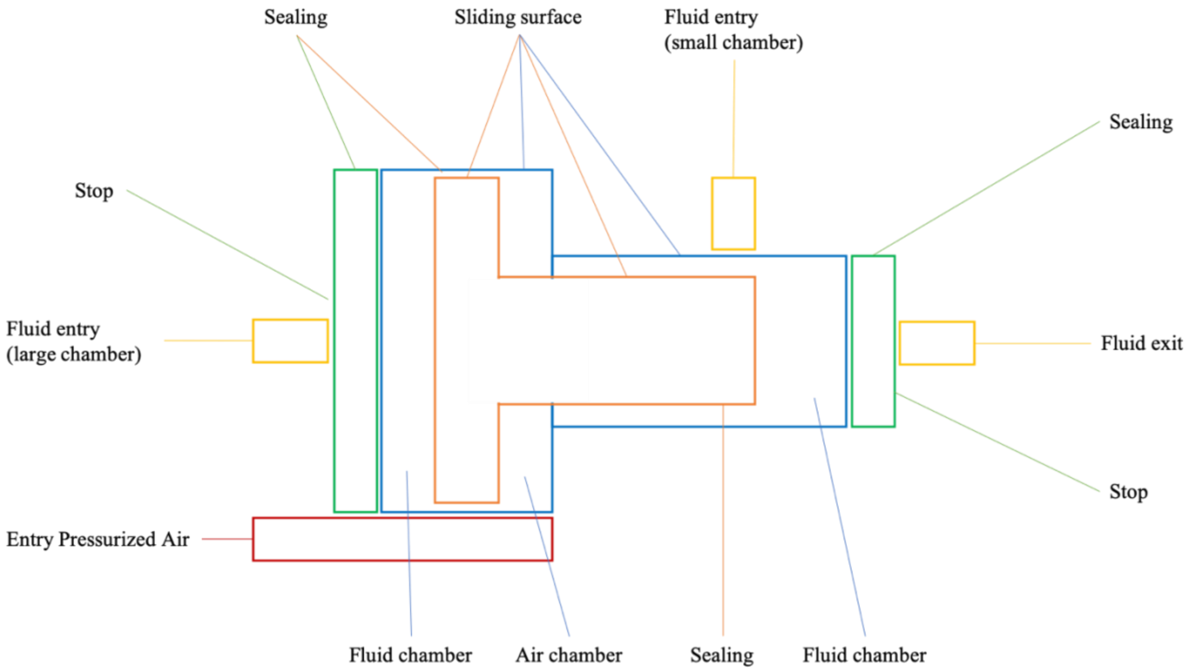

Figure 60. Architecture of the pressure intensifier. For testing the pressurized air chamber is designed.

Dimensioning

The dimension of the pressure is driven by the inner diameter of the chambers. The diameter ratio depends on the intensification factor. The diameters of master and slave have been derived and result in the following pressures

$$p_s = 1.91 \text{ MPa}$$
$$p_{m,grasp} = 1.36 \text{ MPa}$$
$$p_{m,hold} = 0.26 \text{ MPa}$$

The maximum intensification factor is at the hold stage.

$$I_{hold} = \frac{p_s}{p_m} = 7.4$$

The needed diameter ratio between the chambers of the PI

$$\frac{d_l}{d_s} = \sqrt{I_{hold}} = 2.7$$

The PI needs to fit in a tiny space and is therefore designed as small as possible. Using the diameter ratio, the inner diameter of the small chamber is set to 4 mm and the large chamber to 12 mm to account for possible losses.

The fittings have a standard size and do not fit in the tiny space. They are placed on the bottom just outside the base. The fluid is guided by the outer cylinder of the small chamber and large chamber to the fittings.

Geometric Model

The figure below displays the model of the pressure intensifier (Figure 61). In inactive state the piston is at the bottom and the fluid passes the first chamber to the slave. When the PI is active the piston moves upwards by the fluid in the large chamber, closes the small chamber and intensifies the pressure. The fittings are placed at the bottom of the PI because they do not fit in the base's dimension. This requires the fluid to be guided from one part to another to reach the small chamber. To prevent leakage and allow concentric aligning of the hole during assembly a 5 x 2 mm hydraulic hose, PUN-H-2x0.4 [92], is placed in between.

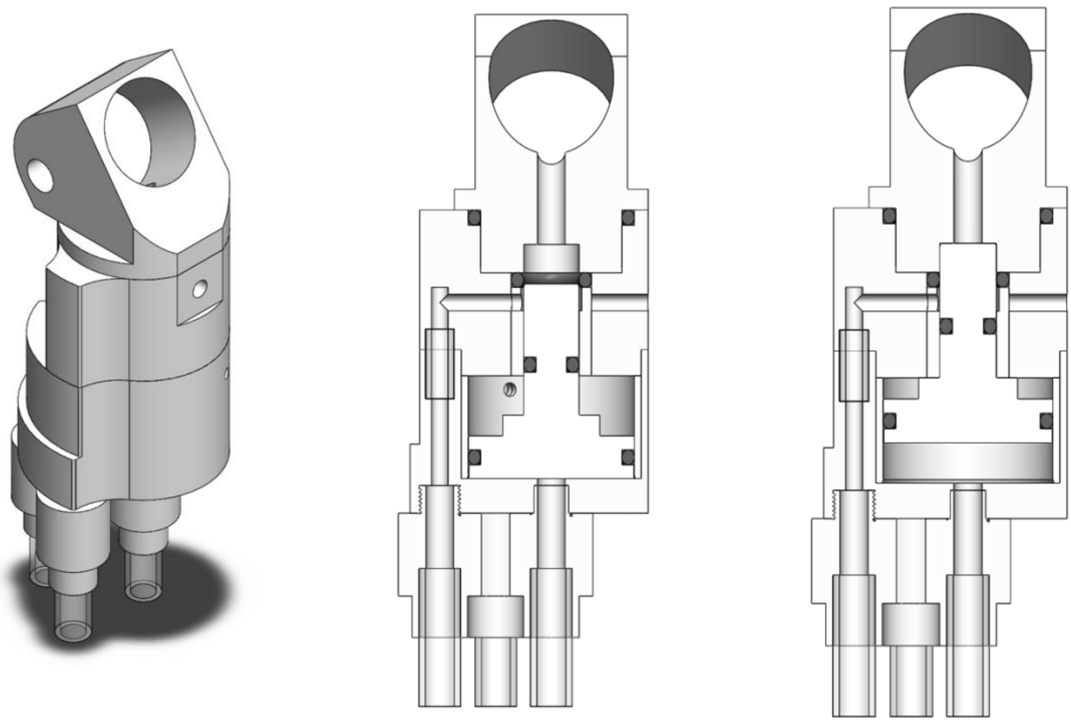

Figure 61. Pressure intensifier (left), section view inactive (middle), section view active (right).

The small chamber is divided into a 6 mm diameter cylinder and a 4 mm diameter cap in which the piston will intensify the pressure. This is done to minimize the chance of the O-ring 6x1 to move through the exit. Just before closing off the chamber high velocity is generated by Bernoulli's principle as the flow area decreases rapidly (Figure 62).

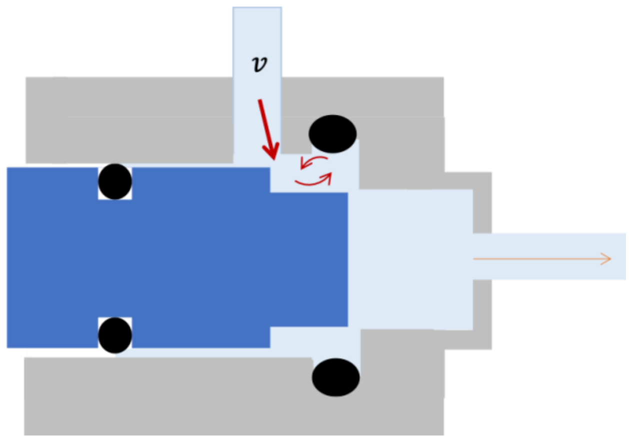

Figure 62. Just before closing off the small chamber high velocity occurs that can cause the O-ring to move. This problem needs to be taken into account during dimensioning of the design.

Model verification

An empty PI, excluding the connector from PI to the slave, weighs 21 grams. The maximum water weight contribution is in the active state 0.34 gram at a volume with height 3.8 mm and diameter 12 mm. The weight contribution of air is in order of nanogram negligible. Combined with the slave the mass equals 33.6 grams. This satisfies the maximum weight requirement of 43 g.

The cylindrical stresses are calculated. At the large chamber the wall thickness is 0.5 mm, the outer diameter 13 mm and maximum pressure is 1.1 MPa.

$$\sigma_{large} = \begin{bmatrix} \sigma_\theta \\ \sigma_l \end{bmatrix} = \begin{bmatrix} 14 \\ 7 \end{bmatrix} \text{ MPa} \ll \sigma_{y,SS316}$$

At the large chamber the wall thickness is 0.5 mm, the outer diameter 7 mm and maximum pressure is 2 MPa.

$$\sigma_{small} = \begin{bmatrix} \sigma_\theta \\ \sigma_l \end{bmatrix} = \begin{bmatrix} 13 \\ 6.5 \end{bmatrix} \text{ MPa} \ll \sigma_{y,SS316}$$

The stresses in the duct are even lower because of the mean diameters. All stresses remain below the yield stress.

V. Implementation in the Tweezer

Position of the slave cylinder

In the concept phase the slave cylinder was placed perpendicular to a thumb angle of 25 degrees. When assigning a body to the slave cylinder it is seen the dimensions exceed the base's dimension (Figure 63).

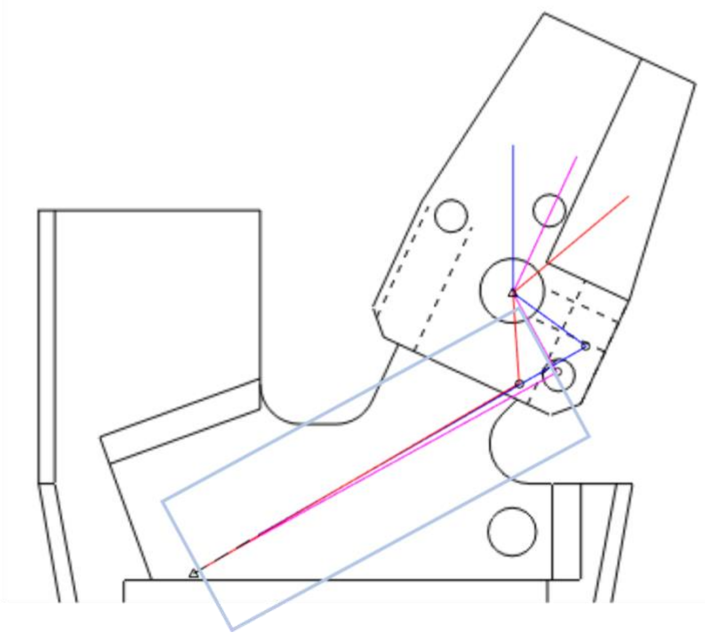

Figure 63. A right section view of Tweezer with slave cylinder (9 x 25mm) perpendicular to a thumb opening of 25 deg (pink) exceeds the design space.

Iteratively, it is chosen to place the slave cylinder perpendicular to a thumb opening of 19 degrees (Figure 64). The angle (ϕ) between slave and the thumb moment arm (r_T) now has a maximum of 123° when the hook is fully open. The maximum required force by the slave equals 97 N.

$$F_s = \frac{M_{pinch}}{r_T \cos(\phi - 90°)} \tag{E. 10}$$

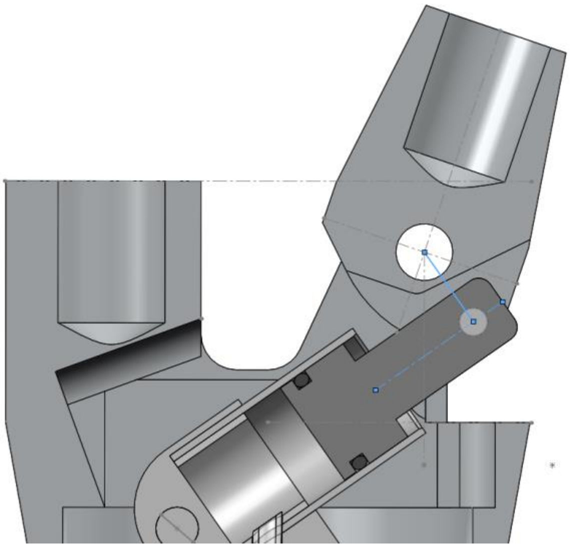

Figure 64. Perpendicularity between the slave cylinder the thumb arm at 19 deg (green line)

At 19 degrees the forces on the slave cylinder are still satisfactory with a slightly increased maximum needed force of 97 N. The slave cylinder pivots on an axle with length 31.5 mm and diameter 3 mm. The maximum force on the axle equals the maximum force induced by the slave cylinder which is at a thumb angle of 50 degrees (Figure 65).

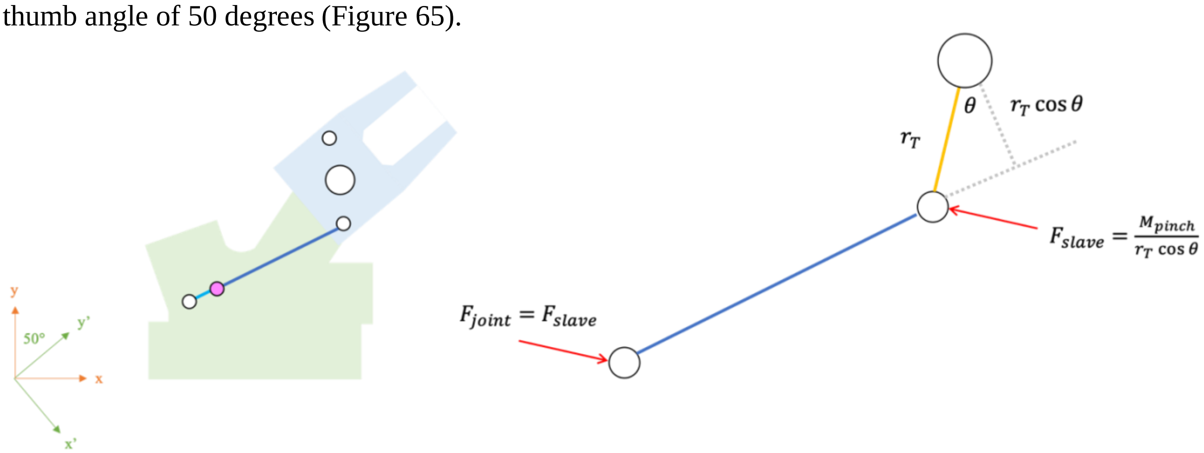

Figure 65. Free body diagram of the slave cylinder analysing the joint force at 50 deg

During closure the slave cylinder pivots with only 2.7 degrees. The pivot axle connected to the base does not need a bearing element and thus has the same diameter as the hole of the connector. The connector is as wide as possible to have the 97 N load distributed over 11 mm to minimize stresses. The axle will not yield, and the displacement is negligible (Figure 66).

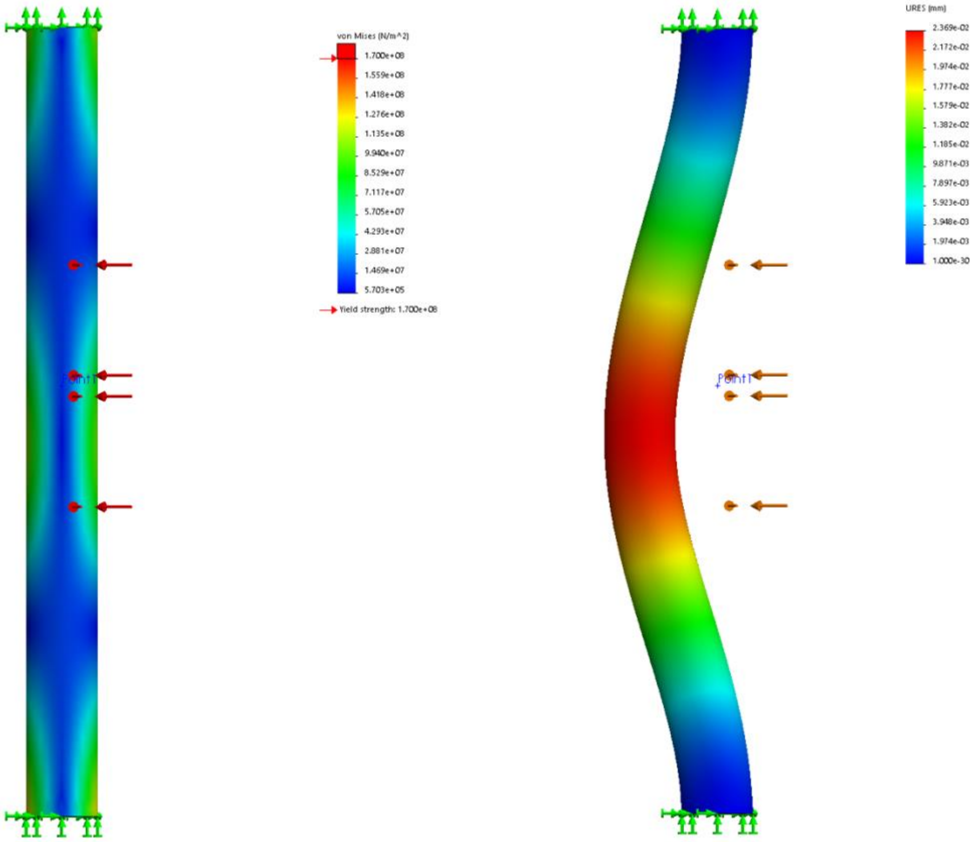

Figure 66. Subjecting the pivot axle to a 100 N distributed load over 11mm: von Mises stress (left), displacement (right)

Since the pressure intensifier is directly connected to the slave cylinder the horizontal position relative to the thumb needs to be chosen such that the pressure intensifier is in the center to allow maximum design space (Figure 67).

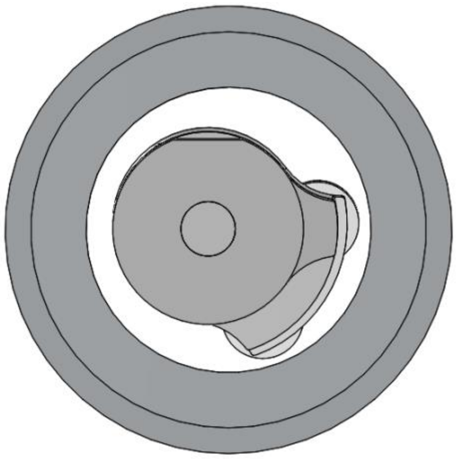

Figure 67. Top section view Tweezer's base with pressure intensifier in the centre.

This results in a total length, from the connection of the slave cap to piston plus the displacement at 19 degrees, of 25.4 mm. The position of the joint thus has been determined (Figure 68).

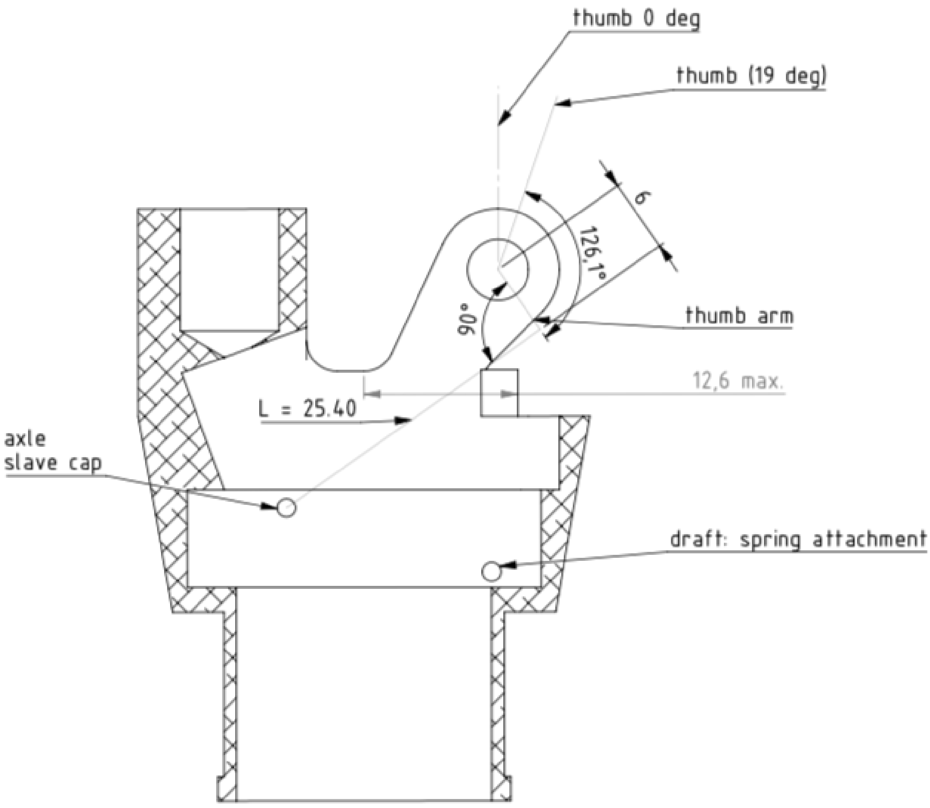

Figure 68. A right section view Tweezer's base with the position of the pivot axle. Perpendicularity of the slave cylinder at 19 degrees and allowing a centre position of the PI result in the position of the pivot axle.

Adjusting the Thumb Socket

The Prehensor required connection at the thumb socket at both sides. The Tweezer only at one. This allows for a larger space to connect the slave piston. Material has been removed to avoid interference between piston and thumb socket. An axle is placed at the thumb arm hole to connect the piston and the spring system.

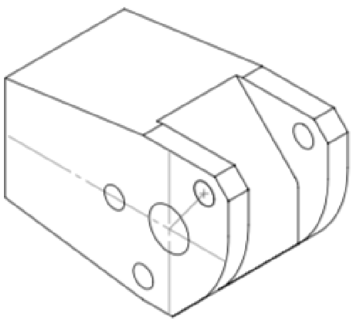

Figure 69. The new thumb socket

Adjusting the Base

Adjustments have been made to the base. The thumb angle is restricted by the mechanical stop in the slave cylinder. To make the system more robust mechanical stops are introduced at the base that blocks the thumb socket exceeding 50 degrees when the system is subjected to non-ideal conditions. Material is removed to eliminate the interferences of the slave cylinder with the base. An axle is inserted for connection of the slave cylinder. The spring is connected to the base.

VI. Spring System

A spring system, attached to the thumb arm axle, needs to preserve an open thumb position when external forces on the system are absent. The spring is placed outside the hydraulic system for easier verification, assembly and maintenance.

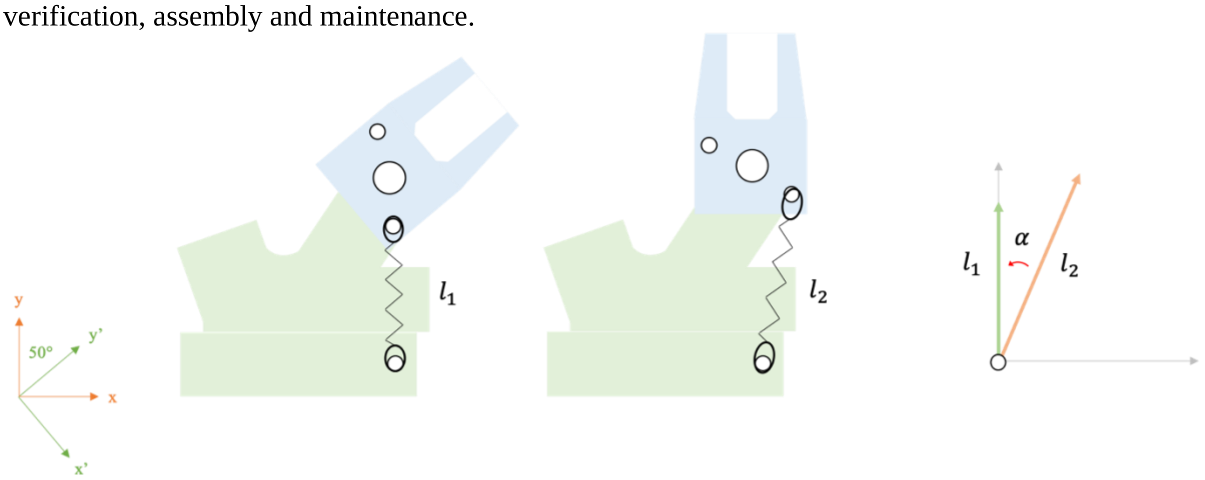

Figure 70. Spring displacement

Assumed is that the spring will only have a planar displacement. The extension spring is attached to the base around which it can rotate freely. The spring therefore only deforms in the axial direction (Figure 70). The attachment as origin the vectors l_1 and l_2 represent the spring in undeformed, open position and deformed, closed position respectively. The spring needs to be placed below the position of the thumb arm hole at open position to ensure elongation at all other angles.

The undeformed length vector $\overrightarrow{l_1}$ is placed vertical to the thumb arm at 50 degrees $\vec{r}_{T,50}$ and is with an undeformed length l_0

$$\overrightarrow{l_1} = \begin{bmatrix} 0 \\ l_0 \end{bmatrix} \tag{E.12}$$

The undeformed length vector $\overrightarrow{l_2}$ equals $\overrightarrow{l_1}$ plus the change of the thumb arm from open to closed position

$$\overrightarrow{l_2} = \begin{bmatrix} 0 \\ l_0 \end{bmatrix} + \vec{r}_{T,0} - \vec{r}_{T,50} \tag{E.13}$$

The deformation can be calculated.

$$\Delta l = |l_1| - \cos\alpha\,|l_2|$$

The elongation does not depend on the undeformed length l_0 but equals $|\vec{r}_{T,0} - \vec{r}_{T,50}| = 2.45$ mm

The angular displacement is given by the angle between the vectors and does depend on l_0

$$\cos\alpha = \left(\frac{l_1 \cdot l_2}{|l_1| \cdot |l_2|}\right) \tag{E.15}$$

The spring's stiffness is determined by the elongation and the spring energy.

$$k = \frac{2E_s}{\Delta l^2} \tag{E.16}$$

The spring stiffness needs to be high enough to return the thumb back from closed to open position. A high stiffness opens the hook faster but also increases the needed actuation force. The desired spring element stiffness will be determined experimentally.

There is very little space of 1 mm between the thumb arm axle and the footing of the spring. A stretched O-ring fits around the axle and to the base. The pre-tension and position are determined later. A small O-ring with a given deformation means percentual large elongation to which there is a limit to break at 250% of its normal length.

F. Development

This section describes the physical birth of the design. The manufacturing choices of the prototype are derived, and the prototype is presented.

I. Manufacturing

Material choice

Parts subjected to hydraulic fluid are made from stainless steel for its corrosion resistance. Sliding parts are made from Polychlorotrifluoroethylene **(**PCTFE). PCTFE does not absorb water and has high strength [48]. Outside parts are made from Aluminium 7075. Parts that come in contact with water are made of Stainless Steel 316. All materials are possible to be machined.

Tolerances

Tolerances in miniature hydraulics are crucial for the prevention of leakage and smooth operation. Parts that need smooth sliding, e.g. piston and cylinder, require an engineering fit tolerance. The sliding fit H7/h7 is chosen which allows accurate location and free movement, including turning [90] [93]. The PI intensifier large and small chamber parts need very precise alignment for the piston. The PI piston floats and makes only contact to the cylinders by the O-rings. Not indicated tolerances are according to ISO2768 [94].

Manufacturing techniques

Always aim for standardized components for economic advantages and known quality. The cylinders are capillary tubes of sizes 6, 8 and 12 mm [95] and are sawn to the correct size. Customized parts are manufactured by milling and turning because of material choice and narrow tolerances possibilities.

O-ring groove

The O-ring is either stretched or compressed (Figure 71). It is fitted with a groove width of $1.1d_s$ and a squeeze of $8\% \pm 2\%\ d_s$ at either side [96]. In practice, $10\%\ d_s$ is sufficient and allows easier manufacturing. The O-rings are lubricated with ROCOL Kilopoise 0001.

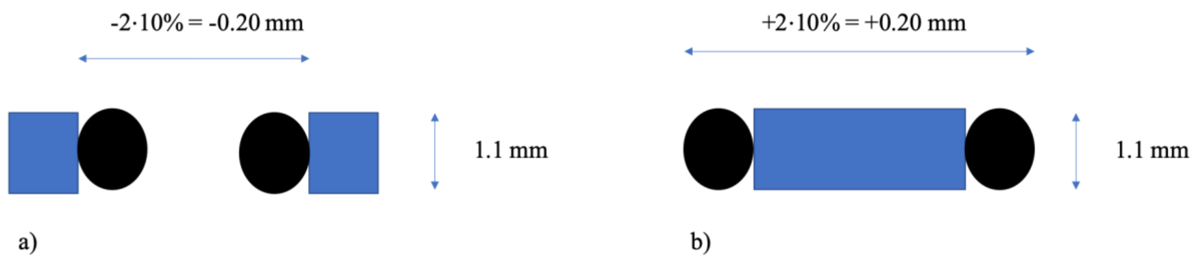

Figure 71. fitting of an O-ring with 1 mm section width a) compressed b) stretched

II. Assembly

Loctite 648 [44] is used to glue the surfaces together and prevent leakage. When gluing it is important that the glue escapes outwards. Any glue inside the cylinder might cause closing of waterways or gluing of sliding parts. Stainless steel has no an active surface. Cleaning on water bases (Ultra Clean Innotec

[97]), polishing the surface with very fine sandpaper and activating the surface using Loctite 7649 activator [98] is important for the glue to work.

III. Prototype

Below the prototype is presented. The master cylinder and its parts (Figure 72) and the PI with the slave cylinder (Figure 73).

Figure 72. master cylinder (left) parts, (right) assembled

Figure 73. (top-left) parts of the slave cylinder, (top-right) assembled PI and slave, (bottom) parts of the PI

Nomenclature

Body-Powered (Prostheses) (BP / BPP), actuation type of prosthesis by means of muscular energy

Electric-Powered (Prostheses) (EP / EPP), actuation type of prosthesis by means of electric energy

Finger, the stationary hook of the split-hook

Hydraulic Tweezer, HT, the voluntary closing version of the WILMER Prehensor with a hydraulic mechanism

Pressure Intensifier (PI), a hydraulic subsystem that can intensify the pressure to generate higher pinch forces

Simplified Version, SV, the prototype that is tested consisting of a connecting element between the base and the slave cylinder without the PI element

Split-Hook, the terminal device of a hook prosthetic consisting of two hooks where one moves towards the other

Thumb, the moveable hook of the split-hook

Voluntary-Closing (VC), operation principle that has an open terminal device in neutral position and that closes the terminal device upon actuation

Voluntary-Opening (VO), operation principle that has a closed terminal device in neutral position and that opens the terminal device upon actuation

WILMER Prehensor, a cosmetic appealing voluntary-opening split-hook prosthetic

WILMER Tweezer, the voluntary-closing version of the WILMER Prehensor

List of Figures

List of Tables

Bibliography

[1] K. Ziegler-Graham, E. MacKenzie, P. Ephraim, T. Travison and R. Brookmeyer, “Estimating the Prevalence of Limb Loss in the United States: 2005 to 2050,” *Arch Phys Med Rehabil.*, pp. 422-9, 2008.

[2] E. Biddiss and T. Chau, “Upper-Limb Prosthetics: Critical Factors in Device Abandonment,” *American Journal of Physical Medicine & Rehabilitation*, vol. 86, no. 12, pp. 977-987, 2007.

[3] M. Egermann, P. Kasten and M. Thomsen, “Myoelectric hand prostheses in very young children,” *Int Orthop.*, vol. 33, no. 4, pp. 1101-1105, 2009.

[4] K. Ostlie, I. Lesjo, R. Franklin, B. Garfelt, O. Skjeldal and P. Magnus, “Prosthesis rejection in acquired major upper-limb amputees: a population-based survey,” *Disability Rehabilition Assistive Technology*, vol. 7, no. 4, pp. 294-303, 2012.

[5] H. Silcox, M. Rooks, R. Vogel and L. Fleming, “Myoelectric prostheses. A long-term follow-up and a study of use of alternate prostheses,” *J Bone Joint Surg A.*, vol. 75, no. 12, pp. 1781-1789, 1993.

[6] D. H. Plettenburg, “Basic requirements for upper extremity prostheses: the WILMER approach,” in *20th Annual International Conference of the IEEE Engineering in Medicine and Biology Society*, 1998.

[7] E. Biddiss, D. Beaton and T. Chau, “Consumer design priorities for upper limb prosthetics,” *Disability and Rehabilitation: Assistive Technology*, pp. 346-357, 2007.

[8] C. Pylatiuk, S. Schulz and L. Doderlein, “Results of an internet survey of myoelectric prosthetic hand users,” *Prosthetics and Orthotics International*, vol. 31, no. 4, pp. 362-370, 2007.

[9] L. Wagner, A. Bagley and M. James, “Reasons for prosthetic rejection by children with unilateral congenital transverse forearm total deficiency,” *Journal of Prosthetics and Orthotics*, vol. 19, no. 2, pp. 51-54, 2007.

[10] F. Routhier, C. Vincent and M. Morissette, “Clinical results of an investigation of paediatric upper limb myoelectric prosthesis fitting at the Quebec Rehabilitation Institute.,” *Prosthetics & Orthotics International*, vol. 25, no. 2, p. 119–131, 2001.

[11] J. Cool, “Technical answers to a medical question (in Dutch),” in *Congresreport of Boerhaavecursus about rehabilitation medicine*, Noordwijkerhout, 1984.

[12] C. Pylatiuk, S. Schulz, A. Kargov and G. Bretthauer, “Two Multiarticulated Hydraulic Hand Prostheses,” *Artificial Organs*, vol. 28, no. 11, pp. 980-986, 2004.

[13] T. Lauren, I. Michelle, P. Pat, B. Chris, S.-W. Lisa, D. Conyers, M. John and R. Tiffany, “A narrative review: current upper limb prosthetic options and design,” *Disability and Rehabilitation: Assistive Technology*, 2019.

[14] S. L. Carey, D. J. Lura and M. J. Highsmith, “Differences in myoelectric and body-powered upper-limb prostheses - Systematic literature review,” *The Journal of Rehabilitation Research and Development*, vol. 52, no. 3, pp. 247-262, 2015.

[15] E. Biddiss and J. Andrysek, “Upper and Lower Extremity Prosthetics for Children and Youth,” in *Paediatric Rehabilitation Engineering: From Disability to Possibility*, CRC Press, 2011, p. 206.

[16] B. Peerdeman, G. Smit, S. Stramigioli, D. Plettenburg and S. Misra, “Evaluation of Pneumatic Cylinder Actuators for Hand Prostheses,” in *The Fourth IEEE RAS/EMBS International Conference on Biomedical Robotics and Biomechatronics*, Rome, Italy, 2012.

[17] G. Smit, D. H. Plettenburg and F. C. v. d. Helm, “The lightweight Delft Cylinder Hand, the first multi-articulating hand that meets the basic user requirements,” *IEEE Transactions on Neural Systems and Rehabilitation Engineering* , vol. 23, no. 3, pp. 431-440, 2015.

[18] D. H. Plettenburg, Upper extremity prosthetics : current status & evaluation, Delft: VSSD, 2006.

[19] S. Landberger and J. Shaperman, “Child prosthetic hand design: no small challenge,” in *Wescon Conference,* Anaheim, CA, USA, 1996.

[20] G. Smit and D. H. Plettenburg, “Efficiency of voluntary closing hand and hook prostheses,” *SAGE Journals,* vol. 34, no. 4, pp. 411-427, 2010.

[21] D. Plettenburg, “The WILMER Appealing Prehensor,” *Journal of Prosthetics and Orthotics,* p. 43–45, 2006.

[22] C. Taylor, “The Biomechanics of Control in Upper-Extremity Prostheses,” *Artificial Limbs,* pp. 4-25, 1955.

[23] D. H. Plettenburg and J. L. Herder, “Voluntary closing: A promising opening in hand prosthetics,” *Technology and Disability,* pp. 85-94, 2003.

[24] C. Light, P. Chappell and P. Kyberd, “Establishing a standard- ized clinical assessment tool of pathologic and prosthetic hand function,” *Arch Phys Med Rehabil.,* p. 776–83, 2002.

[25] K. Berning, S. Cohick, R. Johnson and L. Miller, “Comparison of body-powered voluntary opening and voluntary closing prehensor for activities of daily life,” *Journal of Rehabilitation Research and Development,* p. 253–262, 2014.

[26] J. Shaperman, M. LeBlanc, Y. Setoguch and D. McNeal, “Is body powered operation of upper limb prostheses feasible for young limb deficient children?,” *Prosthetics and Orthotics International,* vol. 19, pp. 165-175, 1995.

[27] M. S. Trujillo, D. M. Russell, D. I. Anderson and M. Mitchell, “Grip Force Control Using Prosthetic and Anatomical Limbs,” *American Academy of Orthotists and Prosthetists,* vol. 30, no. 3, p. 132–139, 2018.

[28] M. Hichert, D. Plettenburg and A. Vardy, “A need for a more user-centered design in body powered prostheses,” in *Proceedings of the Myoelectric Controls/Powered Prosthetics Symposium,* Fredericton, Canada: University of New Brunswick, 2014.

[29] A. Tousi and D. H. Plettenburg, “WILMER Appealing Voluntary Closing Prehensor,” TU Delft, Delft, 2011.

[30] W. J. P., M. F. Glisson, E. L. Brockmeyer and J. K. Hodgins, “A low-friction passive fluid transmission and fluid-tendon soft actuator,” in *IEEE/RSJ International Conference on Intelligent Robots and Systems,* Chicago, IL, USA, 2014.

[31] G. Smit, D. Plettenburg and F. van der Helm, “Design and evaluation of two different finger concepts for body-powered prosthetic hand.,” *Journal of Rehabilitation Research & Development,* pp. 1253-66, 2013.

[32] R. Davies, S. Livingstone and A. Earl, “Power sources and actuators,” in *Proc. Symp. Powered Prostheses,* 1965.

[33] H. Monod, “Contractility of muscle during prolonged static and repetitive dynamic activity,” *Ergonomics,* vol. 28, no. I, pp. 81-89, 1985.

[34] “DINED anthropometric database,” [Online]. Available: www.dined.nl. [Accessed 30 September 2019].

[35] M. Hichert, D. Abbink, A. Vardy, C. van der Sluis, W. Janssen, M. Brouwers and D. Plettenburg, “Perception and control of low cable operation forces in voluntary closing body-powered upper-limb prostheses,” *Plos One,* vol. 14, no. 11, pp. 1-17, 2019.

[36] Sick Sensor Intelligence, “Datasheet PBT-RB025SG1SSNAMA0Z,” 11 11 2019. [Online]. Available: https://cdn.sick.com/media/pdf/6/96/396/dataSheet_PBT-RB025SG1SSNAMA0Z_6038640_en.pdf. [Accessed 20 05 2020].

[37] Feteris Components, “Model FLLSB200 S-beam Junior Loadcell,” [Online]. Available: https://tudelft.auralibrary.nl/koppelingen/documenten/fllsb200s-beamjuniorloadcellfeteris.pdf.

[38] Scaime, “Strain gage conditioner CPJ / CPJ2S,” [Online]. Available: https://scaime.com/product/post/cpj---cpj2s. [Accessed 31 05 2020].

[39] National Instruments, “USB-6008 Multifunction I/O Device,” [Online]. Available: https://www.ni.com/nl-nl/support/model.usb-6008.html. [Accessed 31 05 2020].

[40] D. Ryu, K. Moon, H. Nam, Y. Lee, C. Chun, S. Kang and J. Song, “Micro Hydraulic System Using Slim Artificial Muscles for a Wearable Haptic Glove,” in *IEEE/RSJ International Conference on Intelligent Robots and Systems,* Nice, France, 2008.

[41] R. Bos, “Mechanical design of dynamic hand orthoses: Expanding technology with comprehensive overviews and alternative pathways,” Delft University of Technology, Delft, 2019.

[42] Eriks BV, “Eriks O-ring Handbook,” Alkmaar.

[43] Eriks, “NBR 70 Compound 36624,” 14 8 2015. [Online]. Available: https://shop.eriks.nl/ProductDisplay?storeId=100001&urlLangId=-1&productId=1132441&urlRequestType=Base&categoryId=19542&langId=-1&catalogId=1000&itemFacet=adf_f154815%3A%2210.0%22. [Accessed 9 2 2020].

[44] Henkel Europe, “Datasheet Loctite 648,” 08 2016. [Online]. Available: https://tdsna.henkel.com/americas/na/adhesives/hnauttds.nsf/web/1716575D28E43176882571870000D860/$File/648-EN.pdf. [Accessed 22 04 2020].

[45] Festo AG & Co. KG, “Datasheet plastic tubing PUN-H-3X0,5-NT,” 19 03 2020. [Online]. Available: https://www.landefeld.com/shop/media/festo/datenblaetter/197375_en.pdf. [Accessed 30 03 2020].

[46] Maku GmbH, “Datasheet LF 3200 3281 03 09,” [Online]. Available: http://www.maku-industrie.de/shop/en/datasheet/datasheet/view/product/16996/. [Accessed 31 01 2020].

[47] Landefeld, “QSMY-3 (153370) P/in Y-connect,” [Online]. Available: https://www.landefeld.com/artikel/en/qsmy-3-153370-pin-y-connect-/OT-FESTO015455. [Accessed 09 February 2020].

[48] Fluorocarbon, “What Is Polychlorotrifluoroethylene? (PCTFE),” March 2016. [Online]. Available: http://www.fluorocarbon.co.uk/news-and-events/post/11/what-is-polychlorotrifluoroethylene-pctfe. [Accessed 12 February 2020].

[49] J. v. Frankenhuyzen, “Hydrualic Brake-System for Bicycle”. The Netherlands Patent WO2007/111510 A1, 04 10 2007.

[50] Festo AG & Co. KG, “Datasheet push-in Y-connector QSMY-3,” 19 03 2020. [Online]. Available: https://www.landefeld.com/shop/media/festo/datenblaetter/153370_en.pdf. [Accessed 20 04 2020].

[51] AZoM, “Stainless Steel - Grade 316 (UNS S31600),” 13 09 2001. [Online]. Available: https://www.azom.com/properties.aspx?ArticleID=863. [Accessed 20 06 2020].

[52] ASM Aerospace Specification Metals Inc., “Aluminum 7075-T6,” [Online]. Available: http://asm.matweb.com/search/SpecificMaterial.asp?bassnum=MA7075T6. [Accessed 20 06 2020].

[53] Festo AG & Co. KG, “Datasheet plastic tubing PUN-H-3X0,5-NT,” 19 03 2020. [Online]. Available: https://www.landefeld.com/shop/media/festo/datenblaetter/197375_en.pdf. [Accessed 20 04 2020].

[54] M. Živičnjak, N. Narančić, L. Szirovicza, D. Franke, J. Hrenović and V. Bišof, “Gender-Specific Growth Patterns for Stature, Sitting Height and Limbs Length in Croatian Children and Youth (3 to 18 Years of Age),” *Collegium Antropolicum,* vol. 27, pp. 321-34, 2003.

[55] G. Smit, D. Plettenburg and F. Van Der Helm, “Design and evaluation of two different finger concepts for body-powered prosthetic hand,” *JRRD,* vol. 50, no. 9, pp. 1252-1266, 2013.

[56] N. Smaby, M. Johanson, B. Baker, D. Kenney, W. Murray and V. Hentz, “Identification of key pinch forces required to complete functional tasks,” *Journal of Rehabilitation Research & Development,* vol. 41, no. 2, pp. 215-224, 2004.

[57] K. Ulrich and S. Eppinger, Product Design and Development, vol. 4, New York: McGraw-Hill, 2008.

[58] G. E. Dieter and L. C. Schmidt, Engineering Design : A Materials and Processing Approach, New-York: McGraw-Hill, 2009.

[59] N. Sclater, Mechanisms and Mechanical Devices Sourcebook, New York: The McGraw-Hill Companies, Inc., 2011.

[60] D. D. Frey and L. E. Carlson, “Technical note A body powered prehensor with variable mechanical advantage,” *Prosthetics and Orthotics International,* vol. 18, no. 2, pp. 118-123, 1994.

[61] J. Van Frankenhuyzen, “Hydrualic Brake-System for Bicycle”. Netherlands Patent WO2007/111510 A1, 4 10 2007.

[62] E. W. Versluis, “Design of a Hydraulic Prosthetic Hand Adding an active thumb to the Delft Cylinder Hand,” TU Delft, Delft, 2015.

[63] F. Freudenstein and G. N. Sandor, “Kinematic Elements,” in *Mechanical Design Handbook*, New-York, McGraw-Hill, 2006.

[64] J. P. Kuntz, “Rolling Link Mechanisms,” Delft University of Technology, Delft, 1995.

[65] S. Schulz, C. Pylatiuk and G. Bretthauer, “A new class of flexible fluidic actuators and their applications in medical engineering,” *At-Automatisierungstechnik,* vol. 47, no. 8, pp. 390-395, 1999.

[66] S. Schulz, C. Pylatiuk, M. Reischl, J. Martin, R. Mikut and G. Bretthauer, “A hydraulically driven multifunctional prosthetic hand,” *Robotica,* vol. 23, p. 293–299, 2005.

[67] I. N. Gaiser, C. Pylatiuk, S. Schulz, A. Kargov, R. Oberle and T. Werner, “The FLUIDHAND III: A Multifunctional Prosthetic Hand,” *American Academy of Orthotics and Prosthetics,* vol. 21, no. 2, pp. 91-96, 2009.

[68] S. Schulz, C. Pylatiuk and G. Bretthauer, “A New Class of Flexible Fluidic Actuators and their Applications in Medical Engineering,” *Automatisierungstechnik 47,* vol. 47, no. 8, pp. 390-395, 1999.

[69] D. Ryu, K.-W. Moon, H. Nam, Y. Lee, C. Chun, S. Kang and J.-B. Song, “Micro Hydraulic System Using Slim Artificial Muscles for a Wearable Haptic Glove,” in *IEEE/RSJ International Conference on Intelligent Robots and Systems*, Nice, France, 2008.

[70] D. H. Plettenburg and G. Smit, “A New Voluntary Closing Hook Prosthesis,” in *MyoElectric Controls/Powered Prosthetics Symposium*, Fredericton, New Brunswick, Canada, 2011.

[71] 4. A. J. P. Whitney, M. F. Glisson, E. L. Brockmeyer and J. K. Hodgins, “A low-friction passive fluid transmission and fluid-tendon soft actuator,” in *IEEE/RSJ International Conference on Intelligent Robots and Systems*, Chicago, IL, USA, 2014.

[72] M. LeBlanc, “Current evaluation of hydraulics to replace the cable force transmission system for body-powered upper-limb prostheses,” *Assistive technology: the official journal of RESNA,* vol. 2, pp. 101-7, 1990.

[73] G. Smit and D. H. Plettenburg, “Design of a Hydraulic Hand Prosthesis, with Articulating Fingers,” in *MyoElectric Controls/Powered Prosthetics Symposium*, Fredericton, New Brunswick, Canada, 2011.

[74] “Springs,” [Online]. Available: http://www.thecartech.com/subjects/machine_elements_design/Springs.htm. [Accessed 13 November 2019].

[75] A. Olieman, “Morphological chart,” Delft University of Technology, 12 April 2011. [Online]. Available: http://wikid.io.tudelft.nl/WikID/index.php/Morphological_chart. [Accessed 21 11 2019].

[76] R. Schipperen, “Design of a Variable Mechanical Advantage Mechanism for the Delft Cylinder Hand,” Delft University of Technology, Delft, 2015.

[77] G. Johnson, Concise Encyclopedia of Engineering, New York: McGraw-Hill, 2006.

[78] J. Cool, “Springs (in Dutch),” in *Werktuigbouwkundige Systemen*, Delft, VSSD, 2011, pp. 259-268.

[79] J. Kuntz, “Rolling Link Mechanisms,” Delft University of Technology, Delft, 1995.

[80] D. Frey and L. Carlson, “A body powered prehensor with variable mechanical advantage: technical note,” *Prosthetics and Orthorics International*, vol. 18, pp. 118-123, 1994.

[81] Milwaukee Cylinder, “Design Engineering Guide,” Actuant Corp., 2012.

[82] D. Plettenburg, “The WILMER Appealing Prehensor,” *Journal of Prosthetics and Orthotics*, vol. 18, no. 2, pp. 43-45, 2006.

[83] S. Pugh, “Concept Selection: A Method that Works,” in *Claus- ing, D. and Andrade, R., eds., Creating Innovative Products Using Total Design*, Reading, 1996.

[84] D. M. Anderson, Design for manufacturability: Optimizing cost, quality, and time to market., Cambria CA: CIM Press, 2001.

[85] K. K. Ehrlenspiel, Cost-Efficient Design with 320 figures., Berlin: Springer, 2007.

[86] D. Stienstra, “Introduction to Design for (Cost Effective) Assembly and Manufacturing.,” [Online]. Available: http://me.gatech.edu/files/capstone/L071ME4182DFA. [Accessed 18 November 2019].

[87] J. Van Der Cruijsen, “Redesign of the mechanism of the WILMER Appealing Prehensor,” Delft University of Technology, Delft, 2011.

[88] J. Cool, “Cord and Pulley (in Dutch),” in *Werktuigbouwkundige Systemen*, Delft, VSSD, 2011, p. 15.

[89] International Organization for Standardization, “The ISO System of Limits and Fits - Tolerances and Deviations,” in *ISO Standards Handbook - Limits, fits and surface properties*, Geneva, Switzerland, ISO, 1999, p. Chapter 6.

[90] Granta Design Limited, “CES EduPack software,” Granta Design Limited, Cambridge, UK, 2019.

[91] Landefeld, “PUN-H-2X0,4-NT (133038) Plastic tubing,” [Online]. Available: https://www.landefeld.com/artikel/nl/pun-h-2x04-nt-133038-plastic-tubing/OT-FESTO035907. [Accessed 11 February 2020].

[92] R. Pfeffer, “ISO System of Limits and Fits,” [Online]. Available: http://www.pfeffer.ch/isotolerances.htm. [Accessed 05 February 2020].

[93] International Organization for Standardization, “General Tolerances to ISO2768,” 1989. [Online]. Available: http://www.toplevelcnc.com/wp-content/uploads/2018/04/General-Tolerances-DIN-ISO-2768.pdf.

[94] Salamon's Metalen BV, “Material: SS Capilary Tubes (in Dutch),” 2016. [Online]. Available: https://salomons-metalen.nl/images/general/salomon_catalog_2016.pdf. [Accessed 22 03 2020].

[95] D. Plettenburg, “Pneumatic Seal Friction,” in *A Sizzling Hand Prosthesis*, Delft, Delft University of Technology, 1989, pp. 42-49.

[96] Innotec, “Ultra Clean,” [Online]. Available: https://www.innotec.nl/reinigers/technische-reiniging/ontvetters/ultra-clean-456/. [Accessed 22 05 2020].

[97] Henkel Europe, “LOCTITE SF 7649,” 08 2016. [Online]. Available: https://tdsna.henkel.com/americas/na/adhesives/hnauttds.nsf/web/385739FE3EBAE638882571870000D8B5/$File/SF%207649-EN.pdf. [Accessed 22 04 2020].